

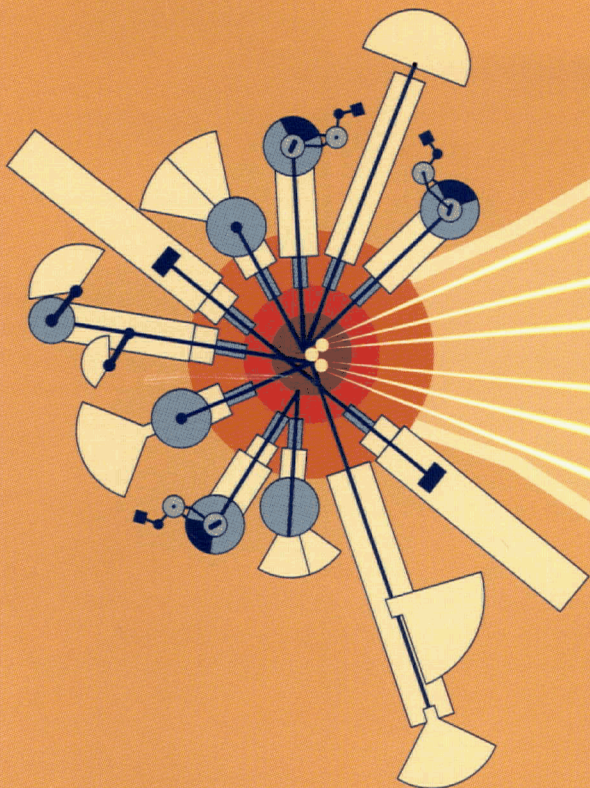
MARTIN MARIETTA ENERGY SYSTEMS LIBRARIES



3 4456 0315428 0

ORNL -- 6574

# ADVANCED NEUTRON SOURCE



OAK RIDGE NATIONAL LABORATORY

CENTRAL RESEARCH LIBRARY

CIRCULATION SECTION

4500N ROOM 175

**LIBRARY LOAN COPY**

DO NOT TRANSFER TO ANOTHER PERSON

If you wish someone else to see this  
report, send in name with report and  
the library will arrange a loan.

UCN-7989 3 9-77

## Progress Report



Advanced Neutron Source

April 1990

Printed in the United States of America. Available from the National Technical Information Service, U.S. Department of Commerce, 5285 Port Royal Road, Springfield, Virginia 22161. NTIS price codes: printed copy, A06; microfiche, A01.

This report was prepared as an account of work sponsored by an agency of the United States Government. Neither the United States Government nor any agency thereof, nor any of their employees, makes any warranty, express or implied, or assumes any legal liability or responsibility for the accuracy, completeness, or usefulness of any information, apparatus, product, or process disclosed, or represents that its use would not infringe privately owned rights. Reference herein to any specific commercial product, process, or service by trade name, trademark, manufacturer, or otherwise, does not necessarily constitute or imply its endorsement, recommendation, or favoring by the United States Government or any agency thereof. The views and opinions of authors expressed herein do not necessarily state or reflect those of the United States Government or any agency thereof.

*Cover shows 11 neutron beam tubes and the footprints of their associated instruments clustered around the Advanced Neutron Source reactor. Also illustrated are the 14 cold neutron guides as they fan out into the guide hall.*

Cover design by Mickie R. McBee  
and Bobbi M. Lee

# Advanced Neutron Source (ANS) Project Progress Report

## Principal Authors

D. L. Selby    R. M. Harrington  
*Oak Ridge National Laboratory*

F. J. Peretz  
*Martin Marietta Engineering*

## Editor

M. R. McBee  
*Oak Ridge National Laboratory*

## Technical Editing

C. M. Chance  
*Oak Ridge National Laboratory*

Date Published - April 1990

Prepared by the  
Oak Ridge National Laboratory  
Oak Ridge, Tennessee 37831  
operated by  
Martin Marietta Energy Systems, Inc.  
for the  
U.S. DEPARTMENT OF ENERGY  
under Contract No. DE-AC05-84OR21400

MARTIN MARIETTA ENERGY SYSTEMS LIBRARIES



3 4456 0315428 0

Contributing Authors

R. G. Alsmiller	R. A. Kisner
J. L. Anderson	R. A. Lillie
R. A. Brown	J. March-Leuba
N. C. J. Chen	B. H. Montgomery
G. L. Copeland	R. E. Pawel
B. Damiano	R. T. Primm, III
F. C. DiFilippo	G. T. Yahr
W. R. Gambill	G. L. Yoder, Jr.

*Oak Ridge National Laboratory*

C. C. Eberle	C. C. Queen
T. J. McManamy	T. L. Ryan

*Martin Marietta Engineering*

R. C. Birtcher	H. R. Thresh
G. L. Hofman	T. C. Wienczek
J. L. Snelgrove	

*Argonne National Laboratory*

E. L. Redmond	J. M. Ryskamp
---------------	---------------

*Idaho National Engineering Laboratory*

M. Ibn-Khayat	M. Abu-Shehadeh
---------------	-----------------

*University of Tennessee*

T. Nishigori  
*Osaka University*

# Contents

	<u>Page</u>
Figures . . . . .	vii
Tables . . . . .	xi
Acronyms . . . . .	xiii
1. Project Management . . . . .	1
1.1 Quality Assurance (QA) Program . . . . .	3
1.1.1 Quality Assurance Staffing. . . . .	3
1.1.2 Quality Assurance Plan. . . . .	4
1.1.3 Quality Program Implementation. . . . .	4
1.1.4 Monitoring of Project Activities. . . . .	4
2. Research and Development. . . . .	7
2.1 Reactor Core Development . . . . .	7
2.1.1 Development of Data and Techniques. . . . .	7
2.1.2 Preconceptual Core Development. . . . .	8
2.1.3 Support to Design. . . . .	10
2.2 Fuel Element Specification. . . . .	10
2.2.1 Impacts of New Reference Core . . . . .	11
2.2.2 HFIR Target Capsule Irradiation Tests . . . . .	12
2.2.3 Fuel Performance Modeling. . . . .	12
2.2.4 Simulation of Irradiation Damage by Ion Bombardment . . . . .	12
2.2.5 Fabrication Development . . . . .	12
2.3 Corrosion Loop Tests and Analyses. . . . .	13
2.3.1 The Corrosion Test Loop . . . . .	13
2.3.2 Corrosion Tests . . . . .	14
2.3.3 Analysis of Test Results. . . . .	14
2.3.3.1 Measurements and Calculations. . . . .	15
2.3.3.2 Summary of Corrosion Loop Experimental Results. . . . .	16
2.3.4 The Corrosion Workshop . . . . .	21
2.4 Thermal-Hydraulic Loop Tests . . . . .	21
2.4.1 Test Loop. . . . .	21
2.4.2 Schedule. . . . .	21

	<u>Page</u>	
2.5	Reactor Control Concepts. . . . .	22
2.5.1	Control Blades vs Control Rods . . . . .	22
2.5.2	Scramming Up vs Scramming Down . . . . .	22
2.5.3	The Use of Burnable Poison . . . . .	23
2.5.4	Control Rod Positions During the Cycle . . . . .	24
2.6	Critical and Subcritical Experiments . . . . .	24
2.7	Material Data, Structural Tests, and Analysis. . . . .	24
2.7.1	Core Pressure Boundary Tube. . . . .	24
2.7.2	Fuel Plate Stability . . . . .	25
2.7.3	Characterization of Irradiated 6061-T651 Aluminum . . . . .	25
2.8	Cold Source Development. . . . .	26
2.8.1	Cold Source Neutronics . . . . .	27
2.8.1.1	Model Development. . . . .	27
2.8.1.2	Cavity Effects . . . . .	28
2.8.1.3	Combined Liquid Deuterium and Liquid Nitrogen-15 System . . . . .	29
2.8.2	Thermal-Hydraulics and Testing Program. . . . .	29
2.8.2.1	Thermal-Hydraulics Analytical Modeling. . . . .	29
2.8.2.2	Thermal-Hydraulic Testing Program. . . . .	30
2.8.3	Development of Safety Philosophy for the ANS LD <sub>2</sub> Cold Source. . . . .	31
2.8.4	Cold Source Instrumentation Development. . . . .	31
2.9	Beam Tube, Guide, and Instrument Development . . . . .	31
2.9.1	Neutron Supermirrors. . . . .	31
2.9.2	Instrumentation Workshop . . . . .	33
2.9.3	Detector Shielding . . . . .	33
2.9.4	Beam Tube and Guide Design. . . . .	34
2.9.5	Very Cold and Ultracold Neutrons. . . . .	35
2.9.6	Instruments Available at Startup . . . . .	35
2.10	Hot Source Development. . . . .	35
2.11	Neutron Transport and Shielding. . . . .	36
2.11.1	Neutron/Gamma Transport in Beam Tubes . . . . .	36
2.11.2	Evaluate Component Heat Sources and Doses. . . . .	36
2.12	I&C Research and Development. . . . .	36
2.12.1	Protection and Control Strategy. . . . .	36
2.12.2	ANS Dynamic Model . . . . .	37
2.12.3	Xenon Transient Calculations . . . . .	39
2.12.4	Flux Calculation at Detector Locations. . . . .	40
2.12.5	Control Rod Drive Magnet and Latch Analysis . . . . .	40

	<u>Page</u>
2.13 Facility Concepts . . . . .	41
2.13.1 Materials Selection Issues . . . . .	41
2.13.2 Waste Management R&D. . . . .	42
2.13.3 Planning for Future Hardware Development and Testing. . . . .	42
<b>3. Design. . . . .</b>	<b>43</b>
3.1 Selection of Preferred Site. . . . .	43
3.2 Site Characterization. . . . .	45
3.3 Balance-of-Plant (BOP) Team. . . . .	46
3.4 Special BOP Tasks. . . . .	46
3.4.1 Decay Heat Removal . . . . .	46
3.4.2 Heat Removal System. . . . .	46
3.4.3 Containment Alternatives . . . . .	46
3.4.4 Site and Building Layout . . . . .	47
3.5 Architectural Engineer Selection. . . . .	47
3.6 Reactor Systems . . . . .	47
3.6.1 Overview . . . . .	47
3.6.2 Pressure Boundary. . . . .	47
3.6.3 Control and Monitoring Elements. . . . .	50
3.6.4 Fuel Element Assembly. . . . .	50
3.6.5 Provisions for Irradiation Capsules . . . . .	50
3.6.6 Seal Configurations for the CPBT . . . . .	51
3.6.7 Refueling and Maintenance Provisions . . . . .	51
3.7 Experiment Systems Design. . . . .	52
3.7.1 Overview. . . . .	52
3.7.2 Beams, Scattering, and Physics Instruments . . . . .	53
3.7.3 Transplutonium Production . . . . .	55
3.7.4 Materials Irradiation Facilities . . . . .	56
3.7.5 Special Isotope Production . . . . .	57
3.7.6 Analytical Chemistry Facilities. . . . .	57
3.7.7 Support Facilities . . . . .	58
3.8 Systems Integration. . . . .	58

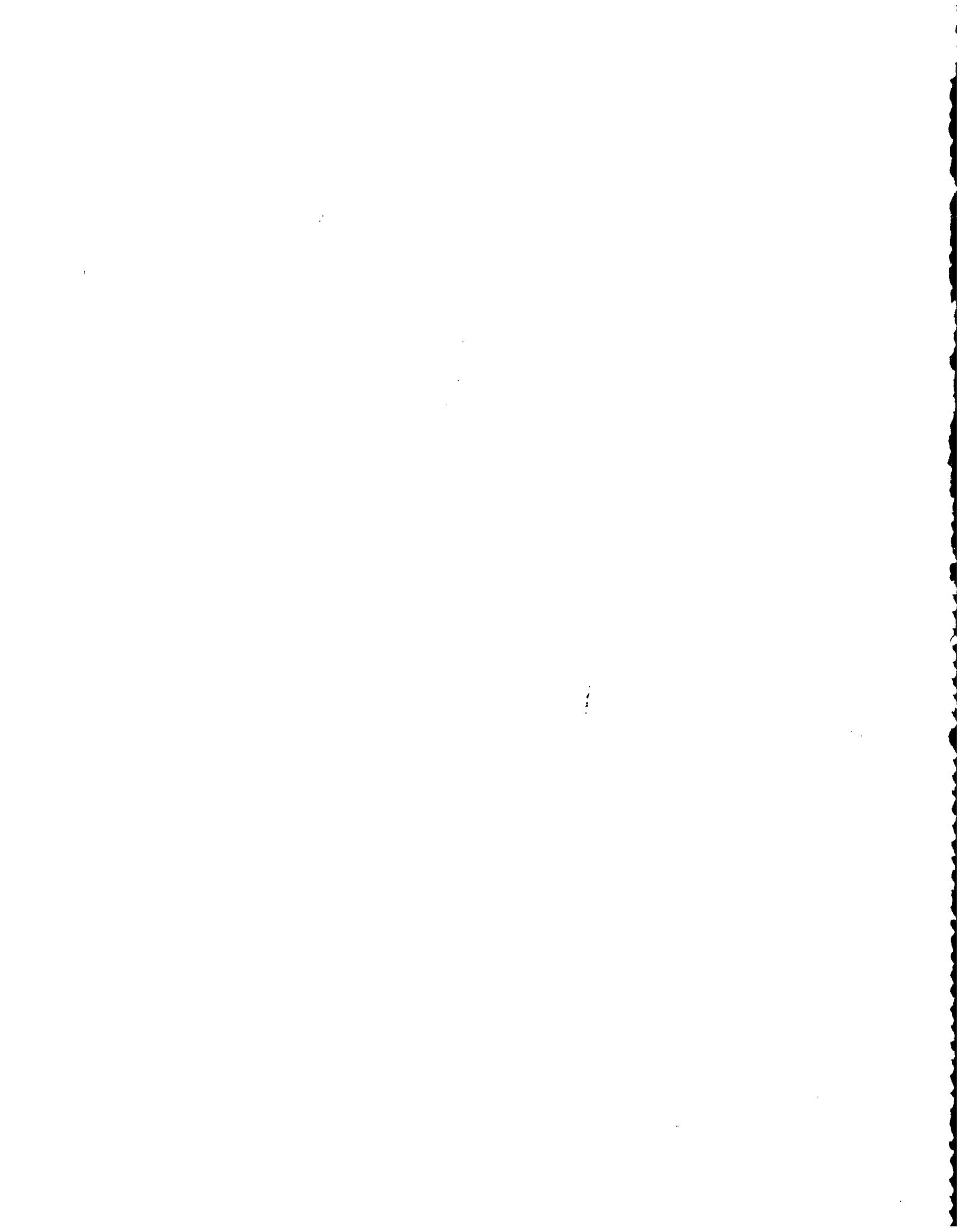
	<u>Page</u>
4. Safety .....	63
4.1 Safety Workshop .....	63
4.1.1 Environmental and Waste Management Issues Session .....	64
4.1.2 Applicable Regulatory Safety Criteria and Goals Session .....	65
4.1.3 Reactor Concepts Session .....	66
4.2 Regulatory Safety Criteria .....	69
4.3 Transient Thermal-Hydraulic Analysis .....	70
4.3.1 RELAP5 Code Improvement .....	71
4.3.2 Development of a RELAP5 Model of the ANS .....	72
4.3.3 Decay Heat Removal Calculations .....	75
4.4 Severe Accident Analysis .....	75
4.4.1 Severe Accident Debris Recriticality .....	76
4.4.2 Severe Accident Initiated Steam Explosion .....	78
4.4.3 Hydrogen Explosion .....	81
4.4.4 Other Ongoing Studies .....	83
4.5 Probabilistic Risk Assessment .....	83
4.5.1 Large Pipe Break Core Damage Risk Study .....	84
4.5.2 Determination of Dominant Accident Sequences .....	88
4.5.2.1 Core Flow Blockage (85% of Total Core Damage Risk) .....	89
4.5.2.2 Reactivity Addition Initiated Transients (8% of Total Risk) .....	90
4.5.2.3 Large Pipe Breaks (4.7% of Risk) .....	91
4.5.2.4 Pressurizer Pump Failures (3% of Risk) .....	91
4.5.2.5 Loss of Secondary Coolant Heat Removal (0.25% of Total Risk) .....	91
4.5.3 Hydrogen-Oxygen Safety Risks .....	92
References .....	95

# Figures

<u>Figure</u>	<u>Page</u>
1.1    Advanced Neutron Source schedule . . . . .	2
2.1    Final preconceptual core geometry. . . . .	8
2.2    Film growth on 6061 Al for CTEST No.4 at three reference positions on specimen . . . . .	16
2.3    Film growth on 6061 Al for CTEST No.10. Interface temperatures and local heat fluxes near beginning and end of test are shown for each position . . . . .	18
2.4    Film growth observed during CTESTS for specimens having near-identical interface temperatures, $T_{\phi/c}$ . Specimen position for given experiment is noted in parentheses; coolant temperatures and heat fluxes are listed as indicated . . . . .	18
2.5    Comparison of film-growth data illustrating importance of coolant inlet temperature, $T_{ci}$ , as "independent" variable. . . . .	19
2.6    Single epoxy involute plate test facility. . . . .	26
2.7    Impact of cold source on calculated neutron spectrum with inclusion of normalized ILI data for reference . . . . .	27
2.8    Neutron guide factors obtained within the guides for three separate cold source cavities . . . . .	28
2.9    LN <sub>2</sub> cold source test facility . . . . .	30
2.10    Neutron transport through a reflecting channel. . . . .	32
2.11    Transmitted beam intensity and polarization (solid lines) as function of angle after transmission through optimized supermirror stack. Incident beam intensity is shown as dotted line . . . . .	32
2.12A    Illumination of single neutron guide. . . . .	34
2.12B    Illumination of guide pare configuration. . . . .	34
2.13    Block diagram of control engine template for ANS. . . . .	38

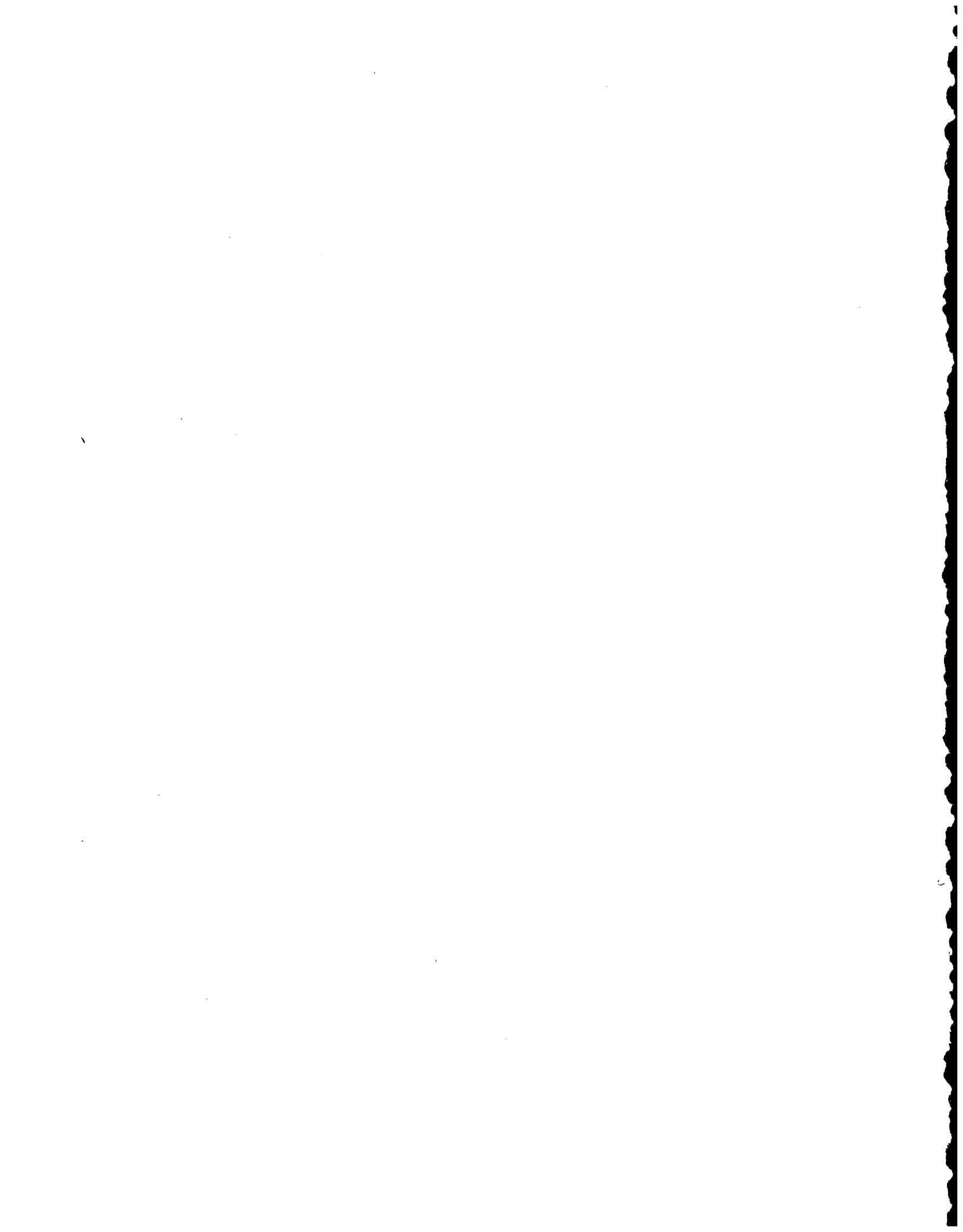
<u>Figure</u>	<u>Page</u>
2.14 Hot spot fuel surface temperatures following loss of main pumping power, and coolant saturation temperatures during slow depressurization. Gas pressurizer is located in low pressure side of pump and has 9 m <sup>3</sup> of D <sub>2</sub> O liquid volume and 1 m <sup>3</sup> of gas volume. Power peaking factors are 2.48 for hot spot and 1.95 for hot streak . . . . .	39
2.15 Reactivity due to Xenon, Samarium, and other fission products following shutdown; otherwise, 57 hours must elapse to reach criticality again . . . . .	39
2.16 Force developed by lifting magnets. . . . .	40
2.17 Control rod in unlatched position. . . . .	41
2.18 Force transfer through ANS latch. . . . .	41
3.1 Melton Valley area and proposed sites . . . . .	45
3.2 Conceptual site plan. . . . .	46
3.3 Elevation view of reactor system. . . . .	48
3.4 Baseline reactor core configuration . . . . .	49
3.5 Pressure containment components . . . . .	49
3.6 Refueling machine shown docked with transfer cell . . . . .	52
3.7 Refueling tunnel concept. . . . .	53
3.8 Plan view of experiment facilities on second floor of reactor building . . . . .	54
3.9 Section of reactor assembly and pool, showing curved very-cold guide. . . . .	55
3.10 Triple-axis spectrometer footprint. . . . .	55
3.11 Section of reactor core showing materials irradiation and transplutonium production targets . . . . .	56
3.12 ANS documentation planning schedule initial release milestones. . . . .	60
4.1 RELAP5 preliminary calculations of (A) primary coolant core inlet and outlet pressures and (B) hot spot fuel plate centerline temperatures after large pipe break (325 diam) from full power . . . . .	73

<u>Figure</u>	<u>Page</u>
4.2 RELAP5 preliminary calculations of primary coolant core inlet pressure after small pipe break (51-mm diam) from full power. . . . .	74
4.3 Comparison of normalized heat flux vs flow predicted by onset of net vapor generation criteria and saturated exit limit (nominal heat flux = 6 MW/m <sup>2</sup> , nominal velocity = 27.4 m/s, T-core inlet = 49°C, and P-core exit = 0.2 MPa). . . . .	75
4.4 Failure envelopes for CPBT (inner wall) and reflector tank (outer wall) loaded by triangular pressure pulse . . . . .	80
4.5 Pressure pulse vs distance for atmospheric pressure detonation of 4, 10, and 18 kg hydrogen. . . . .	82
4.6 Large-pipe-break event tree (FD = fuel damage and NFD = no fuel damage). . . . .	87
4.7 Large-pipe-break fuel damage risk . . . . .	87



# Tables

<u>Table</u>		<u>Page</u>
2.1	ANS reactor final preconceptual core design specifications and comparison with HFIR .....	9
2.2	Flux and spectrum figures .....	10
2.3	Perturbations due to irradiation facilities and capsules. ....	11
2.4	Corrosion test loop: completed tests and parameters .....	15
3.1	Project document preparation dependencies .....	59
4.1	Coolant bulk temperature at core exit predicted by onset of net vapor generation (ONVG) using Saha-Zuber low mass flow rate correlation. ....	76
4.2	Criticality of hypothetical core debris configurations .....	78
4.3	ANS steam explosion pressure pulse estimates and effect on CPBT and reflector tank. ....	81
4.4	Aging probability of failure per weld-year calculated with PRAISDPD .....	86



# Acronyms

AE	Architectural Engineer
ANL	Argonne National Laboratory
ANS	Advanced Neutron Source
ATR	Advanced Test Reactor
B&W	Babcock and Wilcox Company
BES	Basic Energy Sciences
BNL	Brookhaven National Laboratory
BOC	Beginning-of-Cycle
BOP	Balance-of-Plant
CDR	Conceptual Design Report
CPBT	Core Pressure Boundary Tube
DAS	Data Acquisition System
DOE	Department of Energy
EB	Electron Beam
EDX	Energy Dispersive X-ray
EOC	End-of-Cycle
ETD	Engineering Technology Division
FD	Fuel Damage
HFBR	High Flux Beam Reactor
HFIR	High Flux Isotope Reactor
I&C	Instrumentation and Controls
ICANS	International Committee on Advanced Neutron Sources
IGORR	International Group on Research Reactors
ILL	Institut Laue Langevin
INEL	Idaho National Engineering Laboratory
LANL	Los Alamos National Laboratory
LANSCE	Los Alamos Neutron Scattering Facility
LOCA	Loss-of-Coolant Accident
LWR	Light-Water Reactor
NFD	No Fuel Damage
NRC	Nuclear Regulatory Commission
NSCANS	National Steering Committee for an Advanced Neutron Source
ONVG	Onset of Net Vapor Generation
ORNL	Oak Ridge National Laboratory
ORO	Oak Ridge Operations
PC	Personal Computer
PDD	Plant Design Description
PRA	Probabilistic Risk Assessment
PRC	Project Review Committee
PRAISDPD	PRAISE Discrete Probability Distributions
QA	Quality Assurance
QAS	Quality Assurance Specialist
R&D	Research and Development
RDL	Reference Documentation List

REDC	Radiochemical Engineering Development Center
RERTR	Reduced Enrichment for Research and Test Reactors
RT	Reflector Tank
SDD	System Design Description
SEM	Scanning Electron Microscopy
TC	Thermocouple
TEM	Transmission Electron Microscopy
UCN	Ultracold Neutron
UT	University of Tennessee
VCN	Very Cold Neutron

# Project Management

---

At the time of the last progress report, the Advanced Neutron Source (ANS) Project was still at the "preconceptual design" stage; preconceptual design documents initial activities that analyze and select from various project alternatives and develops a brief project definition with preliminary costs and schedules. At the end of 1988, we began "conceptual design," a more formal phase of the work that encompasses the development of a definitive project scope, cost, and schedule sufficient to support the project for Congressional consideration. Although much work remains to be done in the early design activities, a set of reports (*Conceptual Design Reference Report*<sup>1</sup>), which is an intermediate-phase document defining the initial design phase of the project in sufficient detail to support a Congressional request for design-only funding, has been prepared and issued to the Department of Energy (DOE) to support a request for FY 1991 line-item funding to support detailed design.

In response to guidance from DOE and its Basic Energy Sciences (BES) Advisory Committee, the Project schedule and funding profile were replanned to place more of the design work under line-item funding, thus reducing the requirements on the BES operating budget. This new plan calls for line-item funding to begin in FY 1991. The plan is divided into a three-year, design-only project; the first part of which will also provide the data required to submit a request for line-item funds to complete all design and

construction work. This plan for line-item funds to complete all design and construction work was formally accepted by our Headquarters sponsor (the Division of Materials Science) at a major review (the "Ed Temple Review") of the Project in April 1989. The proposed schedules are shown in Fig. 1.1.

The Temple Committee was one of three major external reviewers of the Project in this reporting period. The others were the BES Advisory Committee (August 1988) and the Martin Marietta Energy Systems Independent Review Committee (June 15-16, 1989). All were supportive of the Project and found that the approach taken to safety issues is an appropriate and effective one.

A draft Quality Assurance (QA) Plan for the Project was written and extensively reviewed within Martin Marietta Energy Systems and the DOE Oak Ridge Operations Office (ORO). The QA Plan has now been approved, with minor revisions by both organizations. The preparation, followed by implementation, of a QA Plan at this unusually early stage of a Project is expected to bring later benefits through minimizing the need for rework, the need for retrospective justifications of fitness-for-use of results or equipment, and reduction of design changes. The QA Plan and other Project policies will be implemented through formal procedures, to be followed by all parts of the Project. A Project Review Committee (PRC), consisting of the ANS Project managers, a QA specialist, and chaired by the Project Director, will

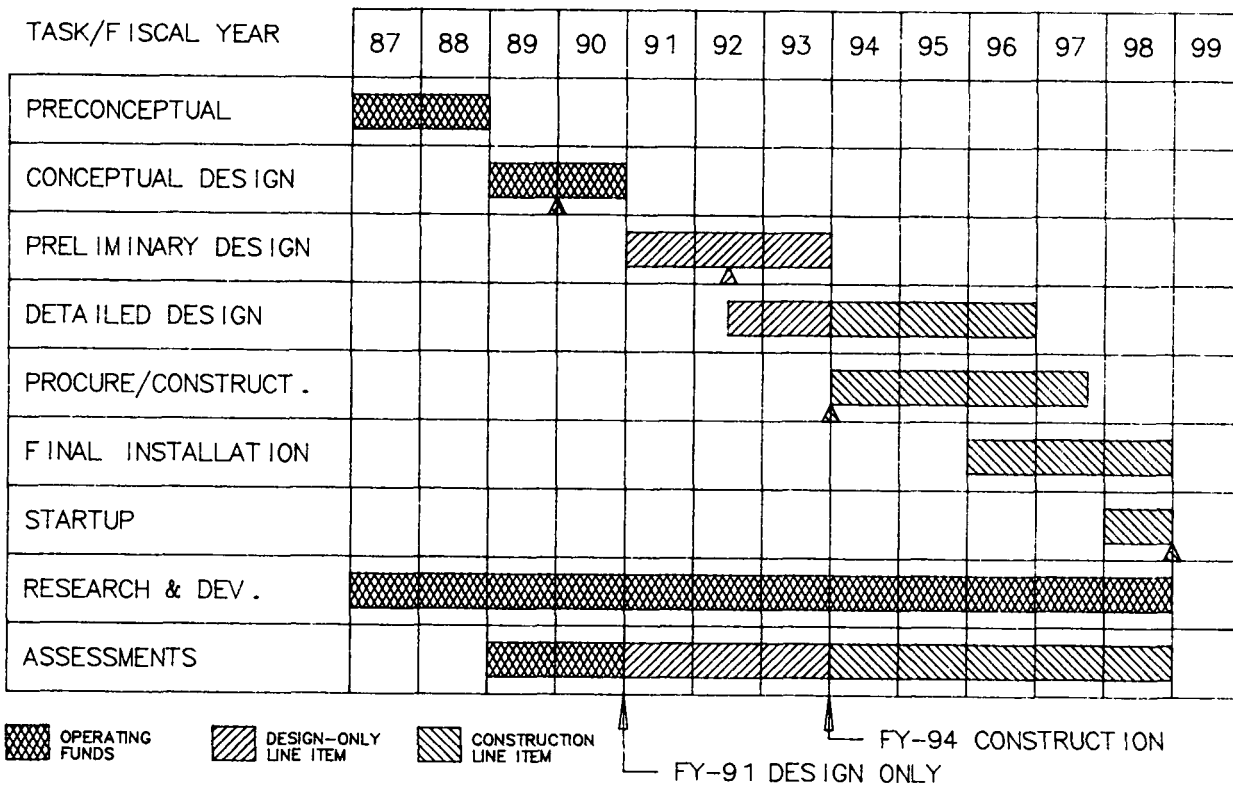


Fig. 1.1. Advanced Neutron Source schedule.

review all proposed policies and procedures and must approve them before issue. Two QA Specialists (QASs) have been assigned to the Project.

We continue to seek and to receive guidance and technical input from the broader technical community. The National Steering Committee for an Advanced Neutron Source (NSCANS) has met twice during this reporting period, reviewing the Project's design work and providing feedback from the user community. Two subcommittees of NSCANS--on materials irradiation testing facilities and reactor design--made visits to Oak Ridge to review their particular areas of interest; the results of these visits significantly and favorably influenced the reactor design.

Two ANS workshops have been held: one at Idaho National Engineering Laboratory (INEL) was devoted to the corrosion of heated aluminum in water, and the other at

Knoxville, Tennessee, focused on all aspects of safety and was much broader in scope. A third workshop on the research instruments for a neutron scattering facility was jointly sponsored by the ANS Project and Brookhaven National Laboratory (BNL) and took place in Oak Ridge. A fourth, to be sponsored jointly by the Los Alamos Neutron Scattering Facility (LANSCE) and the ANS Project, is an international workshop on cold neutron sources to be held in April 1990 at Los Alamos.

The ANS Project has taken the initiative to form an ongoing International Group on Research Reactors (IGORR) to provide a forum for sharing experiences among institutes that are planning or engaged in the construction of new or significantly up-graded research reactor facilities. The Group will be similar to the very successful one established several years ago for spallation neutron

sources and known as the International Committee on Advanced Neutron Sources (ICANS). It is proposed that IGORR will meet every one to two years, and Oak Ridge National Laboratory (ORNL) has offered to host the first meeting in 1990. All of the 13 institutes invited to participate in setting up the Group and planning the first meeting have replied, and only one declined; the institutes invited to help form the Group were all known to be involved in reactor upgrades or new construction. The membership of IGORR and attendance at its meetings will be drawn from all organizations with research reactors. We believe that this initiative will have important benefits to the research reactor community.

The first edition of an ANS newsletter was sent in August to a large mailing list obtained from the following societies: American Physical Society, American Nuclear Society, Biophysical Society, Materials Research Society, and the American Chemical Society. In addition, a monthly news bulletin, concentrating largely on the scientific research applications of the facility, is sent to the National Steering Committee and other interested persons.

In the last year, shortage of funds has again forced a one-year extension to the Project. The Project's minimal 1989 request was for \$8.7 million operating funds and \$350,000 capital equipment funds, but only \$7.8 million operating money was made available to the Project Office. The replanning for design-only line-item funding was aimed at reducing the operating funds requirement in the early years, and the FY 1990 request was reduced from \$15.6 million to \$9.7 million (excluding capital equipment). The result of these budget reductions is to stretch out the Project by one year, even if full 1990 operating and 1991 line-item funding is received. Further reductions will lead to further delays.

The Project's cost accounting and reporting system, newly installed at the time of the last report, has proved to be very effective.

It has been further developed and will allow a smooth transition from operating to line-item funding.

Two of the many technical achievements during this period have been particularly significant in the planning, scheduling, and management of the Project. One was the evolution and documentation of a final pre-conceptual reference core design with which the conceptual design phase could begin. The other was the selection of a preferred site on DOE's Oak Ridge Reservation for the ANS facility; at the very end of this reporting period, survey drilling had just begun to evaluate that site further. These achievements, and the other technical work of this period, are described later in this report.

## 1.1 QUALITY ASSURANCE (QA) PROGRAM

In August 1988, ANS project management made the decision to implement a project-specific QA program. This choice was based on the realization that major decisions made during the preconceptual and conceptual design phases would guide the future development of the ANS. Implementation of a quality program at this early stage of the project could avoid significant rework and resultant schedule delays later. Early implementation of a quality program was also consistent with the project's position of being able to support a facility design review comparable to the U.S. Nuclear Regulatory Commission (NRC) licensing reviews.

### 1.1.1 Quality Assurance Staffing

A QAS was assigned on a part-time basis in August 1989 to develop a QA Plan for the project; one additional QAS was loaned to the project on a part-time basis early in 1989 to assist in program development. In April

1989, the QA staffing level rose to one full-time and one half-time QAS.

### 1.1.2 Quality Assurance Plan

The ANS QA Plan was developed and extensively reviewed within the project. Before project approval of the plan, a team of nuclear industry experts familiar with regulatory trends reviewed the draft plan and the strategy for its implementation. The consensus was that the plan and implementing approach were comparable to, or exceeded, the practices of the current commercial nuclear industry. The plan was approved by the Project in April 1989 and submitted to DOE-ORO for their approval in accordance with DOE-OR Order 5700.6A. Comments were received from DOE-ORO in August, resolved, and the Plan revised in October 1989.

### 1.1.3 Quality Program Implementation

The Project's management strategy demanded that the quality program would not be an add-on program but would be integral to the Project's conduct of operations. The quality-assuring provisions of the program would be incorporated into the procedures to define how management would control the performance of project tasks.

The PRC, consisting of the Project's managers and a QAS, was created to review and resolve issues affecting multiple aspects of the project, such as project procedures. A Commitment and Action Tracking System was implemented to provide a means of ensuring that all project commitments are accomplished. The system provides management with commitment status reports, notices of impending commitment due dates, and notices of overdue commitments.

Project management has initiated the use of a simplified system for individual task

planning by the Task Leaders, with review and approval before work commencement and a simplified task closeout document. This approach has been very successful in several research and development (R&D) tasks and the Preliminary Subsurface Investigations of the proposed site.

A data base of computer codes used on the project has also been established. This data base is used to track the codes used for each task and the validation, verification, or benchmarking status of those codes.

### 1.1.4 Monitoring of Project Activities

Project management has elected to review selected key activities that were completed before the development of the project-specific QA program. This review is a combination of a Peer Review for the technical aspects of the task and a Quality Audit for appropriate supporting documentation and adherence to established procedures. The Site Evaluation Report was reviewed in late FY 1989, with procedural compliance findings identified and resolved. The PS-2 Reference Core Design is scheduled for review in early FY 1990.

Surveillances of the preliminary site subsurface characterization were performed on a frequent basis to ensure compliance with the plan. No deficiencies were identified.

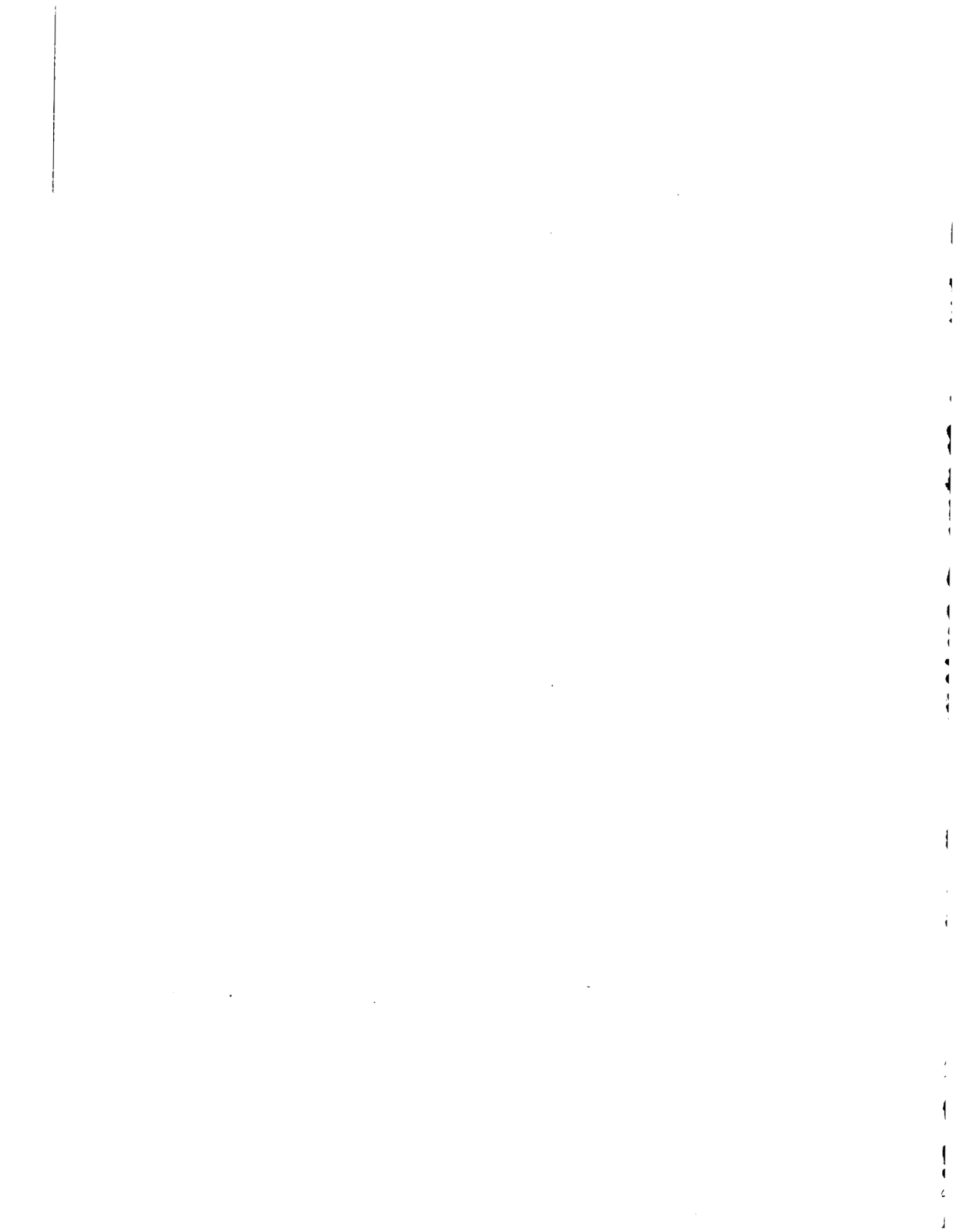
An audit of the design process and fabrication of the HANS-1 Fuel Irradiation Experiment were completed, with some documentation problems identified and resolved.



*The ANS Cold Source Test Facility will be used to examine thermal-hydraulic behavior in a cryogen-filled dewar and to aid in the design and fabrication of the cold source.*



*The ANS Corrosion Test Loop began operation in January 1988 to look at formation of oxide on aluminum clad fuel plates.*



# Research & Development

---

Thirteen R&D tasks have been identified as essential to the ANS Project. These R&D tasks are required to address feasibility issues, to provide some of the data needed for the preparation of the Conceptual Design Report (CDR), to produce the data necessary to make a rational decision when alternative design concepts are identified, and to examine and demonstrate the applicability of technological advances. This chapter summarizes progress on these tasks for the reporting period and includes activities at Argonne National Laboratory (ANL), Babcock and Wilcox (B&W), INEL, ORNL, and University of Tennessee (UT).

## 2.1 REACTOR CORE DEVELOPMENT

The reactor core development has now moved from a preconceptual phase to a conceptual development phase. At the end of the report period tasks had been initiated to lead to a conceptual core geometry by January 1990. The major activities during the report period for this task are summarized in the following sections (Sects. 2.1.1-2.1.3).

### 2.1.1 Development of Data and Techniques

Additional nuclides have been added to the cross-section library developed for use on this project, and cross section sets are in

place for diffusion and transport calculations. Differences in the results of diffusion calculations by different workers have been largely resolved; causes included different methods of deriving spatially weighted cross sections, different ways of reporting results (e.g., clean core vs equilibrium xenon), and different numbers of groups in the cross-section sets.

Comparison of transport and diffusion calculations for an early single-core design confirmed that most diffusion-calculated quantities are sufficiently accurate, with the error mostly arising from the finite size of the computational cells. More recent calculations with a Monte Carlo model have not yet been fully evaluated, but appear to provide even stronger confirmation of the diffusion calculations of reactivity.

A personal computer (PC) version of the BOLD-VENTURE code, prepared as a part of another INEL project by the University of Cincinnati, became available. With few exceptions, the code was written in standard FORTRAN 77. It was, therefore, a good starting point for conversion to CRAY and, in particular, the Livermore CRAY on which 900 hours of time was available to the ANS Project. The conversion was not easy, but was accomplished with a consequent reduction in computing costs.

A steady-state thermal-hydraulics code, originally written for the High Flux Isotope Reactor (HFIR), has been adapted for the ANS. The new version is more flexible, with many of the dimensions and properties that

were embedded in the HFIR coding easily changed to represent design variations. The thermal-hydraulic correlations have been updated (e.g., the critical heat flux correlation—see following paragraph), and recent values for heavy-water ( $D_2O$ ) properties (see below) are also included. The code is now in routine use.

A considerable amount of effort was devoted to developing an improved critical heat flux correlation,<sup>2</sup> and the new correlation is now in use.

During this period, most of the comparative studies of different core designs have taken the major uncertainties into account; that is, the effect of combined uncertainties (in local fuel loading, in coolant channel gap, and in other major variables) in reducing the permissible operating core power below the nominal limiting value was considered. The uncertainties were combined, very conservatively, by multiplication, which is equivalent to assuming that every variable takes its most unfavorable value simultaneously. Such a method is unrealistic, and a proper combination of uncertainties would be based on the statistical probabilities of departures from nominal, reflecting the probabilistic nature of the safety goals (e.g.,  $<10^{-5}$ /year probability of core damage). Some evidence, from hand calculations and from the statistical analysis code used for the Advanced Test Reactor (ATR) at Idaho, indicates that operating power levels (and therefore achievable neutron flux) set by probabilistic calculations may be as much as 10 to 20% higher than the conservative multiplicative approach. Work was therefore begun to evolve a methodology for statistical combination of the uncertainties.

### 2.1.2 Preconceptual Core Development

The major activity in this task area was the development of a final preconceptual reference core design.<sup>3</sup> The new reference core consists of two involute fuel elements, of

different diameters, aligned axially with a small axial gap between them (see Fig. 2.1). The use of different element diameters permits a separate flow of coolant to be provided for each one, thus enhancing the heat removal capability and increasing the thermal-hydraulic margins. The improved cooling allows the elements to be relatively long and thin, so self-shielding is reduced and an acceptable core life can be achieved with a relatively small loading of highly enriched uranium silicide ( $U_3Si_2$ ) fuel clad in aluminum.

The reference design has a fueled volume of 67.4 L, each element having a heated length of 474 mm and a radial fuel thickness of 66 mm. The end-of-cycle (EOC) peak thermal flux in the large heavy-water reflector tank around the core is estimated to be in the range of  $0.8$  to  $1.0 \times 10^{20} \text{ m}^{-2} \cdot \text{s}^{-1}$ . Other key

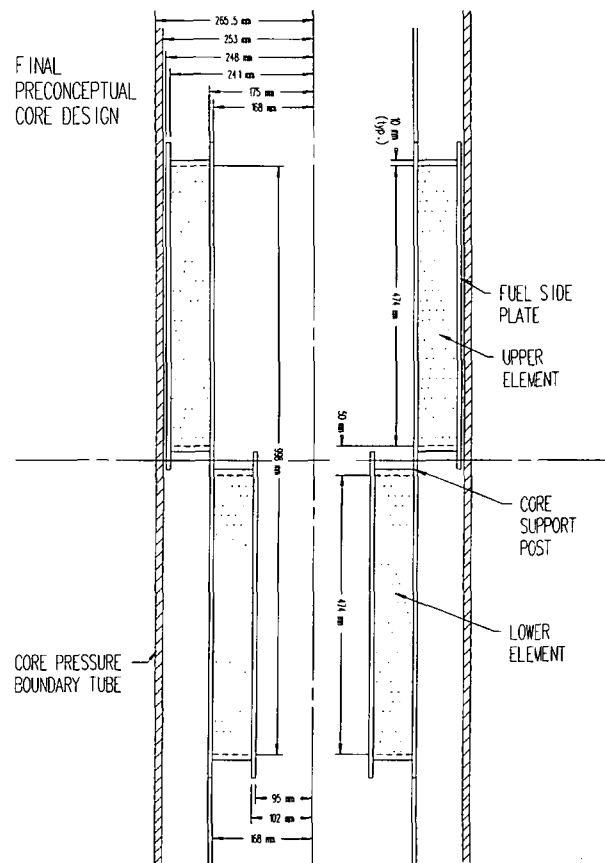


Fig. 2.1. Final preconceptual core geometry.

parameters for this new reference core are presented and compared with HFIR values in Table 2.1.

The lack of symmetry about the mid-plane of the new design is unusual and, at first sight, intuitively unwelcome. However, in addition to the neutron beam production, the ANS is to be designed for materials irradiation testing and transplutonium production as well. It turns out that with the asymmetrical design, the region immediately inside the

larger element is appropriate for fast-flux irradiation testing, and that region immediately outside the smaller element is good for transplutonium reduction (see Table 2.2). Furthermore, the beam tubes are shielded from the materials irradiation positions by the fuel in the upper element and are relatively far removed from the transplutonium production positions, so that the flux at the beam tubes is little affected by the irradiation positions (see Table 2.3).

Table 2.1. ANS reactor final preconceptual core design specifications and comparison with HFIR

Quantity	ANS	ANS notes	HFIR*
Fission power level, MW(f)	350		100
Power transferred to primary coolant, MW(c)	332	Heat convected away from fuel plates	97
Average power density, MW(c)/L	4.9		1.9
Maximum power density, MW(c)/L	8.3	Estimated, fuel grading not yet optimized	4.4
Core life, d	14		20
Core active volume, L	67.4	Fueled volume	50.6
Fuel form	U <sub>3</sub> Si <sub>2</sub>		U <sub>3</sub> O <sub>8</sub>
Fuel matrix	Al		Al
Vol % of fuel in meat, % 12.5/18.0 <sup>b</sup>	15		
Fuel loading, kg U <sup>235</sup>	14.9		9.4
Fuel cladding	6061 Al		6061 Al
Fuel plate thickness, mm	1.27		1.27
Clad thickness, mm	0.254		0.254
Coolant channel gap, mm	1.27		1.27
Coolant (and reflector) H <sub>2</sub> O(D <sub>2</sub> O)	D <sub>2</sub> O(D <sub>2</sub> O)		
Inlet pressure, MPa	3.7		4.1
Inlet temperature, °C	49		49
Heated length, mm	474		508
Coolant velocity in core, m/s	27.4	May be reduced after detailed analysis	16
Core pressure drop, MPa	1.6		0.7
Outlet pressure, MPa	2.1		3.4
Bulk coolant outlet temperature, °C	81		73
Average heat flux, MW(c)/m <sup>2</sup>	6.3		2.4
Maximum heat flux, MW(c)/m <sup>2</sup>	10.7	Estimated; fuel grading not yet optimized	5.6
Maximum fuel centerline temperature, °C	400	Design groundrule	327
Peak thermal flux in reflector, 10 <sup>19</sup> m <sup>-2</sup> .s <sup>-1</sup>	>8	Unperturbed	1.5

\*At 100 MW.

<sup>b</sup>Inner element/outer element.

Table 2.2. Flux<sup>a</sup> and spectrum figures  
[Unperturbed beginning-of-cycle (BOC), nominal power]

Purpose	ANS design criterion	Reference core (BOC)	
		No control rods	With control from top
<b>Scattering</b>			
Peak thermal flux	5	9 <sup>b</sup>	9 <sup>b</sup>
Thermal/fast ratio near peak	80	75-100	75-100
<b>Materials irradiation</b>			
Fast flux	1.4		
Top of irradiation space		1.9	1.3
Center of irradiation space		2.3	1.9
Bottom of irradiation space		2.2	2.3
Fast/thermal ratio	0.5		
Top of irradiation space		0.8	3.5
Center of irradiation space		1.3	5.0
Bottom of irradiation space		1.2	3.0
<b>Transuranium production</b>			
Epithermal flux	0.6		
Top of irradiation space		3.4	3.8
Center of irradiation space		2.4	3.4
Bottom of irradiation space		1.2	1.9
Epithermal/thermal ratio	0.25		
Top of irradiation space		1.5	1.6
Center of irradiation space		1.2	1.4
Bottom of irradiation space		0.9	1.0

<sup>a</sup>10<sup>19</sup> m<sup>-2</sup>·s<sup>-1</sup>.

<sup>b</sup>EOC estimated value.

### 2.1.3 Support to Design

Work continues on optimization of the fuel grading to maximize the power capability of the core. There is evidence that hot spots can be placed close to the inlets of the elements, where the water is coolest, thus improving the incipient boiling and critical heat flux margins and also reducing both the oxide growth rate and the fuel centerline temperature. These optimizations are not yet complete.

The new reference core, besides the neutronic advantages referred to previously, has only about half the power density of the earlier design, greatly enhancing safety margins. Outside reviews of the design by the NSCANS and DOE are very positive.

One remaining issue is stability of the thin fuel plates: a large margin to the critical velocity is desirable, and later design work may call for shorter plate span or lower coolant velocity.

## 2.2 FUEL ELEMENT SPECIFICATION

The U<sub>3</sub>Si<sub>2</sub>/Al mixture continues to be the reference fuel for the ANS reactor core. Irradiation data accumulated during the year through the Reduced Enrichment for Research and Test Reactors (RERTR) Program have continued to show low, stable fuel swelling and excellent retention of fission gases in small discrete bubbles. The fuel

Table 2.3. Perturbations due to irradiation facilities and capsules

	Loss of $K^{eff}$ %	Loss of rendement %	Expected peak thermal flux loss <sup>a</sup> %
Base case - no irradiation facility structural material	-	-	-
Add structural material(10% Al, 90% D <sub>2</sub> O) in both irradiation regions	0.22	<0.1	<0.5 (Al)
Add 10 capsules of steel irradiation specimens	<0.1	<0.1	<0.51 <sup>b</sup>
Add 30 production rods with transplutonium elements <sup>c</sup>	0.93	<0.1	2 <sup>b</sup>

<sup>a</sup>This is greater than the simple loss-of-rendement because the extra fuel loading in the core needed to restore  $K^{eff}$ , and therefore core life, also reduces the rendement.

<sup>b</sup>Will vary almost linearly and additively with the number of capsules or rods.

<sup>c</sup>75% of the campaign, 41 curium targets, and 25% of the campaign, 63 curium targets.

NOTE: Preliminary results--need confirmation from independent calculations.

development efforts this year have concentrated on continued evaluation and analysis of irradiation data on the fuel from the RERTR Program, generation of a computer code to model this behavior, simulation of irradiation damage by ion bombardment, fabrication of capsules for irradiation testing in the target region of the HFIR, and fabrication development for plates.

### 2.2.1 Impacts of New Reference Core

The new reference core described in Sect. 2.1 has a larger volume and a lower fuel loading than previous cores. The lower volume fraction of fuel required is expected to simplify the fabrication process and increase

the fabrication yields of acceptable plates. The incorporation of burnable poison into the plate ends will introduce a new feature in the fuel plate fabrication process. However, the less severe requirement for axial fuel grading will ease a major developmental hurdle in plate fabrication. The specific performance requirements will not change much with the new core, that is, the homogeneity requirements, burnup rates and levels, and temperatures will remain about the same.

The inclusion of burnable poison (15 g of <sup>10</sup>B) in the fuel plate ends for a distance of ~40 mm is proposed to reduce the power peaking at the core ends. If boron carbide (B<sub>4</sub>C) containing natural boron is used, this translates to 96.8 g of B<sub>4</sub>C in a volume of 1.6 L or 2.5 volume %. This volume fraction of B<sub>4</sub>C dispersed in aluminum should fabricate

easily. At first glance, this would be accomplished by adding small compacts of  $B_4C$ -Al at both ends of the fuel compact in the picture frame before hot roll bonding. Areas that will need investigation are the propensity for blistering due to additional tolerances for fitup and the shape of the fuel zone ends.

The June 1989 core calculations for radial and axial grading and a nominal meat thickness of 0.711 mm (28 mils) yield a fuel concentration of 1.37 kg U/L. For  $U_3Si_2$  this is a loading of 1.47 kg/L or 13.2 volume %. This loading fabricates with <1% voids, so the aluminum volume will be ~87%. This low volume fraction of fuel eases several fabrication problems including overall meat thickness uniformity and meat-end thickening (dogboning) during rolling. A large improvement in meat thermal conductivity from the 60 W/m·K envisioned for the highest proposed loadings up to 160 W/m·K for the 13.2 volume % loadings will lower the centerline temperature somewhat. (The affect is not large since most of the temperature drop is over the oxide coating on the plate surface and the oxide-water interface.) The low fuel volume fraction should also improve the mechanical stability of the fuel plates during irradiation.

## 2.2.2 HFIR Target Capsule Irradiation Tests

The first capsule for irradiation testing in the target region of HFIR was completed on schedule in March 1989. The capsule is now awaiting a "normal" cycle for irradiation in HFIR. The capsule contains 18 separate fuel holders each containing two fuel samples. The fuel samples are extremely small mixtures of fuel particles in aluminum powder to minimize heat generation in this extremely high thermal flux. The test consists of  $U_3Si_2$  at planned temperatures of from 250 to 425°C and relative fission rates of 0.5 to 1.0. Additionally,  $U_3Si$  is included at two temperatures. The fuel modules have been completed for

the second capsule test. Final machining and loading into the capsule will await evaluation of the actual temperatures for the first test. This second test will include some  $UAl_2$ ,  $UAl_3$ , and  $U_3O_8$  since these may be viable backup fuels at the lower loadings of the new core.

## 2.2.3 Fuel Performance Modeling

Excellent progress has been made on analytical modeling of the performance of  $U_3Si_2$ -Al fuels as a function of irradiation conditions. The model is expected to be able to track swelling and mechanical behavior as well as changes in the thermal conductivity during irradiation under normal and operational transient conditions. The model has currently been fit to the data generated by the RERTR Program.

## 2.2.4 Simulation of Irradiation Damage By Ion Bombardment

One area of concern is that the high fission rates in the ANS will change the basic irradiation behavior of the fuel particles (e.g., by making the fuel amorphous) and thus make extrapolations invalid. Extremely high rates of damage can be achieved by ion bombardment to study this effect. Preliminary results this year have shown that under very high rates,  $U_3Si_2$  does become amorphous. More work is needed to determine the behavior under damage rates similar to those of the ANS.

## 2.2.5 Fabrication Development

Work this year has shown that using multiple compact meats in fuel plates is a potentially viable method of achieving fuel gradients. The preferred method of varying meat thickness is used successfully in HFIR in the radial direction but has yet to be verified as feasible in the axial and radial directions

simultaneously. Work is currently under way on this concept. Low-deformation methods (i.e., hot-isostatic-bonding) of plate bonding are also feasible for 6061 aluminum alloy but are very difficult. The lower volume fractions envisioned for the new core will probably obviate the need for low-deformation methods of bonding.

## 2.3 CORROSION LOOP TESTS AND ANALYSES

The ANS reactor core will be composed of an array of aluminum-alloy-clad fuel plates immersed in high-velocity heavy water. As the heat from the nuclear fuel passes through the thin cladding into the water, the high thermal conductivity of aluminum and the high heat transfer coefficient governing heat flow from the plate to the water combine to keep the temperatures in the fuel plate at reasonable levels.

It has been found previously, however, that the exposure of aluminum and many aluminum alloys under such conditions typically leads to the growth of an adherent oxidation product separating the fuel plate from the cooling water. At the anticipated high heat flux levels for the ANS core, the presence of this low-thermal-conductivity film may interfere with heat flow and, in certain instances, lead to excessive heating of the fuel plate. The earlier ORNL aluminum corrosion program,<sup>4,5</sup> associated mainly with the HFIR and ATR Projects, resulted in a detailed description of the basic features of the aluminum-water reaction for high heat flux conditions as well as the development of a widely-used, empirical data correlation that described the growth of the product corrosion layer for a comparatively narrow range of experimental parameters in terms of a single system temperature. Since most ANS thermal-hydraulic parameters are outside the range considered by that correlation, additional information, a more extensive data base and, ideally, a modified or new correlation are

required. Thus, the present task was created to investigate the corrosion of aluminum alloys under ANS thermal-hydraulic conditions and thence to establish its effect in defining operating constraints and core lifetime. Specifically, the basic objectives of the corrosion test program are to ensure that excessive fuel and clad temperatures due to corrosion product buildup do not occur during the lifetime of the ANS core and to ensure that the corrosion/erosion processes do not compromise the structural properties and containment capabilities of the fuel cladding. Because of its long history of satisfactory performance as a fuel cladding in experimental reactors, 6061 Al is the present choice for the ANS, and our main series of experiments focuses on this alloy.

### 2.3.1 The Corrosion Test Loop

The Corrosion Test Loop facility, described in earlier reports,<sup>6,7</sup> has been in virtually continuous operation since its installation and checkout in January 1988. Briefly, the test facility is a forced-flow water loop fabricated entirely of 304 L stainless steel components, capable of pressurized operation to 7 MPa and water flows to 2 L/s. The specimen consists of an aluminum alloy test section of partly rectangular cross section with an enclosed rectangular flow channel that is the same width as that between ANS fuel plates. The specimen is surrounded by insulation and pressure backing, welded to large electrodes, and attached to the main section of the loop so that coolant velocities in the specimen channel up to 30 m/s can be achieved. The heat flux (up to  $\sim 20$  MW/m<sup>2</sup>) is produced by self-resistance heating of the specimen by means of a 30-kA dc power supply; downstream of the specimen, the heat is removed by a water-cooled heat exchanger. A low-pressure bypass (or cleanup) line, as in an actual reactor system, provides instrumentation and equipment for maintaining suitable water chemistry within the loop.

The outer surface of the main section of the specimen is instrumented along its central axis with ungrounded, stainless-steel-sheathed (0.5-mm), type N thermocouples. Seven thermocouples are arranged axially 25.4 mm apart on one side; three are located on the other side to provide additional measurements and comparisons. For a given level of electrical power supplied to the specimen and a given coolant flow rate, a temperature profile along the specimen is established. If the thermal-hydraulic loop parameters are then held constant, changes in the temperatures along the specimen can be related quantitatively to the buildup of oxidation products at the specimen-coolant interface. At the high heat fluxes involved in this work, temperature increases from this source in excess of 100°C are not uncommon.

Fabrication of a "test section" for each loop test requires precision electron beam (EB) welding of the two prepared specimen halves followed by conventional TIG welding of the specimen to the massive electrodes. Procedures for accomplishing the welding, instrumentation, and other assembly steps have been developed and improved throughout the report period.

The loop operates under computer control of the electrical and coolant flow parameters, including various safety features. The associated data acquisition system (DAS) records all temperatures, pressures, flow rates, power levels, and water properties at designated time intervals. While, in principle, the test loop and its support equipment are uncomplicated, integrated operation at the required performance level has required continuous attention as well as repair and improvement of several components. While several pump-related difficulties have been troublesome, considerable time and effort have also been expended on the measurement and control of the pH and conductivity of the coolant water in the loop.

## 2.3.2 Corrosion Tests

The previous experimental efforts at ORNL<sup>2,3</sup> examined the corrosion behavior of several aluminum alloys in flowing pH 5 to 7 water under heat transfer conditions. For heat fluxes from 3 to 6 MW/m<sup>2</sup> and coolant flow rates from 10 to 15 m/s, the rate of growth of the corrosion product, boehmite (Al<sub>2</sub>O<sub>3</sub> · H<sub>2</sub>O), was independent of these parameters and appeared to be only a function of the boehmite-coolant interface temperature and the pH of the water. The assemblage of these data (the Griess Correlation<sup>5,8</sup>) has been widely used to predict the extent of corrosion under various reactor conditions.

The limited range of variables addressed in the earlier HFIR-related work required that supplementary experiments be performed under the more severe thermal-hydraulic requirements of the ANS core. Since the last project report,<sup>6</sup> which discussed the preliminary corrosion loop tests, 12 additional tests have been completed on 6061 Al under a range of heat flux and coolant conditions. In these tests, we have paid particular attention to the direct and indirect effects of high heat flux and coolant velocity on the corrosion rate and have also investigated the influence of coolant pH and coolant temperature. Table 2.4 presents the test schedule for this report period, the coolant conditions, and nominal values of the important thermal-hydraulic parameters associated with each test; several of these parameters vary with time and position along the specimen, and in these cases the average values at three positions are listed.

## 2.3.3 Analysis of Test Results

The ANS Corrosion Test Loop Facility provides the means to expose an aluminum

Table 2.4. Corrosion test loop: completed tests and parameters.

PARAMETERS	TEST NUMBER											
	CTEST3	CTEST4	CTEST5	CTEST6	CTEST7	CTEST8	CTEST9	CTEST10	CTEST11	CTEST12	CTEST13	CTEST14
STARTED	6/27/88	8/19/88	9/8/88	12/13/8	1/31/89	3/7/89	3/28/89	4/13/89	5/3/89	6/27/89	7/19/89	8/10/89
COMPLETED	6/30/88	8/24/88	9/22/88	12/23/8	2/23/89	3/23/89	4/7/89	4/25/89	5/18/89	6/29/89	8/02/89	8/31/89
TIME (DAYS)	3	5	15	9	23	14	10	12	15	3	14	21
PH	6.0	5.0+	5.0	4.5	5.0/4.5	5.0	5.0	5.0	5.0	6.0	5.0	5.0
CONDUCTIVITY (uS/M)	140	400+	460	1250	500-1500	500+	500	500	550-	140	600	600?
INLET TEMP (°C)	80	79	75	80	80	43	57	39	39	80	67	49
VELOCITY (M/S)	27.1	27.7	12.8	24.2	24.2	25.4	25.5	25.5	19.2	28.0	27.8	25.6
AV. POWER (KW)	42.0	41.6	19.0	41.8	41.8	42.0	43.0	56.0	42.4	43.0	37.7	22.3
HT. FLUX (MW/M <sup>2</sup> )												
AVERAGE	11.6	11.6	5.3	11.6	11.6	11.7	12.0	15.7	11.9	11.9	10.6	6.2
POS. 2	11.3	11.0	5.2	11.4	10.9	11.3	11.4	14.5	11.6	11.4	10.1	6.2
POS. 4	11.6	11.5	5.3	11.6	11.5	11.7	12.1	15.5	11.9	11.8	10.6	6.2
POS. 6	12.0	12.5	5.5	12.0	12.4	12.1	12.7	17.2	12.3	12.4	11.1	6.2
COOLANT (°C)												
POS. 2	83	83	79	84	84	47	61	45	44	84	71	51
POS. 4	90	90	85	93	91	56	70	56	55	92	78	56
POS. 6	96	97	92	101	99	64	78	67	66	99	84	60
INTERFACE (°C)												
POS. 2	147	146	136	156	146	127	136	146	147	148	131	96
POS. 4	155	154	143	164	156	135	146	158	155	156	139	99
POS. 6	163	165	150	173	168	143	156	175	165	166	147	103
FE-RICH LAYER?	NONE	NONE	LIGHT	HEAVY	HEAVY	LIGHT	LIGHT	HEAVY	HEAVY	NONE	SLIGHT	SLIGHT
OXIDE PRODUCT (> GRIESS?)	YES	YES	SAME	NO	NO	NO	YES	NO	NO	YES	YES	NO
SPALL AT TE-6?	YES	YES	NO	NO	YES	NO	YES	YES	NO	YES	NO	NO

surface to rapidly flowing coolant under heat transfer conditions. During a test, the electrical power generated in the specimen and the coolant conditions are generally held constant so that *changes* in temperature of the specimen (at its insulated side) primarily result from the growth of the corrosion product at the metal-coolant interface. While these changes, per se, are important observations because they imply similar increases in the fuel temperature in the ANS core, they are also useful in obtaining the oxide thicknesses and growth kinetics through established thermal-hydraulic calculations. Certain results and implications of these calculations can be checked by observations and measurements on the reacted specimen surface at the completion of the experiment.

### 2.3.3.1 Measurements and Calculations

The electrical heat generated in the aluminum and rejected to the coolant results in both normal and axial temperature gradients within the specimen. While a relatively steep gradient exists across the specimen to the coolant, the temperatures also increase uniformly from the coolant inlet end to the exit. Thus, the temperature dependences of the physical properties of the 6061 Al must be considered in all calculations. An important consequence of the axial gradient is that (for a constant average power) the heat flux increases at the hot end and decreases at the cooler end. As the reaction products thicken more rapidly at the hotter end, the range of heat flux over the specimen in-

creases during an experiment. Only at a position near the axial midpoint will the heat flux remain essentially constant for the complete test.

Despite these complexities, it is possible in principle to utilize the continuous measurements of specimen temperatures and the controlled loop parameters to calculate the growth rates of the corrosion products along the specimen and to correlate these rates with the local conditions. Several computational schemes have been examined,<sup>9</sup> and two computer programs (still in development) are now in use. The programs, OXCAL and ANSDAT, were written completely independently, but exhibit satisfactory agreement in the computed quantities.

### 2.3.3.2 Summary of Corrosion Loop Experimental Results

It is not the intent of this report to discuss the individual experiments in detail. However, to supplement the information in Table 2.4 and to summarize the status of our investigation, a brief general account of the basic results and their significance is given below.

(1) In virtually every experiment, the temperature increase of the specimen at each point along its central axis (and the calculated product film thickness) increased at a slightly decreasing rate that was eventually recognized to depend on several of the system variables. In experiments exhibiting comparatively high rates of film growth or ones allowed to run for sufficiently long periods of time, partial spallation of the film was eventually initiated at the hotter end of the specimen that resulted in a perturbation of the local heating. To provide for more complete postexperiment examinations, the tests were terminated before spallation had progressed over the entire specimen length.

An example of this behavior is shown in Fig. 2.2, which depicts the oxidation rate curves calculated for three points along the

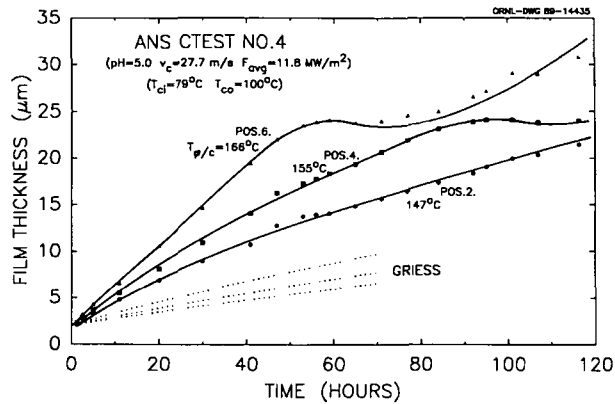


Fig. 2.2. Film growth on 6061 Al for CTEST No.4 at the three reference positions on the specimen.

specimen for CTEST No. 4. (Positions 2, 4, and 6 are located 50 mm apart about the axial midpoint along the specimen's 150-mm active length.) The conditions of the experiment and the local parameters are listed in Table 2.4 and on the figure. The parameters include the coolant velocity ( $v_c$ ), average heat flux ( $F_{avg}$ ), inlet and outlet coolant temperatures ( $T_{ci}$  and  $T_{co}$ ), local coolant temperature ( $T_c$ ), and oxide-coolant interface temperature ( $T_{\phi/c}$ ). The rates of film growth are measurably higher than those predicted by the Griess Correlation for these oxidation conditions. Spallation was observed at Position 6 and 4 after about 60 and 100 hours, respectively, when the apparent thickness of the film approached 25  $\mu\text{m}$ . CTEST No. 3, conducted under similar heat flux and coolant conditions except at pH 6, produced comparable behavior but with even more rapid reactions. However, CTEST No. 5, carried out under less-severe heat fluxes and coolant velocity, produced lower rates having reasonable agreement with the Griess Correlation. X-ray identification of the films on the reacted Al surfaces indicated that the major product was boehmite or "pseudo-boehmite," a poorly crystalline or microcrystalline form.

(2) CTEST No. 6 showed that the corrosion rates were dramatically reduced even at

higher heat fluxes by controlling the pH of the coolant to 4.5 rather than 5.0. CTEST No. 7, where the coolant pH was switched several times during the experiment between these two values, confirmed the effectiveness of the pH 4.5 water in slowing the oxidation reaction even after an initial, rapid-rate excursion at pH 5. While there was a tendency for a degree of "reversibility" in the rate when the pH was increased from 4.5 to 5.0, it was very sluggish. In addition, the posttest appearance of these specimens was characterized by a straw-reddish-brown film that increased in intensity from inlet to outlet end. This film, shown to be mainly an iron-rich layer on the outer surface of the boehmite, appeared to function as an efficient diffusion barrier thus reducing the rate of reaction. Its location solely on the outer surface further suggested that the primary mechanism of boehmite growth was anion diffusion.

(3) To initiate a series of tests appropriate for certain ANS core-specific applications, CTEST No. 8 was conducted at pH 5 with heat fluxes and coolant flow comparable to previous tests, but with the coolant inlet temperature adjusted to give lower local coolant temperatures. Perhaps surprisingly, the rates of film growth were very low, even lower than those predicted by the Griess Correlation. The test was terminated after 14 days with the average film thickness at the hot end of the specimen remaining  $< 10 \mu\text{m}$ . Significantly, a pronounced iron-rich barrier layer was found on the specimen unlike, for example, CTEST No. 4 where no layer was observed and the film growth rates were high.

CTEST No. 9 provided a followup to CTEST No. 8 with the same heat flux and coolant velocity, but with higher (intermediate) coolant temperatures. The observed temperature increases and layer growth were more rapid in this instance, even slightly higher than the Griess Correlation predictions, and the test was terminated at 10 days after spallation was indicated at the hot end

of the specimen. Only a very slight visual indication of the barrier layer was observed on the unspalled film.

(4) CTEST No. 10 was designed to provide further documentation of the significant influence of the coolant temperature that had become evident from the previous tests. This experiment was conducted under the lowest inlet coolant temperature currently attainable in the loop,  $39^\circ\text{C}$ . However, to bring the interface temperatures more in line with previous experiments with higher coolant temperatures, a higher average heat flux was imposed, over  $15 \text{ MW/m}^2$ . Figure 2.3 shows the progress of this experiment in terms of the calculated film thicknesses at the three reference thermocouple (TC) positions. The changes noted above in the interface temperatures and heat fluxes along the specimen are also listed in the figure. At the high power levels of this test, the highest so far, the redistribution of the (constant) average power within the test specimen was comparatively large. For example, 64 hours into the test, the local heat flux variation from TC position 2 to TC position 6 (across the central 100 mm of the specimen) was 14.8 to  $16.1 \text{ MW/m}^2$ ; by the end of the test, it had increased to 13.3 to  $17.8 \text{ MW/m}^2$ . Despite the higher heat fluxes and interface temperatures, the reaction rates were still slightly lower than those predicted by the Griess Correlation. The test was terminated after 12 days, and the specimen exhibited a heavy barrier layer with spallation and severe internal reactions in the hotter third.

An additional test of the strength of the coolant temperature as a variable was conducted in CTEST No. 11 where the heat fluxes and interface temperatures of CTEST No. 4 were duplicated by using lower coolant temperatures but with lower coolant velocity. Despite the equivalence of the former principal variables, the rate of film buildup in this experiment was much less; the iron-rich barrier layer was also present.

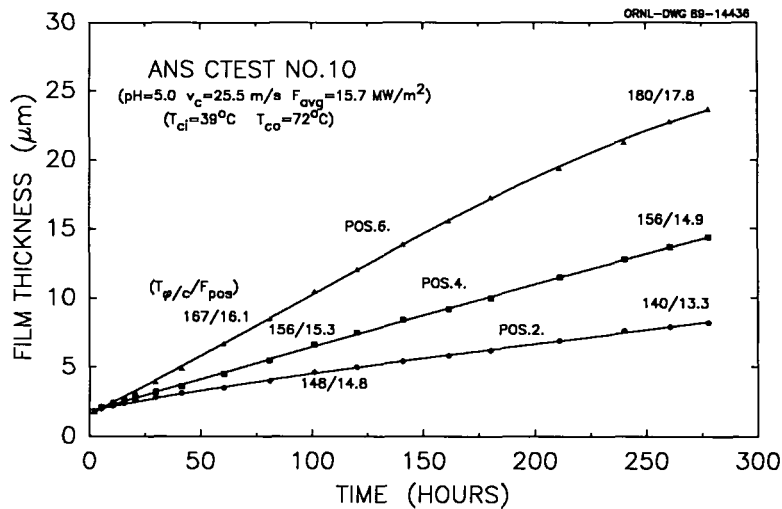


Fig. 2.3. Film growth on 6061 Al for CTEST No.10. The interface temperatures and local heat fluxes near the beginning and end of the test are shown for each position.

At this point in the test sequence, it was apparent that several parameters were contributing to the oxidation behavior and that both negative and positive deviations from the predictions of the Griess Correlation (which, for a given pH depends only upon the inter-

face temperature  $T_{\phi/c}$ ) had been observed, depending upon the coolant temperatures and heat flux. For example, Fig. 2.4 shows rate curves from four different experiments with approximately the same interface temperature at their respective positions on the specimen.

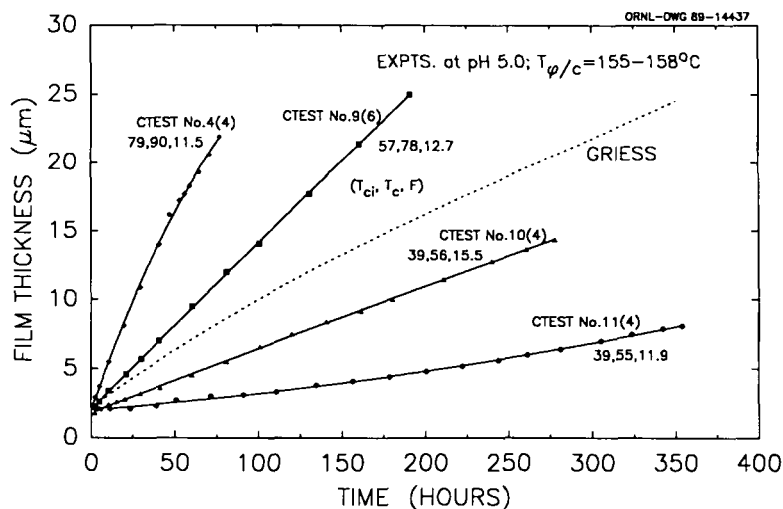


Fig. 2.4. Film growth observed during CTESTS for specimens having near-identical interface temperatures,  $T_{\phi/c}$ . The specimen position for a given experiment is noted in parentheses; coolant temperatures and heat fluxes are listed as indicated.

Compared to the Griess Correlation, a wide range of experimental observations exists. Certainly, the Griess Correlation should not be (nor was it intended to be) used outside the range of data upon which it was based.

(5) As intended, CTEST No. 12 essentially reproduced the results of CTEST No. 3, displaying rapid oxidation rates without the presence of the barrier layer. Thus, with the exception of CTESTS Nos. 3, 4, and 12, all of the reported tests had yielded varying amounts of the iron-rich "barrier layer" on the outer surface of each specimen. The decreased rates (and other characteristics) of oxide growth in these experiments seem to be directly related to the extent of this layer, which from our experimental evidence is clearly influenced by pH and by the coolant temperature—in the specimen and in the rest of the loop.

The basis of CTEST No. 13, was to provide a more direct inquiry into the apparent effectiveness of the coolant inlet temperature  $T_{ci}$  as an important "independent" variable affecting barrier layer formation and aluminum corrosion in the loop experiments, as previous tests had suggested. The conditions of this experiment were set up so that the

local coolant temperature  $T_c$ , local heat flux  $F$ , coolant velocity  $v_c$ , and interface temperature  $T_{\phi/c}$  at TC position 6 were all nominally identical to those of CTEST No. 4 at TC position 2. This was done by decreasing the inlet coolant temperature to 67°C, about 12°C lower than that for CTEST No. 4. The comparison is presented in Fig. 2.5, which is regarded as further evidence that the coolant inlet temperature is at least one of the parameters important in determining corrosion effects. Of course, it should be recognized that this temperature is representative of that in contact with the stainless steel piping of the loop circuitry.

(6) The awareness of the coolant inlet temperature as an important contributor to the film growth characteristics has added still another parameter to our experimental system that must be considered for the ANS. Moreover, the stipulation of the inlet temperature clearly restricts our ability to duplicate all the (apparently important) ANS thermal-hydraulic parameters in the Test Loop. For the present Loop configuration, we must operate within this limitation and devise experiments both relevant to ANS operation and to the evaluation of various system parameters.

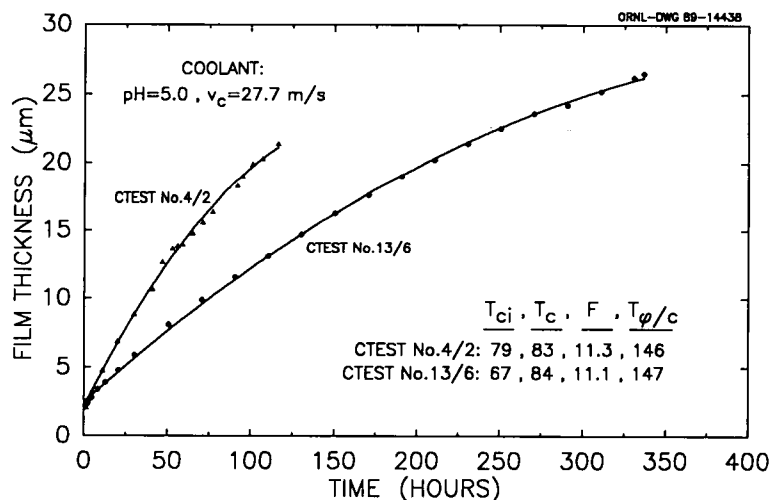


Fig. 2.5. A comparison of film-growth data illustrating the importance of the coolant inlet temperature,  $T_{ci}$ , as an "independent" variable.

CTEST No. 14, using an ANS-related  $T_g=49^\circ\text{C}$ , an average heat flux of  $6.3 \text{ MW/m}^2$ , and a coolant velocity of  $25.4 \text{ m/s}$ , furnished a basis data set appropriate to the near-inlet parts of the core for average heat flux conditions. Very slow film growth was observed for these conditions, and the experiment was terminated only after 21 days.

(7) The physical, chemical, and structural characterization of the product film found on the reacted specimens is being undertaken by several techniques, and only a cursory description will be given here. To date, on various specimens, we have employed standard metallographic procedures, scanning and transmission electron microscopy (SEM and TEM), X-ray structural analysis, energy dispersive X-ray analysis (EDX), and electron microprobe analysis. Simply, for rapidly growing films (without the iron-rich layer), the product is generally a film of very uniform thickness, virtually transparent to the naked eye, and identified as boehmite (from thicker, hotter parts of the specimen) and/or pseudo-boehmite (from the thinner, cooler regions). No other form of oxide or hydrated oxide has been identified as a prevalent reaction product. For slowly growing films (with the iron-rich layer, sensitively detected by the eye as a straw coloration), the films are sometimes quite irregular on a fine scale in thickness, particularly in their early stages of growth. A positive identification has not yet been made for films in this condition, but they appear to be mainly pseudo-boehmite. The iron-rich layer was found by EDX and electron microprobe work to be limited to the outer 5 or 10% of the film. It is comprised not only of iron, but has lesser amounts of chromium and silicon, all occupying the outermost regions. Additional analyses will be required to define the chemical and structural species involved, but the film may well be an Fe-Cr oxide of some sort rather than a Fe-Cr enriched boehmite.

The fact that the iron, chromium, and silicon congregate on the outer surface with

none being observed in the inner portions of the film suggests that the source of these metals is not the aluminum alloy itself, but some other component of the loop system. The lack of mixing of this layer also is consistent with the premise that the mechanism of oxidation is one involving anion diffusion, perhaps of oxygen or hydroxyl ions, within the boehmite. The mechanism by which iron and chromium are transported from the stainless steel sections of the loop by the flowing coolant is largely speculative and must address the fact that the iron concentration in the cooling water is consistently  $<20 \text{ ppb}$ .

(8) Spallation of the boehmite from exposed 6061 aluminum alloy specimens was observed for several tests, both for films with and without the iron-rich overlayer. From our experimental temperature measurements during the tests, spallation was observed to occur when the calculated film thicknesses were between  $\sim 23$  and  $28 \mu\text{m}$ , corresponding to temperature drops across the films of  $\sim 120$  to  $160^\circ\text{C}$ . Griess' earlier work<sup>5</sup> reported spallation for several alloys at  $\sim 50 \mu\text{m}$  for lower heat flux and coolant velocity, so that roughly the same temperature drops were involved. There are several mechanisms by which mechanical stresses in a growing oxide film may increase to the point where spallation occurs, and the precise manner by which the heat flux or temperature gradient leads to the observed influence on this process is not presently obvious. A hypothesis by W. R. Gambill<sup>10</sup> has considered elastic stresses to arise as a consequence of the temperature gradient, arriving at a critical oxide temperature drop rather than a critical oxide thickness for spallation.

Metallographic inspection of cross-sections of such specimens revealed severe attack within the metal underlying the spalled film. The depth of the reaction zone, which seemed to be composed of oxide material and perhaps voids (or bubbles) located on grain boundaries and within the metal grains, in several instances exceeded  $0.2 \text{ mm}$ . Similar

behavior in ANS fuel cladding would be unacceptable. No internal reaction zones were observed beneath unspalled films, even when examination by TEM was accomplished, thus implying that these features were a result of spallation rather than the cause.

(9) The new data accumulated from the Corrosion Loop experiments have shown clearly that several system parameters are affecting the corrosion characteristics of 6061 Al. While higher heat fluxes, interface temperatures, and oxide temperatures are all associated with more rapid film growth, lower coolant pH and lower coolant temperatures (both within the test section and in the remainder of the loop) lead to lower rates of film growth, apparently through the promotion of an iron-rich barrier layer that forms on the outer surface. Our present effort is thus directed to an increased understanding of the product layer growth behavior, particularly the occurrence and influence of the barrier layer; in addition, our experiments are being conducted under core-specific conditions that have direct significance to ANS and will also contribute to the data base from which a new rate correlation will eventually arise.

### 2.3.4 The Corrosion Workshop

The ANS Aluminum Cladding Corrosion Workshop was held at the Idaho National Engineering Laboratory in Idaho Falls, Idaho, on November 16 and 17, 1988, to (1) develop suggestions and directions to support the experimental program for the ORNL-ANS Corrosion Test Loop Facility, (2) define gaps in present knowledge, and (3) make suggestions concerning additional R&D needed to support ANS design and operation. The Workshop had 27 attendees representing 8 organizations throughout the country. A report summarizing the proceedings and conclusions of the Workshop has been published.<sup>10</sup>

## 2.4 THERMAL-HYDRAULIC LOOP TESTS

To characterize the thermal-hydraulic performance of the ANS reactor, key parameters and/or the accuracy of their predictions must be known. This task will include the measurements and the analysis necessary to validate computer models that, in turn, will be used to assess the capability for forced and natural convection under estimated hot channel conditions.

### 2.4.1 Test Loop

Test parameters that will be measured in the thermal-hydraulic test loop are (1) friction factor (pressure drop), including possible roughness effects and heat flux dependence; (2) non-boiling heat transfer coefficients; (3) thermal conductivity of cladding, including oxide thickness variations; and (4) incipient boiling and burnout (critical) heat fluxes.

The majority of the tests will be made using light-water coolant; however, at an appropriate time, the loop will be converted to a heavy-water system, and the data obtained for the light water will be systematically confirmed. The experimental data will provide the basis for validation of computer codes that will be used in the design of the ANS.

### 2.4.2 Schedule

Design and construction are scheduled to begin in March 1990 with operational testing in October 1990. These dates are dependent on the final reference core design being fixed in February 1990.

## 2.5 REACTOR CONTROL CONCEPTS

Significant progress has been made during this report period toward the development of a reactor control concept that integrates the best features of various control options. Four specific activities are discussed in the remainder of this section. These four activities provided the information needed to define what appears to be a workable control concept for the ANS.

### 2.5.1 Control Blades vs Control Rods

Both plate and rod geometries were considered for the poison assemblies used to control the ANS reactor core. In each case it was determined that we would be limited to four assemblies since there is only room for four scram lines in the central hole region of the core. From a mechanical design perspective, it was also determined that the rod geometry would be easier to design than the blade geometry (better stability, less structure required, etc). However, it was felt that the worth of a rod system might be less than that of a blade geometry and thus might not provide adequate reactivity control. Therefore, a study was undertaken to examine the relative negative reactivity worth of rod vs plate control geometry.

Two-dimensional ( $r$ ,  $\theta$ ) calculations were performed since the rod geometry can not be represented in the normal  $r$ - $z$  geometry models. The lack of the third dimension ( $z$ ) considerably affects the absolute worths of the poison but it was felt that the relative worths would be reasonable representations of the potential differences in the two geometries. The blade geometry consisted of 7-mm-thick hafnium plates placed around the perimeter of the central hole at 98 mm. To simplify the model, the hafnium rods were simulated by a circular trapezoid shape rather

than a true circular shape and were symmetrically located in the central hole region. The surface area of the rods was  $\sim 14\%$  higher than that of the plates but the same amount of hafnium was loaded into each geometry.

The results of the analysis indicated that the plate geometry could provide as much as 19% higher worth than the rod geometry. However, it was determined that both geometries provided adequate poison capability and therefore no effective worth penalty was associated with choosing a rod geometry. The decision was thus made to use a rod geometry in the reference control concept.

### 2.5.2 Scramming Up vs Scramming Down

The central hole control rods perform two functions: (1) maintain criticality control and (2) provide rapid reactor shutdown or scram if normal operating conditions are exceeded. The question was raised as to whether it would be best to move the rods out of the core from the top during normal operation and scram down (the normal arrangement for a pressurized-water reactor) or move the rods out of the core from the bottom and scram up. The advantages of the down-scram were that we would be scrambling with gravity and possibly eliminating certain classes of rod ejection events. The up-scram concept was considered because we would be scrambling with flow, involving a simpler structure, and minimizing expected irradiation damage to the scram springs. A study was initiated to examine the neutronics behavior of each approach to see if any overriding effects would decide this issue.

The neutronics analysis indicated a distinct advantage for flattening the power distribution with the down-scram geometry. Without any control there is a higher average power density in the upper element. This power tilt is further skewed when the control rods are operated in the lower element of the

core as in the up-scam geometry. When the rods are operated for most of the cycle in the upper element (down-scam configuration), the initial power tilt is shifted away from the upper element so that the average power densities are approximately the same for both elements. In addition, with the down-scam condition the peak heat flux was moved toward the core inlet (the preferred location) for most of the cycle.

Another factor that favored the moving-up/scramming-down configuration was the incremental worth of the rod during normal full-power operation. Near the EOC when the reactivity worth per millimeter of movement of the rods is at its lowest, the differential worth of the rods in the down-scam geometry was about 25 to 35% higher than that obtained for the up-scam geometry. Thus, for a given acceleration of the rods during scram, the down-scam geometry would take less time to provide a particular negative reactivity insertion that, in certain scenarios, would be a significant safety advantage.

As a result of this analysis, the decision was made to move the rods up and scram down in the reference core geometry. Work was then initiated to provide engineering solutions to the potential problems, as identified earlier, that are associated with the down-scam.

### 2.5.3 The Use of Burnable Poison

The project has always planned to use burnable poison to control some of the excess reactivity associated with the ANS core. Burnable poison has been used in the HFIR and ILL reactors with great success, and it offers several advantages:

1. It would be a fixed part of the fuel plate so that it cannot accidentally be withdrawn.
2. Since it is a fixed part of the fuel plate, it reduces the reactivity levels that must be dealt with in storing, shipping, and loading fresh cores.

3. It can be placed at specific locations in the fuel plates to help flatten the power distribution.

Unfortunately, there is a limit as to how much reactivity we can control using burnable poison. If we put too much burnable poison in the system, it cannot be burned up over a 14-day core life, and we end up with a reactivity penalty due to the residual poison. In analyses for earlier core geometries, a maximum of about one-fourth of the excess reactivity was controlled by the burnable poison. Following the completion of the preconceptual core design studies, a more extensive analysis of the use of burnable poison was performed.

The effects of  $^{10}\text{B}$  as a burnable poison were calculated for the final preconceptual core design, assuming that the  $^{10}\text{B}$  is located in the end caps (top and bottom 10 mm or the fuel element). It was felt that by locating the poison in the end caps the power peaking effects associated with the ends of the elements would be reduced and would thus lead to a flatter power distribution for the core. In the initial analysis of the final preconceptual core, the same amount of boron was placed in each end cap and various total boron loadings were examined.

The initial analysis indicated that 13.44 g of  $^{10}\text{B}$  could be loaded and be used to control as much as half of the excess reactivity without much end-of-life penalty (0.088 g residual  $^{10}\text{B}$  at end-of-life). It was determined that locating the boron in the end caps did reduce the peaking effects, and thus a flatter power distribution was produced. However, it was found that putting the same amount of boron in each end cap was not an efficient approach. Since the worth of the boron was different at each end cap, the desired shift in the peak heat flux was not attained. In a later analysis 3.35 g of  $^{10}\text{B}$  was placed in both end caps of the upper element, while 4.47 g and 2.23 g were respectively placed in the top and bottom end caps of the lower element. Essentially the same level of excess reactivity

was controlled with a much better shift in the power distribution. An interesting and somewhat unexpected result was that the boron burned up at about the same rate as the excess reactivity over the first half of the cycle. As a result, indications are that there would be little movement in the control rods over the first half of the cycle.

## 2.5.4 Control Rod Positions During the Cycle

As part of the control concept evaluation, we wanted to examine the position of the rods as a function of time in the cycle. It was found that as we proceeded with the fuel grading exercise to flatten the power distribution, we changed the position of the rods since fuel grading changes affected the reactivity balance. However in general, we found that at beginning-of-life the rods would be about 3/4 withdrawn so that the bottom of the rods would be 140 to 150 mm above the top of the lower fuel element. At this position the rods are expected to have a differential worth of  $\sim 25$  to 35 pcm/mm. At end-of-life the bottom of the rods would be located  $\sim 10$  mm above the top of the upper element where we reach our minimum differential worth of 8 to 10 pcm/mm. This value is similar to those for the control rod in ILL and is expected to be adequate. This task will provide more specific results when the fuel grading and power distribution over the cycle become better defined.

## 2.6 CRITICAL AND SUBCRITICAL EXPERIMENTS

This task has not been initiated. However, some work has been done to examine the timing of these tasks within the context of the ANS Project and the reactor core development. In the present R&D program a preliminary critical and subcritical experiment plan would be developed over the last half of

FY 1990. This would be followed by approximately a year of preanalysis of the experiments planned and discussion with facility personnel to produce a final experiment plan. The experiments would then start around the beginning of FY 1993 and are expected to last for about a year. Items that we would like to evaluate with these experiments include core reactivity, core power distribution, voiding effects, rod worths, effects of objects in the reflector, startup, and shutdown. Analysis of the experiments would proceed into 1994 and provide input to the final core geometry decision scheduled for late 1994. Additional critical and/or subcritical experiments beyond this schedule may be necessary but have not yet been defined.

The location for performing these experiments has not been identified at this time. However, some conversations have been held with Los Alamos National Laboratory and Argonne (West) National Laboratory. It is our hope that a location for these experiments can be identified by the end of FY 1990.

## 2.7 MATERIAL DATA, STRUCTURAL TESTS, AND ANALYSIS

Long-term successful operation of the ANS requires research in several areas to ensure structural adequacy because of the extremely high neutron fluence and the high coolant flow rates. Work during this report period has focused on three primary areas: (1) core pressure boundary tube (CPBT), (2) fuel plate stability, and (3) characterization of irradiated 6061-T651 aluminum. Progress in each of these areas is discussed in the following sections.

### 2.7.1 Core Pressure Boundary Tube

The CPBT concept employs a primary pressure containment that is of just sufficient

diameter to envelop the reactor core. This allows the surrounding reflector vessel, which contains the various guide tubes and beam tubes, to operate at a relatively low pressure.

After careful consideration of candidate materials, 6061-T651 aluminum was selected as the material for use as the CPBT. Traditional iron-based materials such as SA-533 grade B steel and type 304 stainless steel were eliminated because they would absorb too many neutrons. Zircaloy-4 received strong consideration because of its outstanding nuclear characteristics, but it could not be kept cool enough because of its relatively low thermal conductivity. Although 6061-T651 aluminum is not currently accepted by the *ASME Boiler and Pressure Vessel Code* for Class 1 nuclear construction, it is believed that the service experience in high flux reactors and the existing large data base mechanical properties can be used to obtain its acceptance. An inquiry to the ASME Code Committee concerning use of 6061-T651 aluminum for Class 1 nuclear construction is being prepared. A preliminary fatigue design curve has been constructed for consideration by the ASME Code Committee.

A major consideration other than ASME Code acceptance is how often the CPBT will have to be replaced. The primary limit on CPBT lifetime is expected to be irradiation embrittlement. As discussed in a later section, a major irradiation program is planned to provide data required for estimating the loss of fracture toughness caused by irradiation. The corrosion of aluminum produces a low thermal conductivity layer that is another potential limit on the CPBT lifetime because of the resultant temperature increase.

## 2.7.2 Fuel Plate Stability

Structural stability of arrays of parallel fuel plates with coolant flowing through them has been a problem of intense interest to reactor designers for many years. Analytical treatments of the problem have been published<sup>11-13</sup> as well as experimental studies on

flat plates.<sup>14-17</sup> The primary basis currently being used to evaluate the stability of the ANS involute fuel plates is the Miller approach using detailed, finite element analysis to determine the deformed shape of the involute plates. As a check on the Miller approach, a new analysis method was also developed that employs a bounding assumption that the velocity of the fluid is converted to dynamic pressure on one side of a plate. Analytical predictions indicate that the January 28, 1989, ANS reference core may not have sufficient margin between the planned flow velocity of 27.4 m/s and the calculated critical flow velocity. Possible fixes include decreasing the annular radius of the fuel elements by ~20% with a corresponding increase in length, putting a spacer between the fuel plates, changing the shape of the plate from an involute to a more uniform curvature, and decreasing the coolant velocity.

Although the analytical methods have been demonstrated to compare well with tests on arrays of flat plates, they have not been benchmarked against test data on arrays of involute plates. Benchmark tests of arrays of aluminum involute plates and proof tests of complete dummy fuel elements are planned, but it will be some time before the extensive facilities required for such tests can be assembled. The flow rates and pressures required to ensure that plate instability can be reached are fairly large.

In the interim, the facility shown in Fig. 2.6 has been assembled in which a single involute plate made from epoxy can be tested. The lower modulus of elasticity of the epoxy compared to aluminum reduces the critical velocity so that modest flow rates and pressures are sufficient to produce plate instability. Results from this test will indicate the accuracy of the analytical methods.

## 2.7.3 Characterization of Irradiated 6061-T651 Aluminum

The irradiation program for determining the effect of irradiation on the mechanical

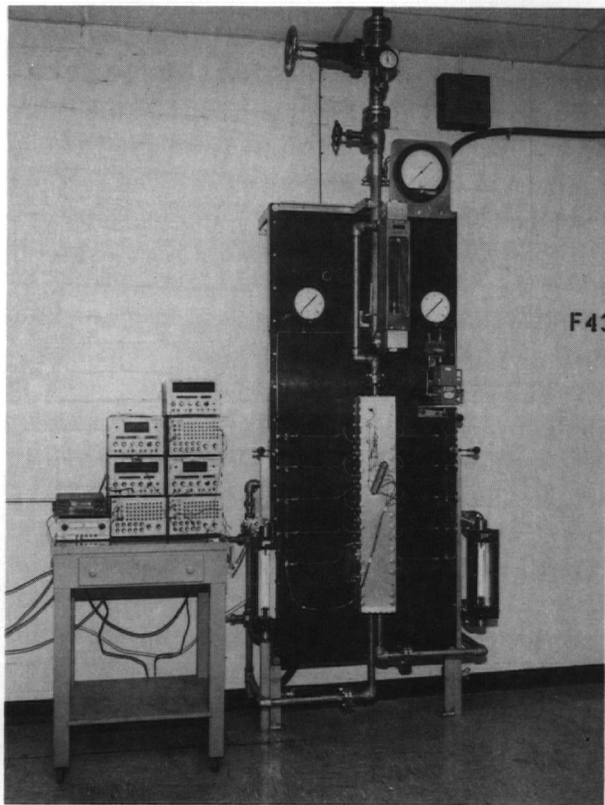


Fig. 2.6. Single epoxy involute plate test facility.

properties of structural materials for the ANS Project was planned. The principal project is the study of the effect of irradiation on 6061-T651 aluminum alloy, which has been selected for the CPBT, the reflector tank (RT), and possibly the cold source as well. Six capsules will be irradiated in the HFIR to study the response of base metal, weld metal, and heat-affected zone metal. Individual capsules will be irradiated to one of three different fluence levels ( $10^{25}$ ,  $10^{26}$ , and  $10^{27}$  n/m<sup>2</sup>). This maximum fluence represents  $\sim 6$  months of operation for the CPBT and  $\sim 30$  years for the reflector tank. Four capsules will contain material typical of the CPBT and will be irradiated at a thermal-to-fast neutron ratio of  $\sim 2$ , close to the predicted ratio for the CPBT. The other two capsules will be irradiated with as high a ratio of thermal-to-fast neutrons as possible. These capsules are in-

tended to provide data for the RT that will see a thermal-to-fast ratio of  $\sim 10^7$ . This thermal-to-fast ratio vastly exceeds that at any existing irradiation facility. Existing information on the effect of irradiation on the mechanical properties of aluminum alloys suggests that the thermal-to-fast neutron ratio may be very significant, with higher ratios resulting in increased degradation of properties. No irradiations for the cold source materials have been planned at this time because there is no practical way of irradiating, maintaining, and testing material at temperatures near that at which the cold source will operate [liquid deuterium (LD<sub>2</sub>) temperature]. Other materials that may require study, such as hafnium, have not been included to date.

Preliminary work has begun to measure the mechanical properties of 6061-T651 in the unirradiated condition, especially the fracture toughness. A 19.1-mm-thick plate of commercial 6061-T651 material was procured. The thickness of the CPBT (12.5 mm) is such that the toughness is expected to be thickness-dependent. Therefore, a range of specimen sizes has been machined, ranging in thickness from 6.4 to 19.1 mm. The irradiation facilities in HFIR make irradiation of standard rectangular specimens difficult. Therefore, circular, arc-shaped, and conventional rectangular specimens have been prepared to determine if specimen geometry affects the measured toughness values. These specimens have been prepared for testing in the laboratory. Specimens will be tested at room temperature to compare with available literature data on the fracture toughness and at 95°C, the approximate operating temperature of the CPBT.

## 2.8 COLD SOURCE DEVELOPMENT

The cold sources will be a very important part of the ANS facility. Present plans include locating two identical cold sources in the reflector region with the center of the

cold source at a point where the thermal flux is  $\sim 80\%$  of its peak value. Based on present concepts each cold source is expected to contain on the order of 4 kg of liquid and 4 kg of gaseous deuterium within the pressure boundary of the cold source. The majority of the work associated with the cold source development over this report period can be divided into four categories: (1) neutronics analysis, (2) thermal-hydraulics and testing program, (3) development of safety criteria, and (4) cold source instrumentation.

## 2.8.1 Cold Source Neutronics

Three aspects of the cold source neutronics work will be discussed in this section: model development, cavity effects, and  $\text{LN}_2\text{-LD}_2$  combined system option.

### 2.8.1.1 Model Development

Although we continue to believe that the optimal shape for the cold source may be

ellipsoidal in nature, most of the neutronics analysis is still performed with a spherical shape for the cold source since the ILL spherical cold source provides good data for benchmarking the methods development. Early in this report period, analysis problems were encountered with unreasonably high predictions of the thermal-neutron flux entering the neutron guides. This problem was traced to the way in which the core and cold source models were coupled and in the assumptions used in distributing the thermal flux into the many energy groups used in the cold source model. The interface between the core and cold source models was improved, and the correct Maxwellian distribution was used to distribute the thermal flux in the appropriate energy group structure. The resulting neutron leakage into the guides is given as a function of wavelength and compared with normalized Institut Laue Langevin (ILL) data in Fig. 2.7. As can be seen from this figure,

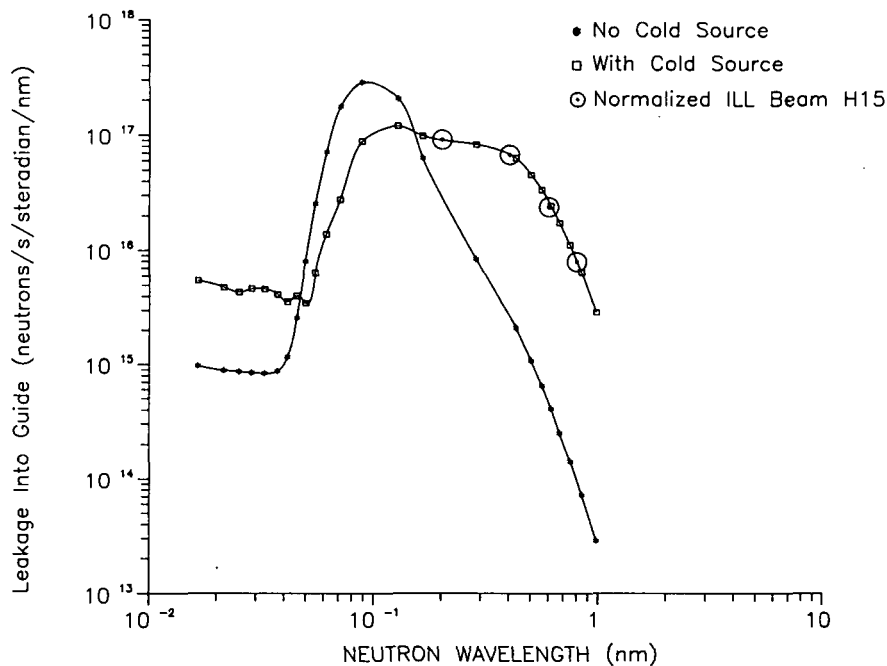


Fig. 2.7. Impact of cold source on calculated neutron spectrum with inclusion of normalized ILL data for reference.

the calculated spectrum is consistent with the measured ILL spectrum.

This, as well as other results obtained over the report period, indicated that the models are now believed to be adequate enough to begin comprehensive cold source geometry studies. At the end of the report period, work was under way to develop models for some nonspherical shapes.

### 2.8.1.2 Cavity Effects

The number and spectrum of neutrons entering a guide depend on the number and spectrum of neutrons that leak out of the cold source surface, which is in direct line of sight with the guide. In a spherical deuterium ( $LD_2$ ) cold source, the peak number of cold neutrons occurs in the central region rather than at the surface. Therefore, a new concept was developed at ILL to introduce a cavity region that penetrates into the cold

source from the surface, which is in direct line of sight with the mouths of the guides. The use of the cavity reduces the absolute cold neutron peak within the cold source; however, when the cavity is properly sized, there is a net increase in the leakage from the cold source surfacing to the guides.

An analysis was initiated to examine different lengths of penetration for a cavity into the 390-mm-diameter spherical cold source used in the present ANS models. Three cavity penetration lengths were considered (other cavity dimensions were the same for all cases and were based on the size of the guide and the need to provide full illumination). The gain factors calculated within the guides for neutrons as a function of wavelength are presented in Fig. 2.8. Based on the three cases considered, the optimal penetration length appears to be  $\sim 190$  mm. At this point gain factors for the cold neutron region are on the order of 50 to 80%. The high

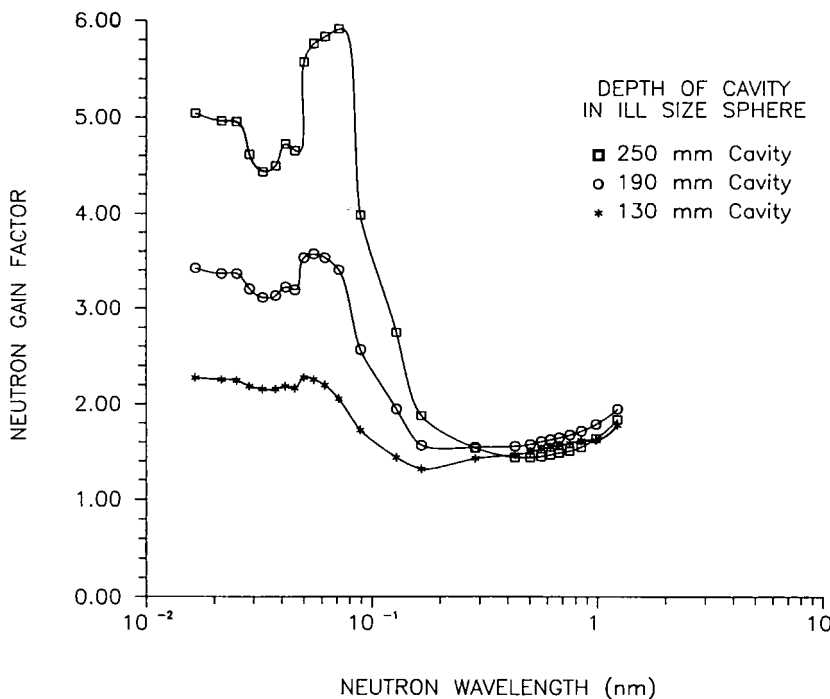


Fig. 2.8. Neutron guide factors obtained within the guides for three separate cold source cavities.

gain factors observed for the higher energy region appear to be caused by the decrease in the effective moderator thickness. The impact of the high gain factor for the higher energy neutrons in conjunction with the use of straight guides in the ANS is not fully understood at this time.

### 2.8.1.3 Combined Liquid Deuterium and Liquid Nitrogen-15 System

A system was examined where the front section of an LD<sub>2</sub> spherical cold source was replaced by LN<sub>2</sub>. Interest in the combined system is motivated by two potential advantages:

1. Because of the flammable nature of deuterium, it is important to minimize the amount of LD<sub>2</sub> in the cold source system. If we could replace the LD<sub>2</sub> in the front portion of the cold source without significant reduction in the number of cold neutrons entering the guide, there would be a considerable reduction in the cold source deuterium inventory.
2. There is a potential problem in that too much heat will be deposited directly in the LD<sub>2</sub> which would prohibit operating the cold source at the preferred location. Replacement of some of the front-face LD<sub>2</sub> by LN<sub>2</sub> would result in a significant amount of the heat load being deposited in the LN<sub>2</sub> where it can be more easily removed.

Early analysis with one- and two-dimensional models indicated that such a combined system could be developed with essentially no change in the cold neutron flux entering the guide. However, later more comprehensive analysis indicated that the combined system would result in a 10 to 15% decrease in the neutron guide cold flux. Although we have not abandoned this idea, we have stopped work in this area for the present. Other options (moving the cold source

back from the core and reducing the size of the cold source) have the potential for reducing the LD<sub>2</sub> inventory and heat load in return for similar decreases in the neutron guide cold flux without requiring the addition of another cooling system.

## 2.8.2 Thermal-Hydraulics and Testing Program

The ANS cold source will experience more severe operating conditions than does the one at ILL. As a result, we have developed a two-coolant system concept, (one to cool the structure and one to cool the LD<sub>2</sub>). Although heat deposited in the LD<sub>2</sub> may be only slightly more than that removed from the ILL LD<sub>2</sub> system, our literature survey has not to date provided proven techniques for predicting our system's thermal performance and stability limits. This information must be obtained to design and operate the cold source successfully. The key issues to be resolved are estimation of (1) system stability and stability limits, (2) liquid level control, and (3) two-phase density for all thermal loading conditions.

An R&D program plan has been developed to address these issues. The objectives of this program are to (1) predict, by use of a thermal-hydraulics model, the cold source stability limits, liquid level, two-phase density, and other thermal-hydraulic behavior; (2) calibrate and experimentally validate the analytical model; and (3) provide interface data required for the reactor system design.

### 2.8.2.1 Thermal-Hydraulics Analytical Modeling

A finite-element model of the cold source was built using PATRAN.<sup>18</sup> This model was then interfaced to the FIDAP<sup>19</sup> fluid dynamics/heat transfer analyzer. A solution to single-phase natural convection was achieved for a simplified set of boundary

conditions and reduced loading parameters using this analysis package. Efforts then concentrated on solving the single-phase natural convection problem with realistic boundary conditions and loading parameters.

A single bubble dynamics model was developed and reviewed during this report period. Some comparison of LD<sub>2</sub> and LN<sub>2</sub> bubble dynamics were obtained using the model. These results support the claim that the LN<sub>2</sub> will satisfactorily simulate the behavior of LD<sub>2</sub> in the experiments.

Bubbly flow limits have been estimated based on the single bubble dynamics calculations and a rather liberal assumption regarding bubble proximity at the phase interface. The results clearly indicate that a large phase interface area is desirable, and a sphere or other geometry that locates the phase interface in a converging cross-section is undesirable from a heat transfer viewpoint.

### 2.8.2.2 Thermal-Hydraulic Testing Program

A good simulation facility is required to achieve the R&D objectives. Based on our present literature search and discussions with cryogenic experts, it appears that an ideal simulation facility cannot be designed and built. As a result, we have chosen a design for the initial cold source experimental facility that incorporates the use of LN<sub>2</sub> heated by resistance wire heaters. This approach was taken for three main reasons:

1. Preliminary calculations indicate that experiments using LN<sub>2</sub> will nicely simulate LD<sub>2</sub> fluid dynamics and heat transfer.
2. LN<sub>2</sub> is a noncombustible, nontoxic fluid that results in a safe inexpensive test facility.
3. Volumetrically heating the moderator to simulate actual ANS cold source conditions is impractical.

In our opinion, the facility's primary limitation is associated with the heating method.

As stated above, the LN<sub>2</sub> in the cold source facility is heated by resistance wires distributed throughout the liquid volume. The spatial heating density can be reasonably simulated at discrete locations. The bubble dynamics and spatial variation of liquid superheat, however, may be altered by the presence of the wires, which will introduce additional nucleation sites and surface boiling phenomena. Despite the stated difficulties, ILL performed much of its R&D work using a similar facility with apparent success.<sup>20</sup> We are confident that LN<sub>2</sub> tests will provide much needed data to predict cold source performance and validate the analytical model.

A picture of the nearly completed LN<sub>2</sub> cold source facility is shown in Fig. 2.9. We expect this facility to be operational during the first quarter of FY 1990.

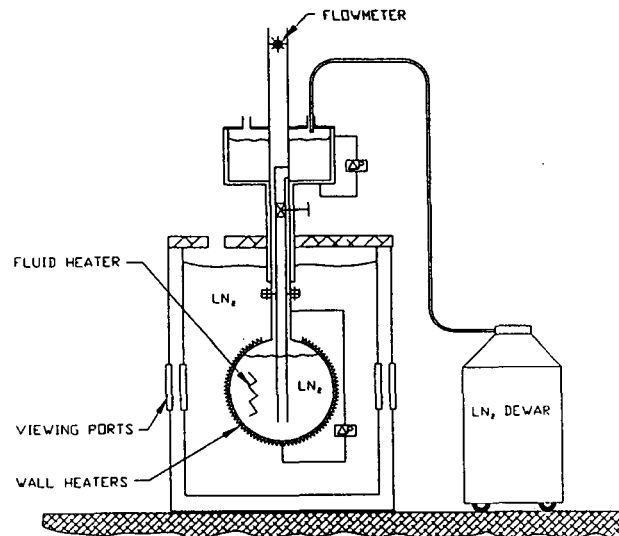


Fig. 2.9. LN<sub>2</sub> cold source test facility.

Additional tests are expected to be performed, including preoperational testing of the prototype cold source system in the 1994 to 1995 time frame. Plans are being developed for these tests but they are not yet complete.

### 2.8.3 Development of Safety Philosophy for the ANS LD<sub>2</sub> Cold Source

Although specific safety criteria for the cold source have not been developed yet, five general safety features required of the cold source have been identified:

1. The cold source must be designed to prevent outleakage of warm or cryogenic deuterium from the pressure boundary.
2. The design must also prevent inleakage of air or water into the deuterium lines.
3. Design features must be included to prevent the occurrence of pressure excursions within the pressure boundary above the design limits.
4. The system must be designed to minimize the opportunity for inadvertent mixing of LD<sub>2</sub> with condensible or oxidizing gases.
5. Provisions must be provided for full and redundant instrumentation and controls needed for operation and safety.

During the coming year, these safety characteristics, along with others that may be identified for the cold source or as part of an interface with the reactor control system, will be developed into a set of specific design criteria for the cold source.

### 2.8.4 Cold Source Instrumentation Development

One of the objectives for the cold source R&D program is to develop techniques and devices deemed necessary to monitor the cold source during normal and abnormal conditions. An ultrasonic probe has been developed for monitoring the cold source liquid level, density at various axial locations within the LD<sub>2</sub>, and the axial temperature profile within the LD<sub>2</sub>. This device has been tested in an LN<sub>2</sub> vat and will be tested further as

part of the LN<sub>2</sub> cold source facility testing program.

## 2.9 BEAM TUBE, GUIDE, AND INSTRUMENT DEVELOPMENT

The beam tube, guide, and instrumentation R&D program is currently giving highest priority to the optimization of beam transport systems that lie on the critical path for the reactor design, such as beam tube geometries, which affect reactivity, and guide tube dimensions, which strongly influence the heat load on the cold sources. The longer-term effort will focus more on the instruments themselves, and groundwork is also being laid toward this goal. We have benefited from collaborations with many groups, particularly at BNL (Neutron Scattering and Light Water Reactor Systems Groups), the National Institute of Standards and Technology (Neutron Scattering Group), and the University of Rhode Island, as well as within ORNL (Solid State and Instrument & Controls Divisions). The polarizing supermirror program within Solid State Division, which has contributed substantially to the ANS R&D program, won a 1989 R&D-100 award.

### 2.9.1 Neutron Supermirrors

Our supermirror research has primarily focused on the very difficult questions of design and fabrication of multilayer, thin-film neutron supermirrors, but success in this area only provides a partial answer to the problem of producing polarizing supermirror stacks: fabricating long, optically flat mirrors is nontrivial, and it is preferable to make short sections and then to stack them up to span the beam. Unfortunately, the topology of a stack is not equivalent to that of a mirror but that of a channel, which has quite different characteristics. Fig. 2.10 illustrates the problem. (The solid lines indicate neutrons

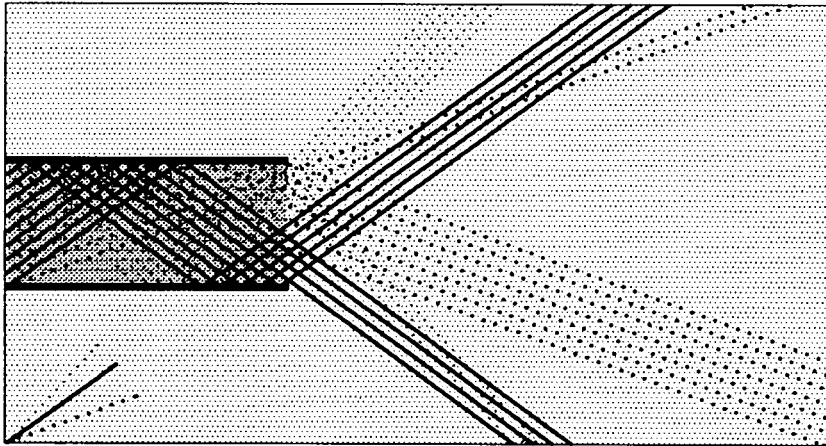


Fig. 2.10. Neutron transport through a reflecting channel.

travelling in the mean beam direction, with dotted lines indicating the extent of divergence that must be handled in the beam.) A channel can only be designed for perfect reflection of an exactly parallel beam; any divergence causes some parts of the beam to be transmitted without reflection, and other parts to be doubly reflected (which is equivalent to direct transmission).

We have general phase space arguments that indicate the directions to take to avoid this problem, but (as for essentially all problems involving divergent beam optics) we have not been able to deduce analytic solutions that would permit design optimization. Numerical studies have been initiated using Monte Carlo simulation and ray-tracing techniques. Figure 2.11 shows a typical result for a bilayer

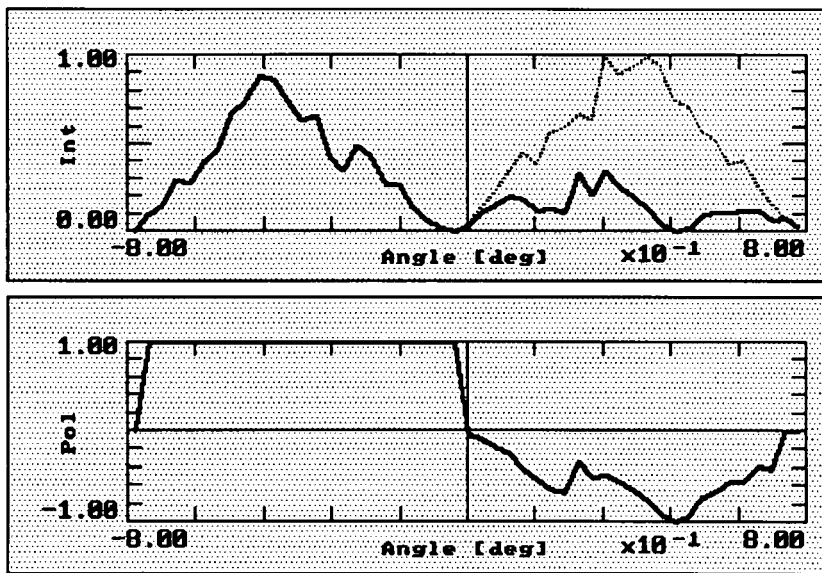


Fig. 2.11. Transmitted beam intensity and polarization (solid lines) as a function of angle after transmission through an optimized supermirror stack. The incident beam intensity is shown as a dotted line.

stack with complex mirror characteristics for a beam of realistic divergence. These first results already show a 50% improvement in efficiency over the simple system of Fig. 2.10, while adding relatively little to the cost of fabrication. We expect even better results as the calculations are further refined.

## 2.9.2 Instrumentation Workshop

A joint BNL/ORNL International Workshop on Neutron Scattering Instrumentation was held at the Garden Plaza Hotel in Oak Ridge, Monday, June 5-7, 1989. Co-chaired by John Axe (BNL) and John Hayter (ORNL), the workshop was sponsored by DOE's Division of Materials Sciences. About 50 neutron scattering instrumentation experts from 19 laboratories in 8 countries attended. The purpose of the workshop was to review the status and limitations of current neutron scattering instrumentation, to discuss and exchange plans for new instruments, and to stimulate thinking about innovative instrumentation concepts to meet the needs of the U.S. neutron scattering community into the 1990s and beyond.

The workshop was organized into plenary sessions in the mornings and divided into parallel working groups each afternoon. The first morning was spent reviewing current and future plans at a several major reactor centers worldwide, and the second morning was devoted to discussion of innovative ideas. The seven working groups considered 3-axes and backscattering, time-of-flight, single-crystal diffraction, powder and liquids diffraction, small-angle neutron scattering, and reflectometry, special techniques, and detectors. In the final morning session, each chairman gave a short summary of the main conclusions reached by his group. The working group discussions were animated and fruitful, and justice cannot be done to them in a limited space. The interested reader is referred to the full report of the workshop proceedings,

which will be distributed to workshop participants and to others on request.<sup>21</sup> As a first step in the ANS neutron multidetector R&D program, a survey of current detector capabilities and limitations was prepared for the workshop by S. A. McElhaney of I&C Division; this report has been extended and will also be available on request.

## 2.9.3 Detector Shielding

The shielding around a thermal or cold neutron detector usually comprises two functional parts: a good neutron moderator, followed by a good absorber (e.g.,  $^{10}\text{B}$ ). In the past, the moderator region has consisted of a hydrogenous material such as water or paraffin, often loaded with an absorber such as  $^{10}\text{B}_2\text{O}_3$ ; such materials require a separate mechanical support structure, which may itself scatter background. More recently, the trend has been toward using moderator materials which also have suitable intrinsic mechanical properties to permit fabrication of the detector shielding from the moderator material itself. A typical example is high-density ( $950\text{-kg}\cdot\text{m}^{-3}$ ) polyethylene, which is readily available, easily machinable, and has appropriate neutronics properties. Several new materials offer the possibility of improved shielding performance, but currently no systematic study is available. In conjunction with BNL, we are now studying the feasibility of using neutron transport calculations to optimize new shielding designs, using a 69-group ANISN model. The three neutron spectra that contribute to the detector flux will be determined with this model: (1) the spectrum leaking from the biological shield; (2) the spectrum leaking from the monochromator shield; and (3) the beam spectra. The results of the calculation will be presented in the form of attenuation factors for each spectral group, evaluated from the ratios of detected to incident neutrons, together with error estimates.

## 2.9.4 Beam Tube and Guide Design

Many of the new techniques developed at ILL and elsewhere have been implemented in the design of the beam tubes at the new Saclay reactor, with the result that beam fluxes per source neutron are higher at Saclay than at ILL. An analysis of this flux gain indicates, however, that while a useful gain is available for "easy" experiments, there is *no* gain in practice for experiments that push the state-of-the-art; we expect the latter types of experiment to dominate at the ANS. The physical reason for this is that the flux gain is achieved by an increase in divergence, which usually needs to be removed again by collimation for high-resolution work. In this case, the extra flux is actually delivered toward the spectrometer as *noise* rather than signal, and we would have been better off without it. These results are being studied to produce new designs that provide real gains at high resolution in the ANS beam tube configurations, together with ways of relaxing the in-pile collimation for those experiments that can take advantage of higher flux produced by increased beam divergence.

The detailed optimization of neutron guide dimensions for different classes of experiments is also the subject of intense R&D activity. Figure 2.12(A) shows a section of a single guide looking at a cold source, which is assumed uniformly bright over its surface, within the angular limits of accep-

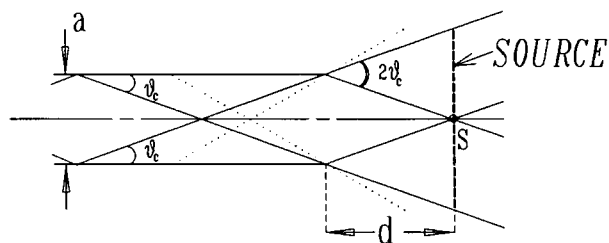


Fig. 2.12(A). Illumination of a single neutron guide.

tance of the guide. The key parameter is the critical angle for the mirror material that coats the guide:  $\theta_c$ , which is typically of order  $1^\circ \text{ nm}^{-1}$ . Reference to Fig. 2.12(A) shows that, for a given source size at a given distance from the guide entrance, there is a maximum value of this angle if the guide is to be *fully illuminated*, a critical requirement for many experiments on straight guides. Since  $\theta_c$  increases linearly with wavelength, it is clear that the choice of a particular guide/source geometry imposes a saturation wavelength  $\theta_{\text{max}}$  for the guide, beyond which the geometry rather than the wavelength imposes the maximum divergence for which the guide is still correctly illuminated. Choosing the maximum value of  $\theta$  to be  $1^\circ$  means that the guide divergence would be as large as possible up to  $\theta_{\text{max}} = 1 \text{ nm}$  for a nickel mirror coating, or  $\theta_{\text{max}} \approx 0.3 \text{ nm}$  for a supermirror coating.

The guide configuration envisaged for the ANS is based on a number (currently 7) of guides viewing a given cold source from the same horizontal plane. Figure 2.12(B) is a plan view of a pair of such guides, with angular separation  $\beta$ ; for the special value  $\beta = 2\theta_c$ , this geometry provides a region (between the end of the guide and B) where the source size is independent of distance. This arrangement is well matched to our present conceptual design values of  $\theta_c = 1^\circ$  and  $\beta = 2^\circ$ . At these angular values, the

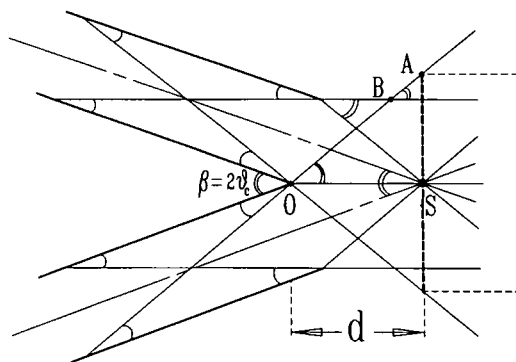


Fig. 2.12(B). Illumination of a guide pair configuration.

points  $A$  and  $B$  essentially coincide. (Angles in the figure are greatly exaggerated.) Within this approximation, the source width remains constant at  $s = 2a$  for all source distances  $d \leq a/2$ . A feeling for the distances involved may be obtained from numerical examples for  $\theta_c = 1^\circ$  and  $\beta = 2\theta_c$ :

- $a = 50$  mm (probable lower limit on guide width):  $s = 100$  mm for  $d = 1432$  mm;
- $a = 80$  mm (probable upper limit on guide width):  $s = 160$  mm for  $d = 2292$  mm.

### 2.9.5 Very Cold and Ultracold Neutrons

The best current method of ultracold neutron (UCN) production is to use a neutron turbine to Doppler-shift the energy of a very-cold neutron (VCN) beam to lower values, because a VCN beam can be transported through sufficiently thin windows with absorption losses only; a UCN beam will be totally reflected at all angles by likely window materials. Thus both the VCN and UCN beams will interface to the reactor *via* VCN guides having a typical cutoff wavelength of 7 nm. To maximize solid angle and to minimize window material, it is proposed to base the design on the current ILL concept, in which the VCN guide actually starts *inside* the top of the cold source so that only a relatively thin cryogenic window intervenes. The many safety questions raised by this configuration will require careful study.

### 2.9.6 Instruments Available at Startup

A first step in instrument optimization is, of course, to select which instruments will be installed. Although instruments have been identified with each beam or guide station on the ANS, it is not expected that all of these

instruments will be in place at the time of reactor startup. Apart from any question of funding (and the availability of appropriately trained manpower, independently of funding), there are cogent reasons for not planning to fill all available stations; having some free beams permits flexibility in incorporating new instrument concepts that have been formulated late in the construction stage and provides workstations for further development of new ideas during ANS operation. A preliminary proposal for the initial complement of instruments that might be considered as "core" instruments and constructed as an integral part of the ANS project was approved at the NSCANS Committee meeting in Arlington on June 12, 1989. The likely mix of core scattering instrument types follows:

- $H2$  Liquids
- $H4$  3-axis
- $T1$  Single Crystal
- $T2$  Single Crystal
- $T3$  Polarized Single Crystal
- $T4$  High-Resolution Powder
- $T5$  High-Intensity Powder
- $T6$  Diffuse Scattering
- $T11$  3-axis
- $T12$  3-axis
- $D1$  Time-of-Flight
- $D2$  Neutron Spin Echo
- $D3$  20-m SANS Camera/Reflectometer
- $D4$  40-m SANS
- $D12$  3-axis
- $L4$  Backscattering
- $L7$  Interferometer
- $L8$  3-axis

### 2.10 HOT SOURCE DEVELOPMENT

The hot source is another planned R&D activity that has not been initiated. This task continues to receive low priority for two reasons:

1. In our opinion, providing an adequate hot source capability is not a feasibility issue.

Thus, we can delay initiation of this task until it begins to affect other aspects of the project. With the limited resources of the project, this frees up resources for items that are more pressing.

2. During the coming year, ILL plans to improve its hot source performance by redesign. If we wait until this effort is underway, we may learn something from a staff with more experience in hot source performance optimization than we have available to the ANS project.

If the ILL effort does not materialize, it will be necessary to proceed with this task in FY 1991.

## 2.11 NEUTRON TRANSPORT AND SHIELDING

This R&D task was defined to deal with issues involving neutron transport analysis. Although very little reportable work was performed under this task, there was some activity in two subtasks: neutron/gamma transport in beam tubes and evaluation of component heat sources and doses. The status of these two tasks is reported in Sects. 2.11.1 and 2.11.2.

### 2.11.1 Neutron/Gamma Transport in Beam Tubes

A transport model of the PS-2 core was developed, and a beginning-of-cycle (BOC) calculation was performed to compare with diffusion calculations of the PS-2 core. The absolute value of the peak thermal flux, the location of the peak, and  $k_{eff}$  obtained by the transport calculation compared very favorably with the diffusion calculations. However, it was found that the transport cross-section set did not contain the information on fission products necessary to provide neutron and gamma sources associated with burned fuel. Since the fission product gamma sources are

significant (accounting for as much as half the total near the end of the cycle) additional cross-section work was required before this task could continue.

When the fission product cross-section work was completed, a beam tube neutron and gamma source was generated. A transport model of the beam tube was then generated, and the transport of the neutron and gamma source down the tube was evaluated. At the close of the reporting period the initial results had been obtained but were considered to be unrealistic. The problem appeared to be associated with the number of angles directed down the beam tube.

### 2.11.2 Evaluate Component Heat Sources and Doses

An analysis was initiated to estimate the neutron and gamma heating loads for various reactor and reflector tank components based on the PS-2 core conditions. To perform this task the neutron and gamma sources developed in the neutron/gamma transport in beam tubes task were used. Therefore, the delays discussed in Sect. 2.11.1 also applied to this task. At the close of the reporting period the heat loads for regions out to the light-water pool had been calculated, but no critical evaluation of the data had been performed.

## 2.12 I&C RESEARCH AND DEVELOPMENT

### 2.12.1 Protection and Control Strategy

The ANS protection system will have fast response to deal with both analyzed and un-analyzed transients and to reduce the necessary margins between set points and the onset of fuel damage. Two independent sets of safety/shutdown rods will be used to ensure high reliability. The four inner rods are used

for control as well as safety and shutdown and hence will always be in a region of high reactivity worth. The eight outer rods, fully withdrawn from the core during normal operation, provide additional shutdown margin and will be located to have ample reactivity worth to provide safety response for anticipated transients. Thus, the two rod systems comprise redundant and independent shutdown means.

Neutron and gamma flux detectors will be located in the light-water RT, avoiding the region close to the core where fluxes are too high and access is too limited. The curve of neutron attenuation vs distance from the core pressure boundary is very steep in the light water so that small changes in detector position can cause large changes in output. In addition, the neutron attenuation is sensitive to the introduction of neutron-absorbing impurities such as boron. The gamma flux in the same region is relatively unaffected by impurities and is less sensitive to position changes. Gamma detectors will be used in conjunction with the neutron detectors to provide high confidence in the reactor flux measurements. Because of the susceptibility of the leakage flux at the detectors to perturbations from position errors, water contamination, or beam tube influences, the measurement system will incorporate an automatic recalibration feature to compare the flux measurements with heat power calculated from core coolant flow and differential temperature measurements. This scheme was developed for use on the HFIR and has been adopted by a number of commercial nuclear power plants, because of similar flux calibration problems.

The control strategy for the ANS is being developed using the control engine concept. The control engine is a design technique to identify a correct and acceptable approach using a template of control system architecture. This results in a comprehensive and tailorable system approach to operations and maintenance. The design is arranged hierarchically and facilitates a distributed

hardware approach with flexible, but controlled and reliable communication paths. The system will include both continuous and discontinuous (discrete event) control features, performance analysis and diagnostics, validation of signals, commands, strategy, and configuration, multifunctional operator interfaces and displays, and a "lifeboat" system that establishes stable local control of processes should higher level communication be lost. A representative template of the control engine concept is shown in Fig. 2.13.

A few features, unique to high-flux reactors, demand special consideration. Because the ANS is to be a user facility of national importance, reliable scheduling and high availability are very important. Unscheduled spurious shutdowns present a special problem because of the rapid rate of xenon growth following shutdown. A maximum of 20 minutes is available to restore power operation before xenon poisoning inhibits restart. This number will decrease later in the life of a core. Burnable poison in the fuel will provide nearly constant available excess reactivity for a significant fraction of the core life. Extraordinary measures will be taken to reduce spurious shutdowns but some, such as those caused by momentary off-site power outages, are unavoidable. A diagnostic system is essential to determine quickly and reliably the source of such shutdowns and to provide confidence that safety concerns do not exist to hinder rapid restart. The rapid restart will be accomplished with a comprehensive automated system that frees the operator for his proper role of supervising the operation and observing for unexpected or undetected problems. Special maneuvering limitations or maneuvering requirements for successful recovery will be programmed into the system.

## 2.12.2 ANS Dynamic Model

The development and validation of the ANS dynamic model continues. This model is coded in ACSL language that provides for

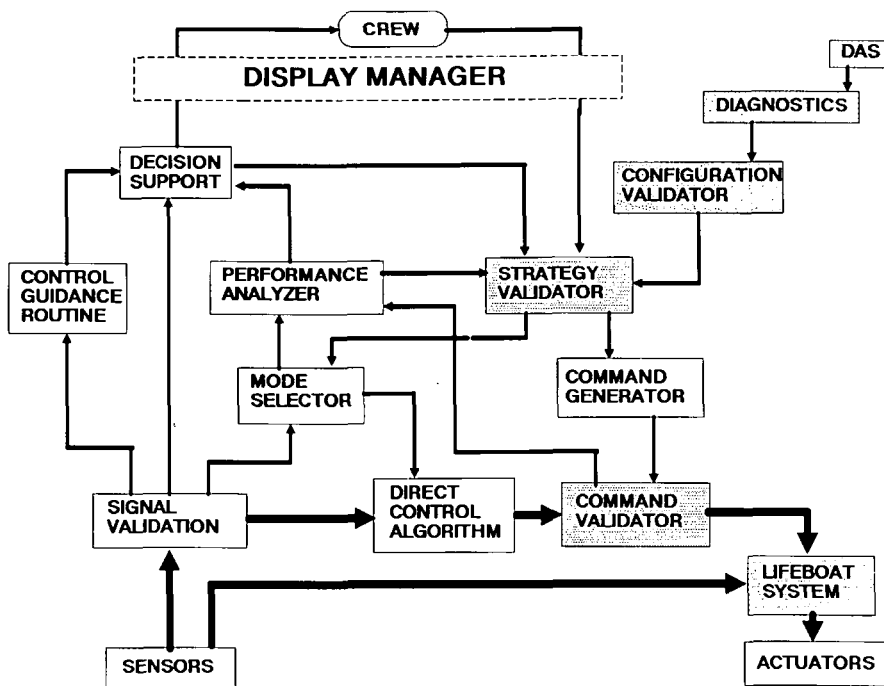


Fig. 2.13. Block diagram of a control engine template for ANS.

great modularity and ease of reconfiguration. Most of the modules used in the current model have been validated against available data. For instance, the core neutronics/thermohydraulics module has been benchmarked against SPERT-II data, and the pump and cooling circuits modules have been benchmarked against HFIR pump coastdown experiments. When experimental data are not available, the modules have been validated by ensuring that they conserve mass and energy and that they respond reasonably for known simple transients.

The ANS dynamic model has been used to evaluate the transient behavior of the ANS reactor following a loss of energy to main circulating pumps. Two cases have been considered depending on whether the pony motors function properly or if they fail to operate, resulting in natural circulation conditions. Figure 2.14 summarizes the main results of this transient study for the current

assumed parameters that define the ANS reactor and cooling circuits. In this figure, the fuel surface temperature at the hot spot of the hot channel is shown as a function of time. The dotted lines in Fig. 2.14 represent the transient coolant saturation temperature following a depressurization caused by a small break of the sizes labeled. These are the main results from this simulation: (1) Regardless of the depressurization rate, the hot spot surface temperature does not reach saturation temperature; thus, there is no boiling or damage to the fuel when the pony motors are available. (2) If pony motors are not available, any reasonable depressurization rate will result in local boiling and possible fuel damage at the hot spot location. Thus we conclude that following loss of pumping power, damage to the core can be avoided by maintaining either pony flow or coolant pressure.

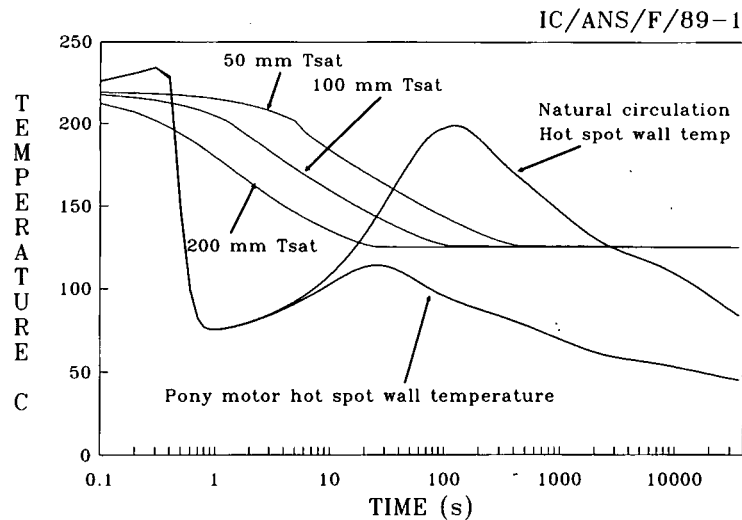


Fig. 2.14. Hot spot fuel surface temperatures following loss of main pumping power, and coolant saturation temperatures during a slow depressurization. Gas pressurizer is located in low pressure side of pump and has  $9 \text{ m}^3$  of  $\text{D}_2\text{O}$  liquid volume and  $1 \text{ m}^3$  of gas volume. Power peaking factors are 2.48 for hot spot and 1.95 for hot streak.

### 2.12.3 Xenon Transient Calculations

The effect of xenon, samarium, and other neutronic poisons on the transient behavior of the ANS reactor has been evaluated. To this end, the BOLD VENTURE computational system has been used to model the fission product dynamics following a reactor shutdown. This calculation results in shutdown  $K_{\text{eff}}$  values that take into account not only the buildup of xenon and other fission products, but also the reactivity effects of flux redistributions due to isotope buildups. The main results of this study are summarized in Fig. 2.15. We conclude from these data that the peak negative reactivity value following a shutdown is of the order of  $\$60$  and occurs in  $\sim 12$  hours. If  $\$10$  worth of positive reactivity is available to the control

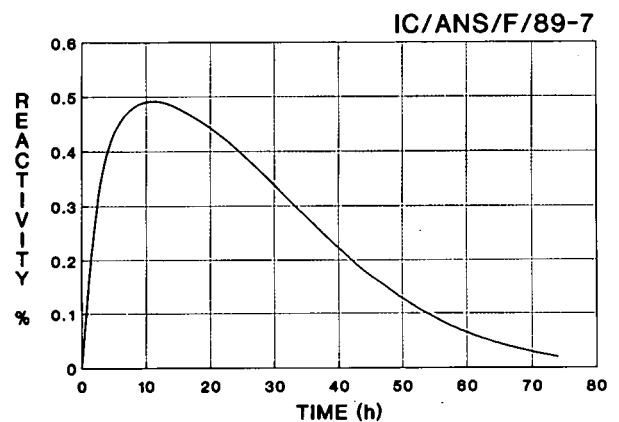


Fig. 2.15. Reactivity due to Xenon, Samarium, and other fission products following a reactor shutdown.

system, reactor restart would be possible only within the first 21 minutes following the shutdown; otherwise, 57 hours must elapse to reach criticality again.

## 2.12.4 Flux Calculation at Detector Locations

The attenuation of neutron flux in the H<sub>2</sub>O pool outside the D<sub>2</sub>O reflector has been studied with a BOLD VENTURE model of the PS-2 66-Li core. The main results of this simulation show that the neutron flux attenuation is 1 decade per every 74 mm of H<sub>2</sub>O. The optimal detector location (flux of 10<sup>14</sup> m<sup>-2</sup>·s<sup>-1</sup>) is located 270 mm away from the reflector boundary. Flux calculations were also performed to study the effect of solid bodies of neutron absorbers on flux at the detector location. From these calculations it was determined that absorbers located more than 100 mm away from the detectors will not significantly affect their efficiency.

## 2.12.5 Control Rod Drive Magnet and Latch Analysis

A computer code has been written to calculate the force developed by electromagnets of the type proposed for use in the scram mechanism of the ANS. The program is based on an analysis presented in ORNL report, *Design and Experimental Evaluation of Electromagnets in Research Reactors*.<sup>22</sup> The program input consists of parameters describing the magnet geometry, coil current, magnetic properties, and the desired force, and the program returns the optimum outer radius, magnet length, and the number of coil turns.

This program has been used to perform parametric studies to determine the magnet space requirements. Results for one of these studies, showing the maximum force developed for a range of magnet outside radii, is shown in Fig. 2.16. In addition to parametric studies, this program should be useful during the design of the control rod drive electromagnets.

A force analysis of the control rod drive latch mechanism also has been performed.

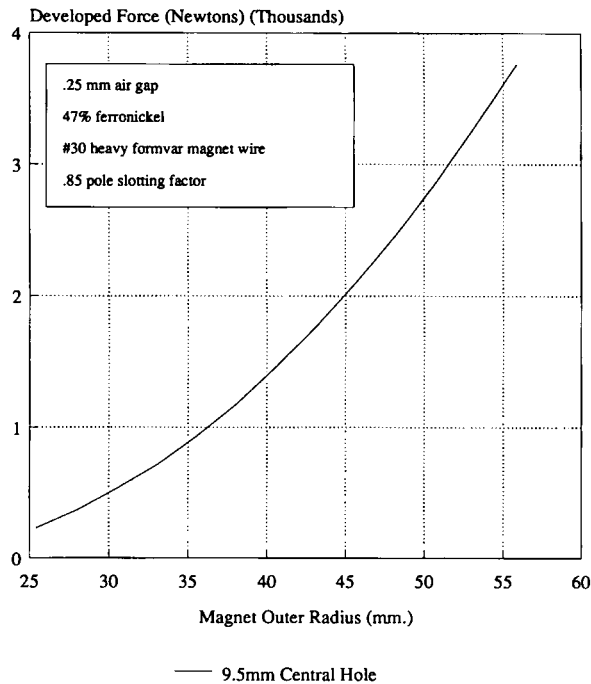


Fig. 2.16. Force developed by lifting magnets.

When engaged, the latch mechanism holds the control rod in a cocked, ready-to-scram position and upon release allows insertion of the control rod. The force applied to the latch (exerted primarily by the control rod weight and accelerating spring force) is distributed between the release rod guide tube and the latch release rod, which is supported by the control rod magnet. To obtain an accurate prediction of the required magnet force, it is necessary to know the distribution of force through the latch.

The latch consists of four disks, supported by the release rod, which protrude through slots in the release rod guide tube (Fig. 2.17). The control rod, which is concentric with the latch release rod guide tube, rests on the protruding portion of the disks. When the release rod is dropped, the disks retract and allow the control rod to clear the latch mechanism and scram.

The known quantities in the analysis are the material properties, the applied force, and the latch geometry, which is described by the

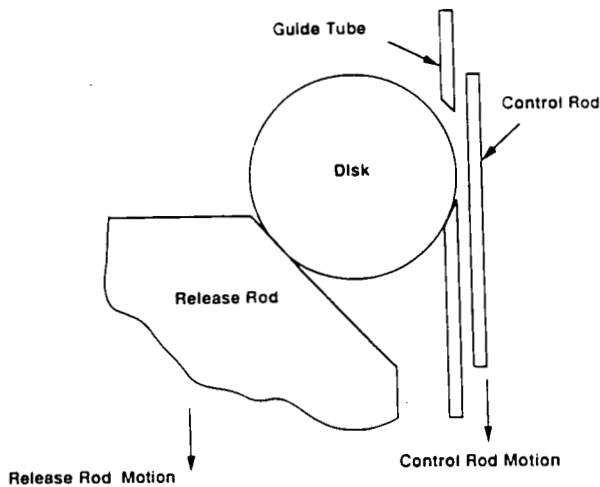
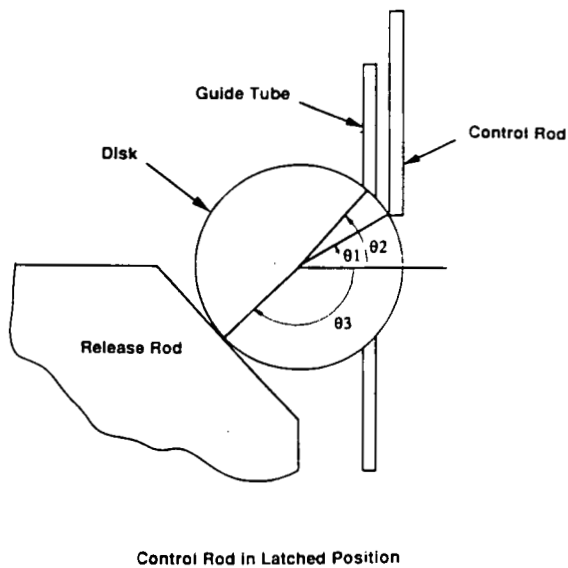


Fig. 2.17. Control rod in unlatched position.

disk radius and the angles  $\theta_1$ ,  $\theta_2$ , and  $\theta_3$  (Fig. 2.17). The analysis determines the force carried by the release rod and the release rod guide tube. Parametric studies have been performed to determine the effect of latch geometry on the force transferred to the magnet. Results from one study (Fig. 2.18) indicate that for all combinations of latch geometry, the majority of the applied force is carried by the release rod guide tube and is not supported by the control rod drive magnet, thus allowing use of relatively small

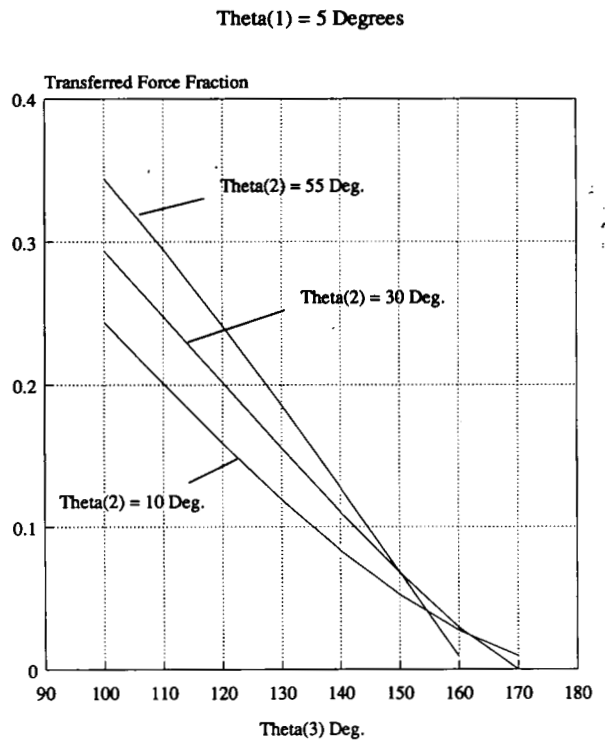


Fig. 2.18. Force transfer through ANS latch.

magnets. Other results are shown in Fig. 2.18: (1) a greater portion of the applied load is carried by the release rod as the release rod face becomes more horizontal (as  $\theta_3$  decreases) and (2) increasing the protruding portion of the disk (increasing  $\theta_2$ ) also increases the portion of the load carried by the release rod. The results of the parametric studies should be useful in designing the ANS latch mechanism and also in determining the force requirements for the control rod drive magnets.

## 2.13 FACILITY CONCEPTS

### 2.13.1 Materials Selection Issues

Support from ORNL's Engineering Technology Division was provided to the reactor systems design team on the selection of materials of construction. Specific examples include input on the use of Type

6061 aluminum as the general material of construction; unclad hafnium for control cylinders; specialty materials, such as steel springs for control drive mechanisms; and Inconel parts in the control drives where additional hardness is required beyond that provided by aluminum.

Support was also provided on the application of Sect. III of the *ASME Boiler and Pressure Vessel Code*. Specific applications include the review of data on 6061 Al and Zircaloy-2 in other sections of the code (these materials do not appear as a Sect. III, Class 1 material), recommendation of allowable stress values for use in scoping the design of the CPBT, and calculation of recommended thicknesses for the CPBT using either of these materials.

### 2.13.2 Waste Management R&D

The priorities of waste management R&D were the definition of anticipated waste and effluent streams associated with the ANS, evaluation of the compatibility of these streams with the existing and planned monitoring, treatment and disposal facilities at ORNL, and the identification of any new or interfacing systems that might be required to allow for handling of all ANS streams. Also a priority was the identification of any waste form development and testing that could be required as a result of issues new to the ORNL waste organization, especially those which might require long-term retention testing. Progress in the former area paralleled the development of facility design concepts during the reporting period. Organizational complexities slowed progress on evaluations of waste form R&D activities; this subject is being re-evaluated at the end of the reporting period in light of the new Laboratory organization on waste R&D.

### 2.13.3 Planning for Future Hardware Development and Testing

Longer-term activities dealing with facility concepts R&D are the developmental and testing activities needed to confirm the adequacy designs for key component designs, including the refueling machine, the control drive assemblies, and the CPBT seal systems. In some cases the test activities can be conducted under this WBS element; others will require significant procurement and construction, and can become new WBS elements under either the R&D or the design tasks. Initial input was made to the task plans prepared for the DOE project reviews, but considerable additional planning will take place as such needs in the design are clarified.

---

### 3.1. SELECTION OF PREFERRED SITE

The ANS site selection process began in FY 1988 with a goal of identifying a preferred site on the Oak Ridge Reservation. The process used for selecting the candidate sites is documented in ORNL/TM-11419, *Oak Ridge Reservation Site Evaluation Report for the Advanced Neutron Source*.<sup>23</sup> The report develops the criteria used to screen the reservation for potential sites, describes the screening process by which several potential areas were identified, and further compares the options, leading ultimately to the current ANS proposed site.

The three main DOE plants are intensively developed areas located in a largely undeveloped reservation. Some of the undeveloped areas, however, have been used extensively for environmental research and/or waste management. The reservation offers a number of sites where the ANS could be isolated from large population centers, yet be in close proximity to the scientific infrastructure needed by a major research facility. The basic task of the site selection process was to eliminate the less desirable sites on the reservation and focus on one proposed site that would be subject to a much more detailed physical evaluation.

The four principal criteria considered were safety, environmental protection, cost minimization, and operational compatibility. All the criteria used in the site evaluation are listed in Exhibit 3.1. In the first stage of the

three-stage procedure used for this study, the criteria were used to first screen out large areas of the reservation. For the second and third stages, a more general set of criteria was used to make a comparative analysis of three or four alternatives.

The results of the first stage revealed four candidate areas: Melton Valley, east of ORNL; the Interchange area between the Y-12 and K-25 Plants at the intersection of Route 95 and Oak Ridge Turnpike; and two areas west of the Y-12 Plant along Bear Creek Road at the intersection of Route 95.

In the second stage of the evaluation, a comparison of the four candidate areas formed the basis for selecting the Melton Valley area as preferable because of its proximity to ORNL, availability of utility services, and lower risk of intruding on the habitat of a protected species.

The third stage of the evaluation used the same comparative criteria employed in the stage-2 analysis, but this time concentrating on the Melton Valley area. The three sites in the Melton Valley area (Fig 3.1) (R, adjacent to the HFIR; C, the central site; and E, the Eastern site) were evaluated; the eastern site was selected as the preferred one. A conceptual site plan showing a preliminary building arrangement (Fig 3.2) was developed for the Eastern site. This recommendation was submitted to the DOE Land Use Committee for its approval in June 1989. Approval was received shortly thereafter and led us to begin further studies of the site to identify both its surface and subsurface characteristics.

### Exhibit 3.1. ANS site selection criteria

#### 1. SAFETY

##### 1.1 Geology/Seismology

- 1.1.1 Five Miles from Capable Faults
- 1.1.2 Competent Bedrock Foundation

##### 1.2 Meteorology

##### 1.3 Population

- 1.3.1 Low Population Zone (LPZ) Entirely Within Reservation
- 1.3.2 Inner Exclusion Area Avoids Public Roads & Evacuation Routes
- 1.3.3 Outer Exclusion Area Excludes Main Plant Sites
- 1.3.4 Population Center Distance  $>1.33 \times$  LPZ Distance
- 1.3.5 Population Density  $<500$ /square mile

##### 1.4 Hydrology

- 1.4.1 Avoid Areas Subject to Probable Maximum Flood
- 1.4.2 Dependable Water Supply
- 1.4.3 Discharges Meet Water Quality Regulations

##### 1.5 Industrial, Military, and Transportation Facilities

#### 2. ENVIRONMENTAL PROTECTION

##### 2.1 Species, Habitats, and Ecological Systems

##### 2.2 Water Quality

##### 2.3 Air Quality

##### 2.4 Archeological, Cultural, and Historical Resources

##### 2.5 Social and Economic Systems

#### 3. ENGINEERING AND SITE DEVELOPMENT COSTS

##### 3.1 Foundations, Grading, and Drainage

- 3.1.1 Avoid Slopes  $>25\%$
- 3.1.2 Avoid Knox Formations
- 3.1.3 Avoid Faults

##### 3.2 Roads, Utilities, and Relocations

##### 3.3 Containment, Safety, and Waste Treatment Systems

#### 4. OPERATIONAL COMPATIBILITY

##### 4.1 Compatibility with Surroundings

##### 4.2 Proximity to Related Facilities and Services

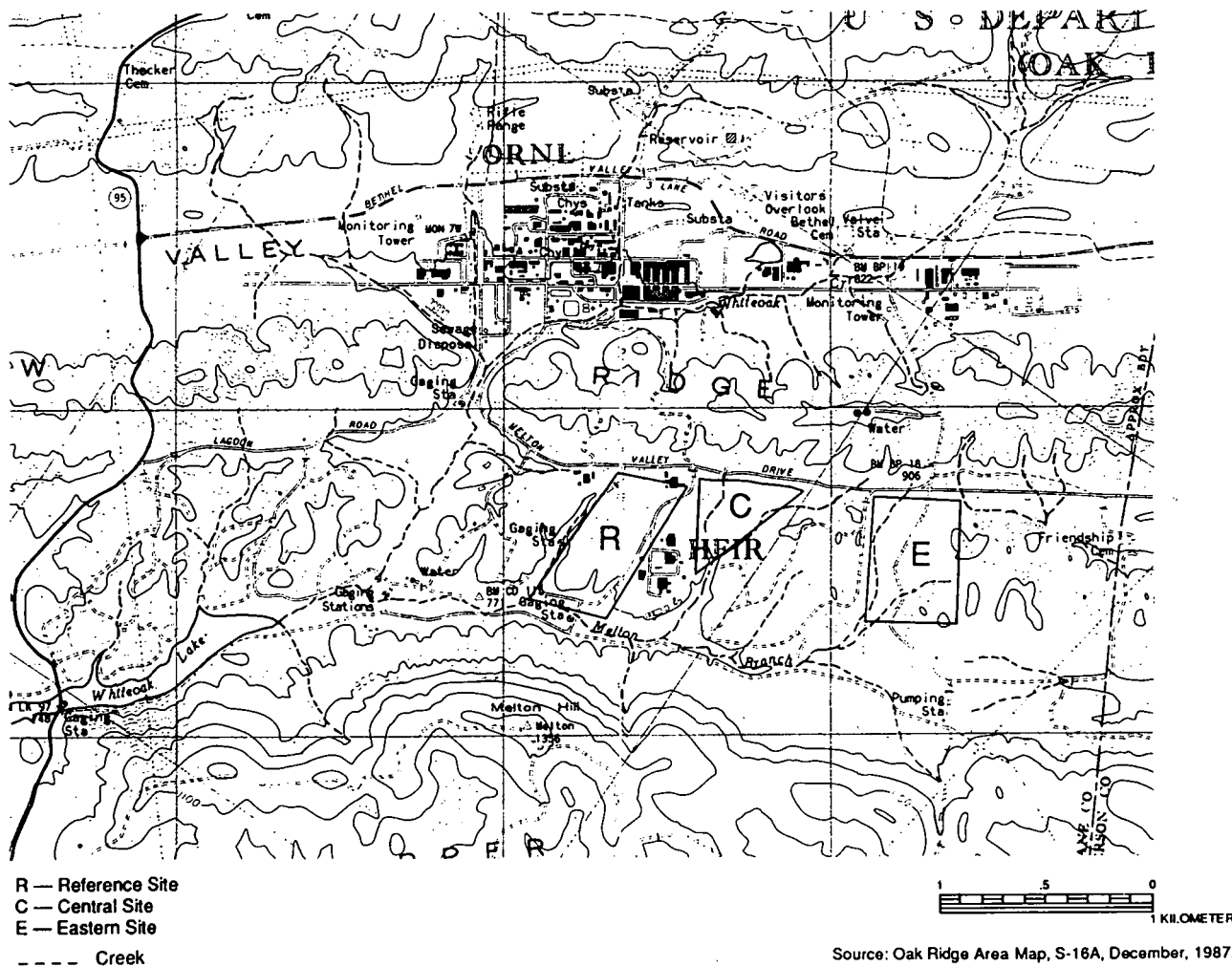
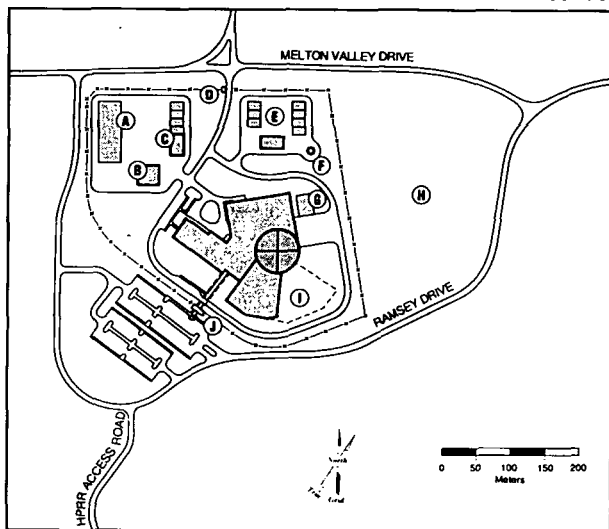


Fig. 3.1. Melton Valley area and proposed sites.

### 3.2. SITE CHARACTERIZATION

Following selection of the ANS proposed site, work was begun to define the surface and subsurface features of the site in more detail. The goal is to identify, as early as possible, any characteristics that might make the site unsuitable or prohibitively expensive to develop. Preliminary environmental surveys of the site and adjacent streams were accomplished to determine if the area had any endangered animal or plant population that

would be disrupted by the ANS construction. The State of Tennessee was asked to review the area for any significant archaeological features and has requested that a formal archeological survey be performed. To date, no listed species or significant archeological features have been identified that would prevent development. A preliminary investigation into the structural integrity of the underlying rock strata began late in FY 1989. Further characterization will be done based on the results of this initial study and the specific needs of the ANS design.



## INDEX

- |                                      |                             |
|--------------------------------------|-----------------------------|
| Ⓐ PROCESS WASTE HANDLING AREA        | Ⓕ STACK                     |
| Ⓑ DETRIITIATION FACILITY             | Ⓖ FILTER PITS               |
| Ⓒ AUXILIARY COOLING TOWER/PUMP HOUSE | Ⓗ FUTURE DEVELOPMENT        |
| Ⓓ VEHICULAR PORTAL                   | Ⓘ GUIDE HALL EXPANSION AREA |
| Ⓔ REACTOR COOLING TOWERS/PUMP HOUSE  | Ⓣ PEDESTRIAN PORTAL         |

This conceptual layout is intended to demonstrate feasibility only; further study will be required to ensure that the final layout is integrated into the ORNL site development plans.

Fig. 3.2. Conceptual site plan.

### 3.3. BALANCE-OF-PLANT (BOP) TEAM

In December 1988, the project had sufficiently matured so that facility issues became important to its continued development. A team of engineers and architects was formed to focus on the design of buildings, structures, land development, and the experiment and reactor interface. The team is oriented to developing the BOP activities that will be accomplished over the next five years by working on early conceptual planning of the facility and concentrating on several specific issues that have a significant impact on the facility scope and layout. In November 1988, the BOP conceptual design activities were formally initiated. Early priorities included developing a five-year task plan and planning for an upcoming DOE review. Following the

review, the site characterization and specific design study tasks (discussed in later sections) were identified and the study efforts initiated. This team will form the core of engineers that will ultimately perform the ANS facilities design. However, the near-term activities will concentrate on developing design criteria for the architectural engineer (AE), who will become an essential team member late in FY 1990.

### 3.4. SPECIAL BOP TASKS

In the absence of full funding for design of the ANS facilities, specific topics were selected to focus the effort of the BOP team on the more critical, unresolved design issues.

#### 3.4.1 Decay Heat Removal

This study task is intended to determine the optimum method of removing heat from the reactor core during an emergency reactor shutdown and to evaluate the capability of an alternative heat removal system to safely limit the severity of an accident.

#### 3.4.2 Heat Removal System

This task addresses removal of heat from the reactor core during normal operating conditions and the development of the conceptual design of the reactor cooling system after considering such issues as overall equipment reliability, decay heat removal space requirements, etc.

#### 3.4.3 Containment Alternatives

This study will review the reference dual-containment concept, evaluate alternatives, and recommend a new baseline containment philosophy. In addressing containment, the recommendation will evaluate security requirements, free access to experiments, experiment equipment layout, and other requirements impacting the containment/building design.

### 3.4.4 Site and Building Layout

This task is focused on the functional and organizational layout of the office building, the support building, the reactor building, and the guide hall and will optimize the layout based on functional communication, maintenance requirements, reactor operations waste removal and handling, etc.

## 3.5. ARCHITECTURAL ENGINEER SELECTION

Discussions have been held with DOE regarding selection of the AE that will design ANS. Preliminary planning of the selection process and work on an advertisement for the *Commerce Business Daily* have begun. The AE will be placed under contract in the summer of 1990 if sufficient funding is available.

## 3.6 REACTOR SYSTEMS

### 3.6.1 Overview

The majority of the effort on the reactor system this year has been focused on refining the conceptual configuration based on the new core geometry. These refinements have been in the area of the CPBT, control rods, shutdown rods, irradiation sample provisions, isotope production rod provisions, and refueling concepts. An overall view of the reactor system is shown in Fig. 3.3.

Several key issues had previously been identified for special study. The lower connection of the CPBT was identified as posing particular problems in designing the connection that allows withdrawal of the CPBT up through the overall assembly while satisfying the requirements of Sect. III, Class 1 of the *ASME Code*, and in developing a test and inspection plan for ensuring the quality of the connection during operation. Cooling concepts and radiation damage for the CPBT need further study. An ASME Code case will be

required for the use of either aluminum or zircaloy in an ASME Sect. III, Class 1 component.

It was decided early in the year that the core geometry would be a two-element core. The two elements would be separated and staggered to provide an enhanced cooling configuration as shown in Fig. 3.4.

### 3.6.2 Pressure Boundary

The pressure boundary system is made up of four basic component assemblies, the upper stationary pressure containment assembly, the diverter, the lower stationary pressure containment assembly, and the CPBT (Fig. 3.5).

Refinements in the area of the CPBT configuration include generating more realistic methods of supporting the fuel elements, performing preliminary thermal analysis, and studying different configurations for sealing arrangements. The CPBT is an open-ended tube with a flange at the upper end for support and seal. The lower end has a series of vanes and a series of support cylinders to straighten and smooth the flow and to support fuel element and isotope production rod assembly. The lower end of the CPBT interfaces with the remainder of the pressure containment system with a set of radial seals. The design of the CPBT is based on using 6061 T6 aluminum.

Initial thermal analysis performed on this configuration indicates that the thermal expansion of the CPBT amounts to 1.5 mm. This translates into a thermally induced stress (if both ends of the CPBT are restrained) of 21.6 MPa, which is well below the allowable limit for the material being used. The 0.5-MN thermally induced load on the CPBT creates a critical buckling problem, which indicates that some compliance would be required in the system. The provisions for this compliance will be discussed later in the discussion of seal configurations.

The stationary portions of the pressure containment system were originally conceived to be made of 304 stainless steel. Because of

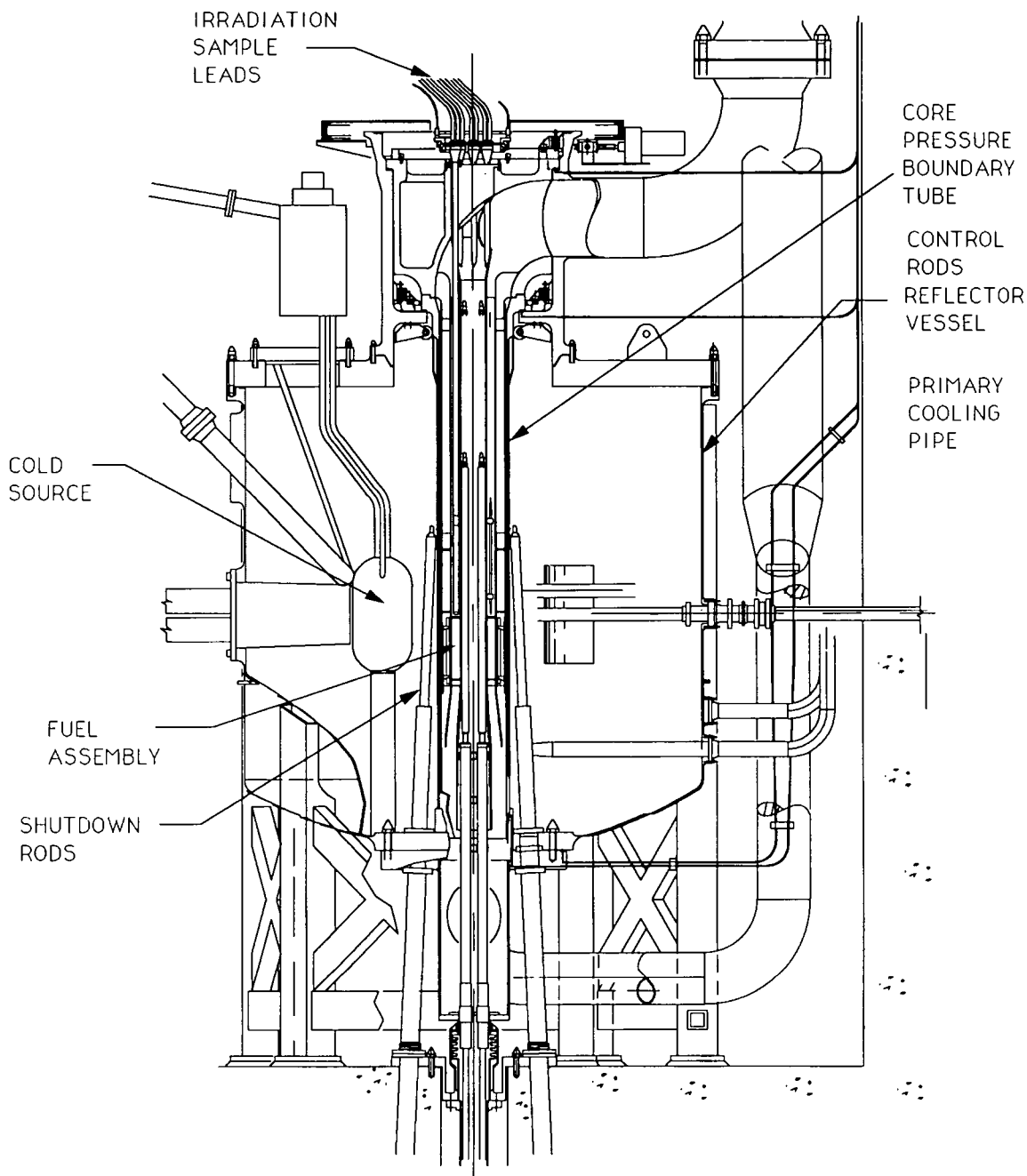


Fig. 3.3. Elevation view of the reactor system.

neutronic considerations, the decision has been made to design these components in 6061 aluminum (same as the CPBT).

The lower part of the primary pressure containment forms the interface to the lower part of the CPBT and the control rod system.

The piping leading into this part of the pressure containment system had to be split into two flow paths above midplane of the reflector vessel to miss the various beam tubes coming out of the reflector vessel. Each branch of the primary coolant pipe in this

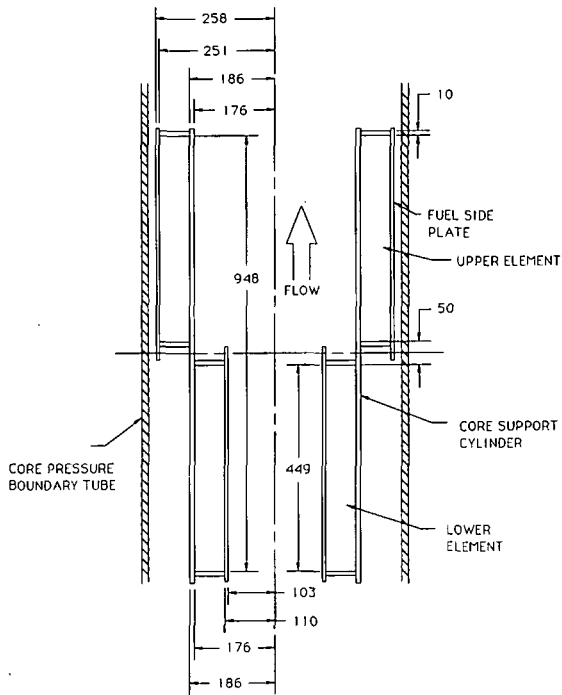


Fig. 3.4. Baseline reactor core configuration.

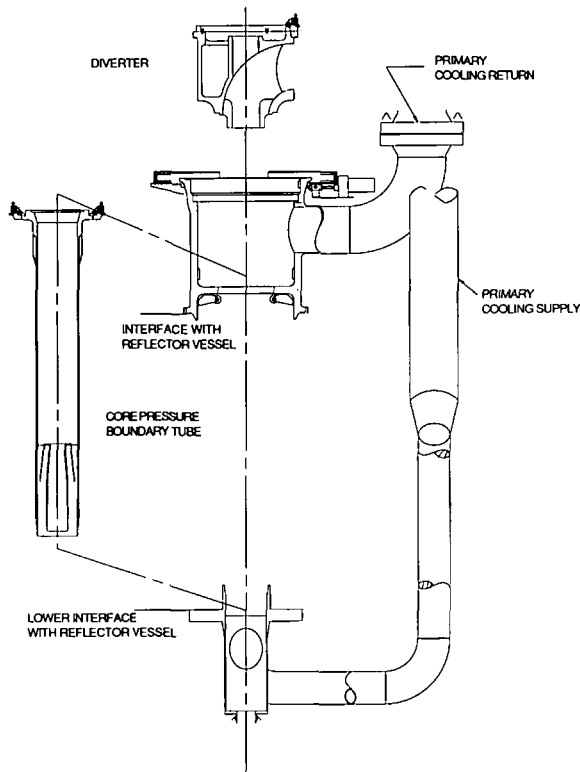


Fig. 3.5. Pressure containment components

area is made up of 16-in. aluminum pipe. These two branches "Y" back together at the lower assembly below the interface for the CPBT at a 45° angle. Every attempt is being made to guide the inlet flow into the pressure containment body in a way that would minimize turbulence and vibrations on the control rod elements. Seismic support for this assembly will be obtained by mounting directly to the bottom to the reactor pool.

The upper portion of the pressure containment assembly is somewhat more complex. The fuel elements, control elements, and CPBT will be removed through the top of the system. The upper stationary pressure containment system has the interface for the upper portion of the CPBT, the top of the reflector vessel, and the refueling system.

The upper portion of the assembly includes a flow diverter that channels the flow from the CPBT into the piping of the primary cooling system. This diverter, a removable plug that forms the upper closure for the primary pressure containment, is held in place by a large retaining ring with many tabs and slots around the upper portion of the periphery. These slots fit between tabs on the stationary part of the containment system. The bottom of the tabs on the stationary system are tapered as are the upper portions of the tabs on the diverter retaining ring. These tapered surfaces form mating wedges. As the diverter tabs are inserted through the slots on the stationary portion, the retaining ring can be rotated to engage the tabs on the retaining ring and the tabs on the stationary part. The tapered surfaces allow the retaining ring to be forced down onto the diverter, forcing it onto the seals that form the pressure boundary.

This diverter also forms the interface for the removable radiation sample assembly to be discussed later. The diverter not only has to withstand the pressure loads of the primary coolant system but also has to provide restraint for the fuel element assembly against the flow loads. These loads are reacted from

the fuel element assembly to the diverter through a support cylinder that is part of the fuel element but can be removed in a hot cell.

The upper portion of the pressure containment was, at one time, located within the reflector vessel. Because of heavy water volume considerations, thermal expansion, and design configuration considerations, this assembly was moved to a location above the reflector vessel. This arrangement requires the upper portion of the pressure containment to be removed if maintenance is to be done within the reflector vessel. Because most of the components, being supported by or penetrating the reflector vessel boundary, are designed to be removed as complete assemblies, it is unlikely that routine maintenance within the reflector vessel will have to be performed. This configuration is not considered to be a problem.

### 3.6.3 Control and Monitoring Elements

The design of the control rod system has gone through several iterations. Early concepts included eight control rods, four of which moved upward and the remaining four downward. The rods that move in the upward direction were designed to scram downward. Those that moved downward were not used in a scram mode.

The present design includes four hafnium rods that are moved as a unit for shim and control purposes, but each rod has the capability of being scrambled individually. These rods are driven from beneath the reactor assembly in a subpile room. The control element portion of the control rods can be removed and replaced from above the reactor assembly in the same manner as the fuel elements. The majority of the support for the control rod assembly comes from beneath the reactor system. Guides are placed within the cylinders, forming part of the core support and irradiation sample assemblies to give support and stability to the control rods.

The shutdown rod assemblies are in the low-pressure area of the reflector tank. These rods were at one time parallel to the CPBT nestled in close to the CPBT. This configuration required that the drive, or reset mechanism, for these rods incorporate a flexible link to bypass the lower flange of the primary coolant system and the reflector vessel.

After obtaining vendor information and performing design studies, it was determined that these flexible links had more backlash than could be tolerated in the shutdown system. Several configurations were studied further, and a configuration that employed direct linkage to the drive and reset mechanism was chosen. This required that the shutdown rods be angled toward the CPBT  $\sim 2.5^\circ$ . This is the configuration currently shown on the baseline conceptual design.

Currently, eight shutdown rods are spaced around the CPBT in a nonuniform manner. Nonuniformity is required to miss the primary coolant inlet at the bottom of the reflector vessel. Preliminary neutronics studies and analysis are being done to determine if this spacing is adequate.

### 3.6.4 Fuel Element Assembly

The fuel element assembly is made up of fuel elements, the support cylinders, and a safety latch system that latches the fuel element assembly to the CPBT. This latch is provided so that the fuel element assembly cannot be removed from the CPBT unless an absorbing cylinder is in place to simulate the shutdown rods and the control rods before removal of the fuel element.

### 3.6.5 Provisions for Irradiation Capsules

Requirements for the irradiation capsule provisions within ANS were to provide facilities equal to or better than those provided in the HFIR. After several meetings with the

user community, a configuration was arrived at to provide locations for five noninstrumented sample holders and five instrumented sample holders. Current configuration shows the noninstrumented sample holder to be our generic capsule assembly, and the instrumented capsule is similar to that used on HFIR.

Both sets of capsules are supported on a cylinder that interfaces with a plug in the diverter. This cylinder extends from the diverter into the fuel element region and provides a location for the capsules adjacent to the upper fuel element. The noninstrumented capsule assemblies are mounted in such a way that their radial location can be adjusted before installation. This allows location of the capsule to be set to tailor the spectrum to which the capsules are exposed. The instrumented sample capsules are long assemblies that interface with the plug inserted into the diverter. At the present time, the disconnect for the leads for the instrumented capsules are under study. During refueling operation, these leads will have to be disconnected before removal of the radiation capsule assembly or the diverter assembly.

### 3.6.6 Seal Configurations for the CPBT

As mentioned earlier, there are several design areas where specific studies have been initiated to look into design issues. One issue has been the seal configuration for the CPBT. There are four basic configurations for sealing the CPBT to the nonremovable portion of the pressure containment system:

1. a conventional face-type seal arrangement with face seals or flange seals at each end of the CPBT;
2. a face seal at the upper portion of the CPBT, but a radial seal at the lower end of the CPBT to allow for thermal expansion, manufacturing tolerances, and other movement between the two systems;

3. interfaces between the CPBT and the mating systems that form a controlled leakage interface using a labyrinth seal or another arrangement rather than a hard seal; and
4. a design with the CPBT as an integral part of the fuel element.

This fourth configuration could have seals of any of the other three types. This particular study is still under way. No conclusion has yet been reached. The advantages and disadvantages of these configurations are still being evaluated and will be documented in a report of the task team activities.

### 3.6.7 Refueling and Maintenance Provisions

Because the expected fuel element life of the ANS is projected to be 14 days, remote refueling or just refueling of the ANS is a big consideration. With the availability requirements imposed on the reactor, the initial indication is that the refueling cycle must be complete within a two-day period. The refueling process is further complicated by the fact that the primary coolant within the reflector tank is heavy water. The entire reactor assembly is submerged in a pool of light water. It is necessary to perform the refueling operations while maintaining separation of the light-water and heavy-water inventories.

Three different methods of refueling the ANS have been examined; this issue is the topic of another special design study task. The system that best fits our needs has not yet been determined.

The first method involves a completely self-contained refueling machine with an elaborate manipulator and a number of storage dollies (for components removed from the reactor) supported and moved on a series of tracks (Fig. 3.6). A three-dimensional, animated computer model of this method was generated to test the validity. Several things were learned from this model. Further

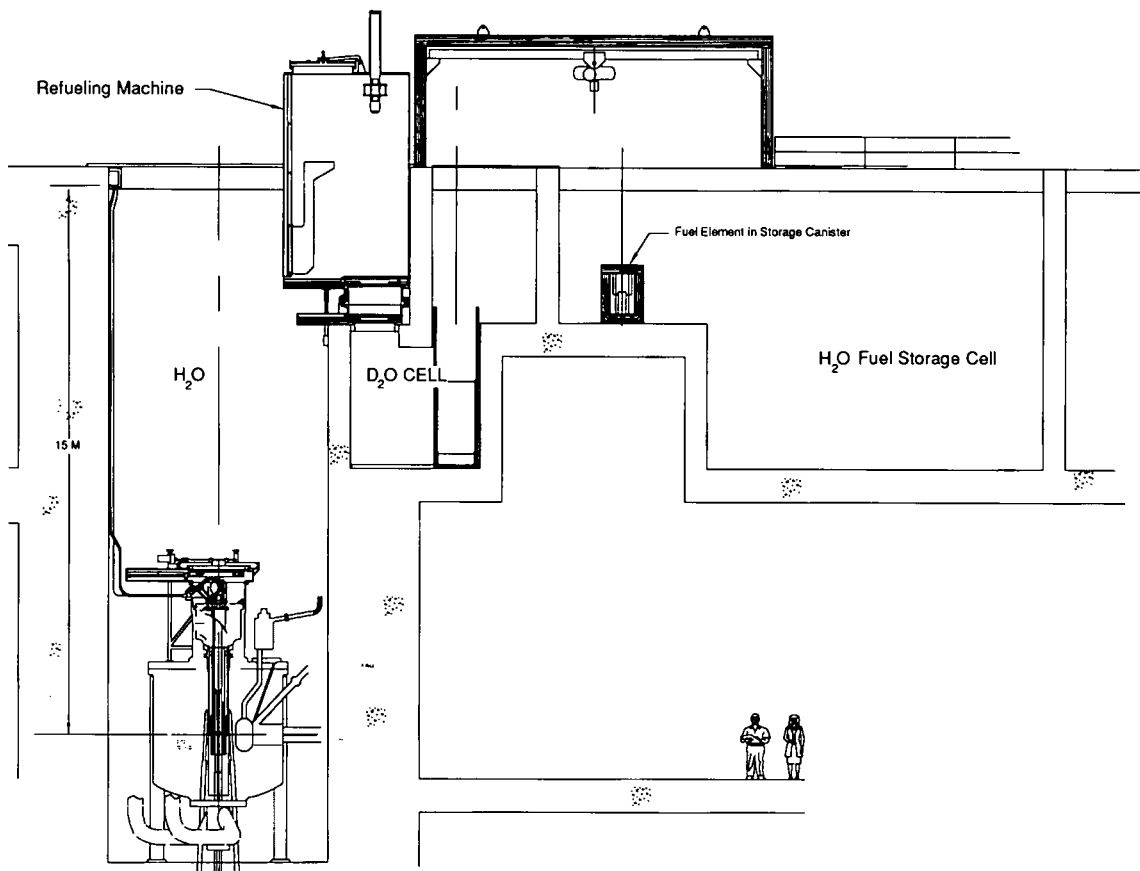


Fig. 3.6. Refueling machine shown docked with transfer cell.

studies and design configurations will be initiated.

The second configuration is a modification of the first with the volume of the refueling machine drastically reduced. The number of storage dollies or fixtures is also reduced, and the manipulator system greatly simplified (Fig. 3.7).

A third configuration is a system in which a cylinder, permanently installed at the top of the reactor system filled with heavy water, ascends to the presurface of the light-water pool. Intersecting with this cylinder is a tunnel through which components from the cylinder are moved to a transfer cell. This whole system is filled with heavy water.

## 3.7 EXPERIMENT SYSTEMS DESIGN

### 3.7.1 Overview

The design effort for the neutron beam transport systems and scattering experiments has continued in the same directions. In general, the emphasis has been on identifying the design requirements and space requirements rather than beginning actual hardware design. Minor changes in beam tube layout have been made to improve access. Cosponsored by ORNL and BNL, a workshop on Neutron Scattering Instrumentation brought

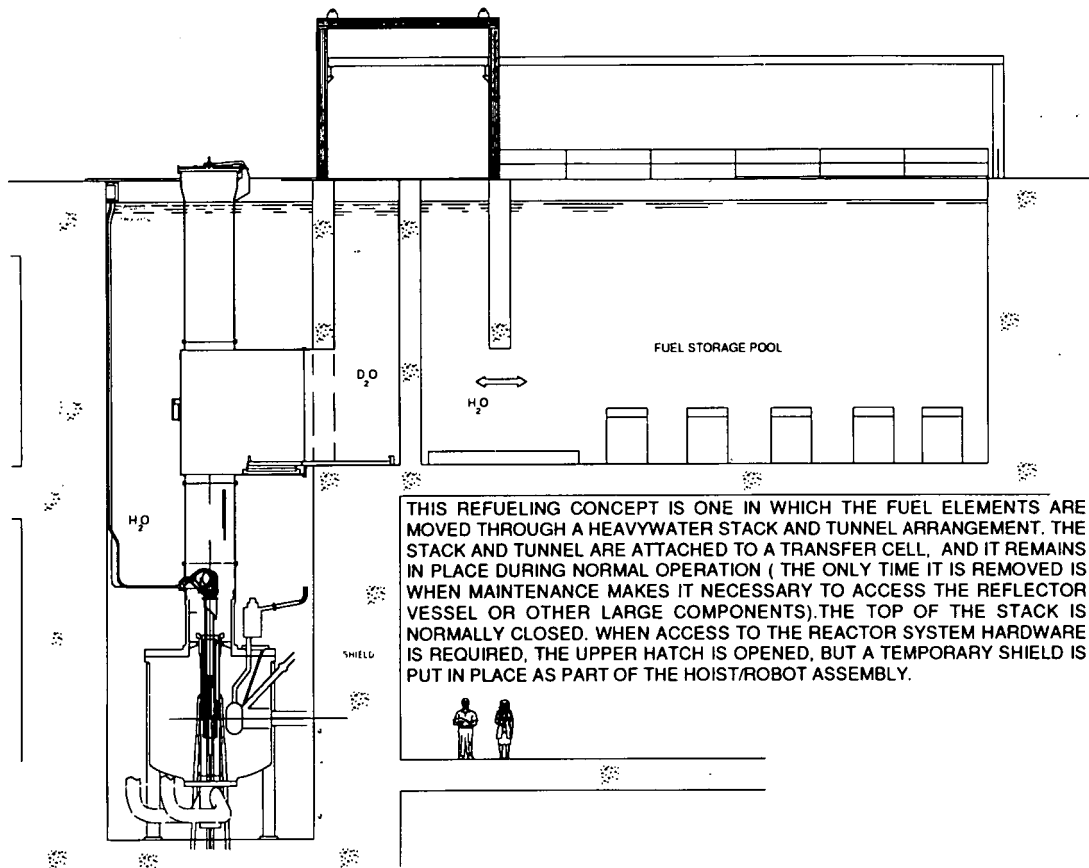


Fig. 3.7. Refueling tunnel concept.

together leading experts in this area. Their recommendations for instrumentation requirements will be used to help develop scattering instruments for ANS.

Other work on experiment systems focused on defining the flux, space, building, and support requirements for transplutonium production, special isotope production, materials irradiation facilities, and analytical chemistry facilities. In-core and reflector vessel irradiation facilities were defined, and conceptual drawings were prepared. Initial work was also started on the materials irradiation control room and the analytical chemistry laboratory in which neutron activation analysis will be performed. Initial layouts were also prepared for hot cells that will be needed to support the various experimental programs.

### 3.7.2 Beams, Scattering, and Physics Instruments

Few changes have taken place in the layout of instruments in the beam room and guide hall shown in the last progress report. The major changes in the beam room layout are the reduction in hot beams from four to two and the addition of one thermal tangential tube. In the guide hall, two outside guide tubes have been added, making a total of seven horizontal guides from each cold source. These additional guides are either strongly curved or bent and provide a clean cold beam to an analytical station and to a nuclear and fundamental physics experiment.

Since the latter involves a significant inventory of liquid hydrogen, it has been located in a cubicle with the walls arranged such that it extends outside the guide hall building.

The major effort on definition of new beam facilities is covered by the planning for a VCN guide coming out of the neck of each cold source and the arrangement of experiment stations on the second floor of the reactor building (Fig. 3.8). These VCN guides are arranged such that the guide enters the cold source through the vapor annulus above the liquid deuterium, so the very low end of the neutron spectrum does not have to pass through a thick wall to enter the guide. The

VCN guides are curved on about a 10-m radius (Fig. 3.9). One of them feeds a UCN turbine, which reflects the neutrons off a receding mirror surface to achieve extremely slow velocities. A cluster of instruments surrounds the turbine. The other VCN guide may be used directly for neutron optics or other applications. Figure 3.8 also shows a slant guide to an analytical station and a slant thermal beam to a small fission target, from which fission-fragment heavy ions are accelerated for charged particle experiments.

The desired footprint of the triple-axis spectrometer has been determined and is shown in Fig 3.10. It varies for the guide hall

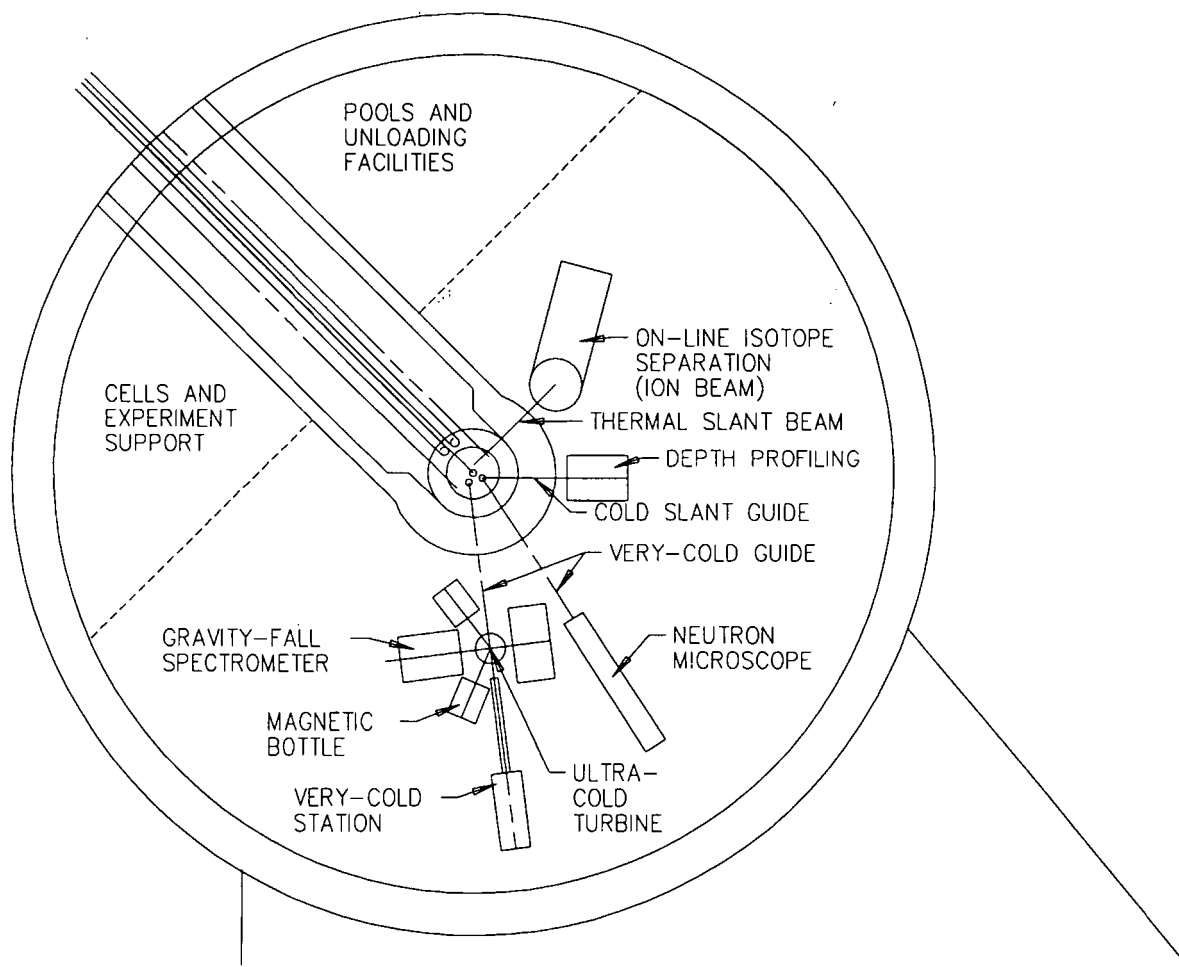


Fig. 3.8. Plan view of experiment facilities on the second floor of the reactor building.

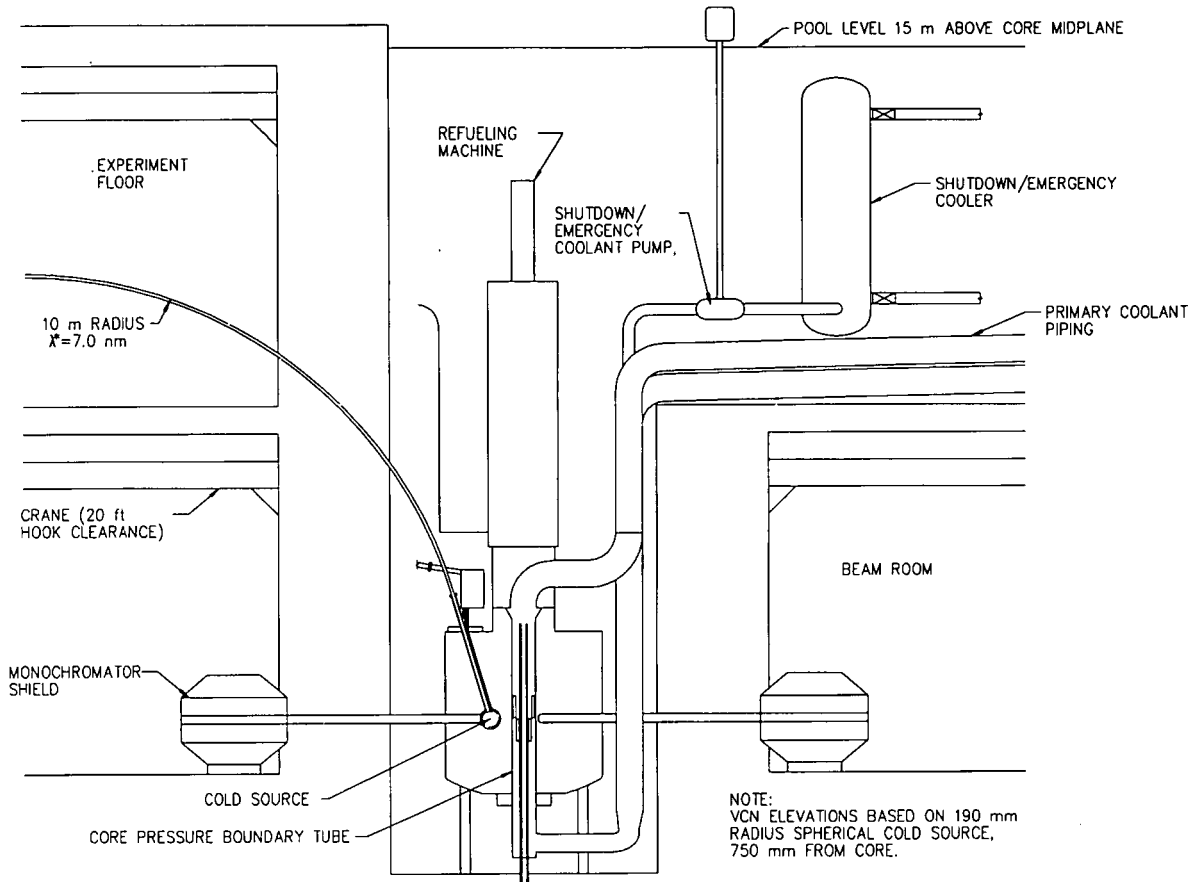


Fig. 3.9. Section of reactor assembly and pool, showing curved very-cold guide.

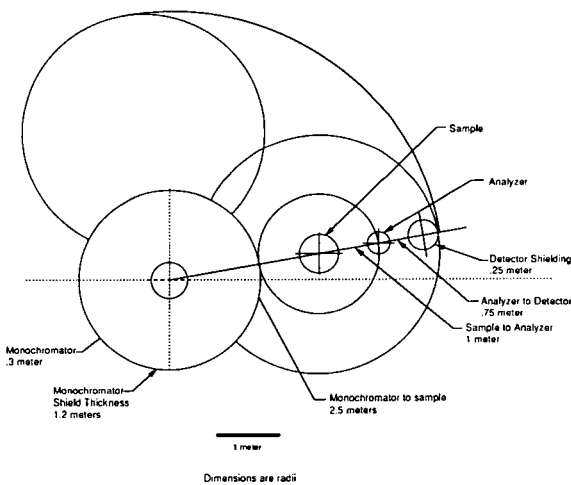


Fig. 3.10. Triple axis spectrometer footprint.

triple-axis spectrometers that have smaller monochromators. Incorporation of more well-defined experiment footprints may impact the beam guide locations.

### 3.7.3 Transplutonium Production

The fundamental criteria provided through NSCANS for transplutonium production are to provide the capability for an annual production of 1.5 g of  $^{252}\text{Cf}$  and 40 g of  $^{254}\text{Es}$ . The criteria are based on the HFIR's production capability for  $^{252}\text{Cf}$  sources (for medical, radiography, and analytical applications) and for  $^{254}\text{Es}$  sources (for heavy element research in the Large Einsteinium Activation Program).

With the present core configuration it is possible to locate the transplutonium target rods where they have less influence on the flux at the horizontal beam tubes. Thus, there is no longer a significant conflict between full-time transplutonium production and optimal use of the scattering facilities. The present concept is based on transplutonium rods located outside the lower fuel element as shown in Fig. 3.11. A portion of the primary coolant flow is diverted to cool the target rods only. Coolant for the target rods does not enter the fuel element. The basic pellet and handling configuration of the existing rods at the HFIR will be retained (except for length) to minimize the impact on the Radiochemical Engineering Development Center (REDC). The rods will be locked to the

shroud that diverts the coolant. An effort will be made to design this shroud so it can be removed separately from the fuel element. Thus, the rods can either be left in place or removed at the end of the fuel cycle.

The current concept defines the reactor end of a hydraulically operated rabbit tube located just outside the CPBT and adjacent to the upper fuel element. Epithermal flux at this location is the best available in the reflector vessel. This rabbit tube is designated primarily for small-quantity transplutonium isotope production where a high epithermal flux is desirable. With a capacity of nine HIFR type rabbits that have a total capacity of  $15.9 \text{ cm}^3$ , the tube will be offset radially at the upper end so it penetrates the flat head of the reflector vessel.

### 3.7.4 Materials Irradiation Facilities

Conceptual drawings now show the primary materials irradiation facilities located inside the upper fuel element, but outside the group of four control rods. Five positions for instrumented experiments and five positions for noninstrumented experiments are planned. The latter positions may also be utilized for transplutonium isotope production when not being used for irradiation experiments. The entire group of experiments is mounted onto an assembly that can be removed and replaced as a unit during refueling of the reactor. Instrumentation leads must be remotely disconnected and reconnected. A conceptual design for this disconnect, while deemed feasible, has not been devised at this time.

Two irradiation positions for larger instrumented materials experiments are located in the reflector vessel. At each position the experiment assembly is placed within a closed-end facility-tube. Conceptual drawings show the lower end of each facility-tube adjacent to the upper fuel element, but outside the CPBT. These facility-tubes are slanted, so their upper ends avoid the reactor refueling port. Heavy water flowing through the

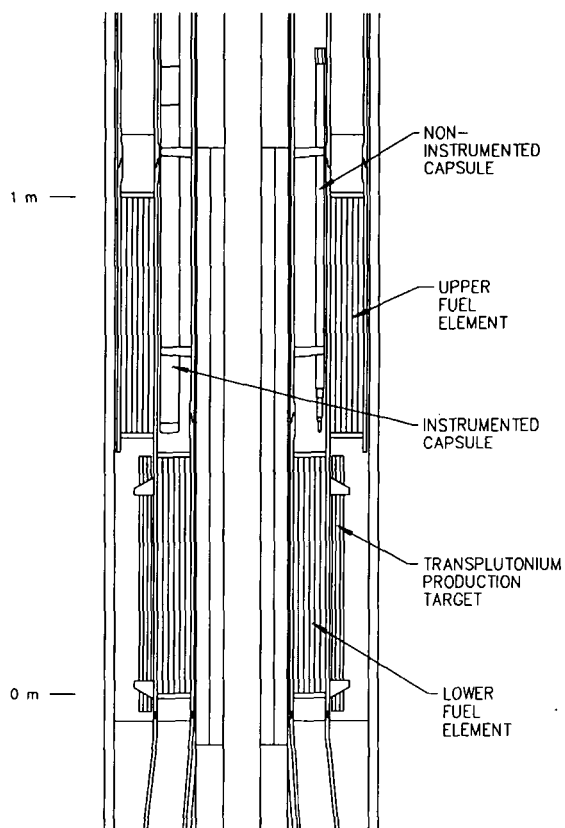


Fig. 3.11. Section of reactor core showing materials irradiation and transplutonium production targets.

facility-tube in a closed loop will be used to cool these two positions. Changing the heavy water to light water will permit the experiments to be remotely removed into the reactor pool and remotely replaced. The need to provide space for shutdown rods just outside the CPBT limited the proximity of these irradiation positions to the upper fuel element. These positions will provide higher thermal flux, and significant epithermal flux, but less fast flux than those positions located inside the upper fuel element.

### 3.7.5 Special Isotope Production

Irradiation facilities for the production of special isotopes (aside from the transplutonium production programs) will have a range of thermal neutron fluxes available. Conceptual drawings prepared to define these facilities and allocate space show seven irradiation positions in the reflector vessel. Each position is located at a different radius from the vertical centerline of the reactor core, thereby providing thermal fluxes from  $4 \times 10^{18} \text{ m}^{-2} \cdot \text{s}^{-1}$  to  $1 \times 10^{19} \text{ m}^{-2} \cdot \text{s}^{-1}$  in  $10^1$  increments. At each position the isotope target assembly is placed within a closed-end facility-tube that penetrates the reflector vessel head. Heavy water flowing within the facility-tube in a closed loop will cool each isotope target. Changing the heavy water to light water will permit the isotope target to be remotely removed into the reactor pool and remotely replaced. The isotope targets are usually not instrumented. Where the neutron flux is appropriate, materials irradiation experiments (instrumented or noninstrumented) may be installed at these isotope irradiation positions.

Three hydraulically operated rabbit tubes have been designated for special isotope production. Conceptual drawings have been prepared to define the reactor end of these tubes and allocate space for them in the reflector vessel. One of the tubes is located where the thermal flux is near a maximum ( $\sim 8 \times 10^{19} \text{ m}^{-2} \cdot \text{s}^{-1}$ ). This tube is offset

radially at the upper end, so it penetrates the flat head of the reflector vessel. The other two tubes are straight within the reflector vessel and are located where the thermal flux is  $2 \times 10^{19} \text{ m}^{-2} \cdot \text{s}^{-1}$ . Each of these rabbit tubes have a capacity of nine HFIR type rabbits.

### 3.7.6 Analytical Chemistry Facilities

Traditional neutron activation analysis facilities use a pneumatically operated rabbit tube to place a specimen into the reactor irradiation zone for a predetermined time and then retrieve it. Three pneumatic rabbit tubes are currently proposed for the ANS. Conceptual drawings show where these tubes will terminate in the reflector. The chosen locations are near the edge of the reflector vessel where internal heating rates resulting from neutron and gamma flux are  $< 1 \text{ W/g}$  of aluminum. Thermal neutron flux will be nominally  $4 \times 10^{18} \text{ m}^{-2} \cdot \text{s}^{-1}$ . Each rabbit tube will be a different size for added versatility. They will accept rabbits of 200-, 40-, and 1-cm<sup>3</sup> capacity. One shielded cell with manipulators will house the loading/unloading stations for the 200- and 40-cm<sup>3</sup> rabbits. The pneumatic tube for the small rabbit will terminate in an adjacent hood. The small rabbit will be the same size as ones currently in use at the HFIR. This small rabbit system will be useful for measurement of short-lived nuclides; for example, delayed neutron counting for uranium.

A proposed floor plan of the chemistry laboratory has been prepared. This laboratory includes chemistry laboratories, counting-rooms, one irradiation control room, one Class 100 clean room, one sample preparation room, one storage room, several offices, and a restroom. It is imperative that the counting room have a low-level irradiation background away from <sup>60</sup>Co, other gamma emitters, and cosmic rays.

Current plans also include a neutron capture, prompt gamma-ray analysis facility that utilizes cold neutrons. This facility will be

located at the end of a curved neutron guide tube at one side of the guide hall where it can be extensively shielded from gamma rays and fast neutrons.

A neutron depth profiling instrument is envisioned on the second floor of the reactor building at the end of a slanted neutron guide tube from one of the cold sources. Having a very low gamma-ray background is not as critical for this instrument.

A gamma irradiation facility will be located at one of the spent-fuel storage positions. The canister that contains the spent fuel will have an axial hole, so an access tube can be used to place specimens within the central zone of the fuel element for irradiation.

### 3.7.7 Support Facilities

Work on support facilities for experiment systems has been confined to identifying the basic support requirements and their impact on plant structures and systems.

A materials irradiation experiment control facility will be required on the second floor of the reactor building for use in monitoring the instrumented materials irradiation experiments that will be placed within the reactor. Located in this area will be a shielded valve box, instrumentation panels, a data logging system, inert gas supply and cleanup systems, and shielded gas transfer lines. This facility must adjoin the reactor pool wall to minimize the length of instrumentation leads and gas transit times to experiment capsules. Experiment controls will interface with reactor set-back controls. A preliminary list of utilities, services, storage, and office requirements has been prepared.

A hot cell complex in support of the transplutonium, special isotope, and materials irradiation programs will be needed. Work will include disassembly of irradiated capsules, assembly of new capsules using previously irradiated specimens, loading and unloading of hydraulic rabbit tubes, and transfer of irradiated specimens or rabbits to shipping casks or temporary storage.

The present sketches show a hot cell bank with restricted zone behind the cell bank for cell maintenance, an operating gallery, restricted cask transfer and specimen storage areas, a contamination control area, and C-zone change room. This must be considered an alpha-gamma facility because of the potential for release of alpha contamination within the hot cells. The location of this two-story complex has not been decided.

A transplutonium target handling facility will be located in the storage pool. At this location the transplutonium target rods will be attached to and removed from the target holder (lower flow diverter) using long-handled tools. Irradiated rods will be placed in storage racks for a short decay period before being placed in a shipping cask. All operations are done under water to minimize damage to the target rods during handling and to dissipate heat.

## 3.8 SYSTEMS INTEGRATION

Among the many elements comprising systems-related work, a particular item that has been completed during this reporting period illustrates this aspect of the project's activities. That item is the interrelationship among the many plans and assessments that have been identified as relevant for the ANS. An extensive review has been conducted to define the interdependencies among the plans and assessments in the form of information from any one of them that is needed to document completion or updating of another. Review of the timing requirements for documents was also undertaken to ensure that the schedule for preparation fully supports input to other documents as required.

This systematic evaluation verified the origin of the principal requirements; identified the need for each of the plans, assessments, and reports identified; and promoted a thorough analysis of the hierarchical relationships, dependencies, and schedules proposed.

The review, of course, focused upon the work planned to be accomplished through the design-only line-item phase. The documents included in the project's planning base have been proposed for initial draft and release as part of the conceptual design activity, which limits the level of detail, but allows for early identification of needs and interactions between them. The documents will be baselined, controlled, and updated as the project progresses beyond the conceptual design phase.

The results of the evaluation indicate that the document planning base identified for the project is appropriate, that the scheduled activities are timely, and that sufficient content can be developed for the conceptual design phase. A particularly valuable output of the

study is the compilation of the total planned activities in a format that serves as a management tool to ensure proper assignment of responsibility, coordination, and implementation of the work. Table 3.1 and Fig. 3.12 present the results of this study in tabular and schedule formats.

Table 3.1 provides information on the preparation dependencies among all of the plans and assessment reports. The approach was to identify each document as the origin of information that might be required by another. Each of the other documents was then reviewed to answer the question: is information from the origin document necessary for completion or update of this document? The result is a matrix indicating which

Table 3.1. Project document preparation dependencies

No.	Documents Title	Dependencies																											
		B1	2	3	4	5	6	7	8	9	10	11	12	13	14	15	16	17	18	19	20	21	22	23	24	25	26	27	28
B1	Project Management Plan					x	x																						
B2	QA Plan					x	x																						
B3	Project Control Manual		x	x	x					x																			
B4	Project Procedures Manual		x					x	x	x	x				x	x	x	x											x
B5	Concept Design Report																					x	x		x		x	x	x
B6	Construction Validation Report							x	x	x	x	x	x	x	x			x	x	x		x	x	x	x	x	x	x	x
B7	Systems Engineering Plan				x																	x	x		x				x
B8	Configuration Management Plan				x									x	x			x	x			x	x		x		x		x
B9	Test & Evaluation Plan										x	x										x	x		x				
B10	Construction Management Plan							x					x	x	x			x	x										x
B11	Human Factors Plan																				x		x	x		x	x		
B12	Risk Assessment								x														x	x	x	x	x		
B13	Waste Management Plan										x							x	x	x			x	x				x	x
B14	Security Assessment																						x	x	x	x	x	x	
B15	RAM Plan										x		x								x		x	x	x	x	x		
B16	Decommissioning Plan												x									x	x						x
B17	Data Management Plan								x	x	x					x	x			x									
B18	Records Management Plan								x	x	x			x		x	x	x											
B19	Value Engineering Plan											x	x										x	x	x				
B20	Operation Readiness Plan								x	x	x	x	x	x	x	x	x	x	x	x	x		x	x	x	x	x	x	x
B21	Plant Design Description								x				x		x	x						x		x	x	x	x		
B22	System Design Description								x				x	x								x		x	x	x	x		
B23	PSAR																						x			x	x	x	
B24	FSAR													x	x								x	x		x	x		
B25	PRA																						x		x				x
B26	Site Selection Report																												
B27	Environmental Assessment																						x		x				x
B28	EIS													x			x							x	x				x

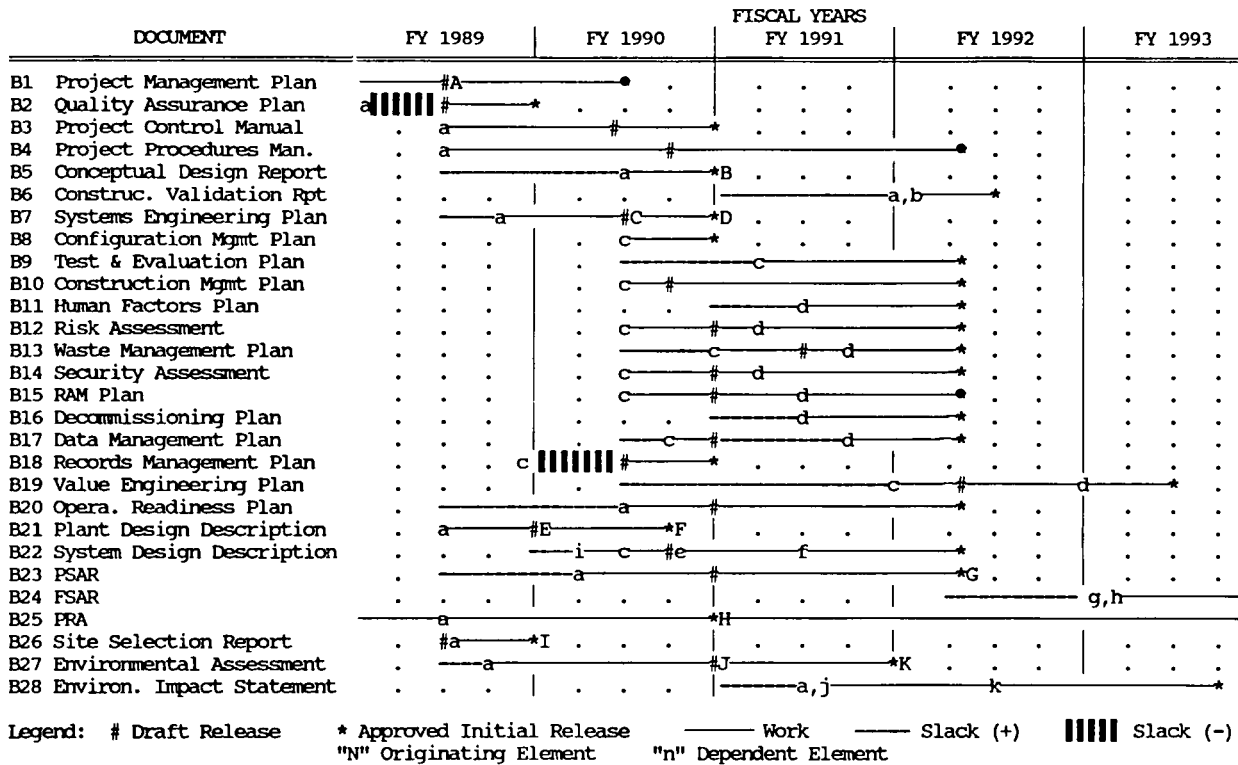


Fig. 3.12. ANS documentation planning schedule initial release milestones.

documents require input from each other for completion.

Figure 3.12 addresses the subject of document release timing and indicates the scheduled work for each of the documents through an initial approved release supporting the conceptual phase of the project. Updates and revisions to most of the documents will occur during subsequent project phases, and detailed schedules will be developed at the appropriate time.

The information illustrated in this figure includes the durations of the initial work planned for each document (solid lines) as well as the milestone points associated with a draft release and the initial release for an approved document. The scheduling of draft releases has been an important component of the project's conceptual phase planning because this allows early initiation of parallel work on lower-level documents based on the

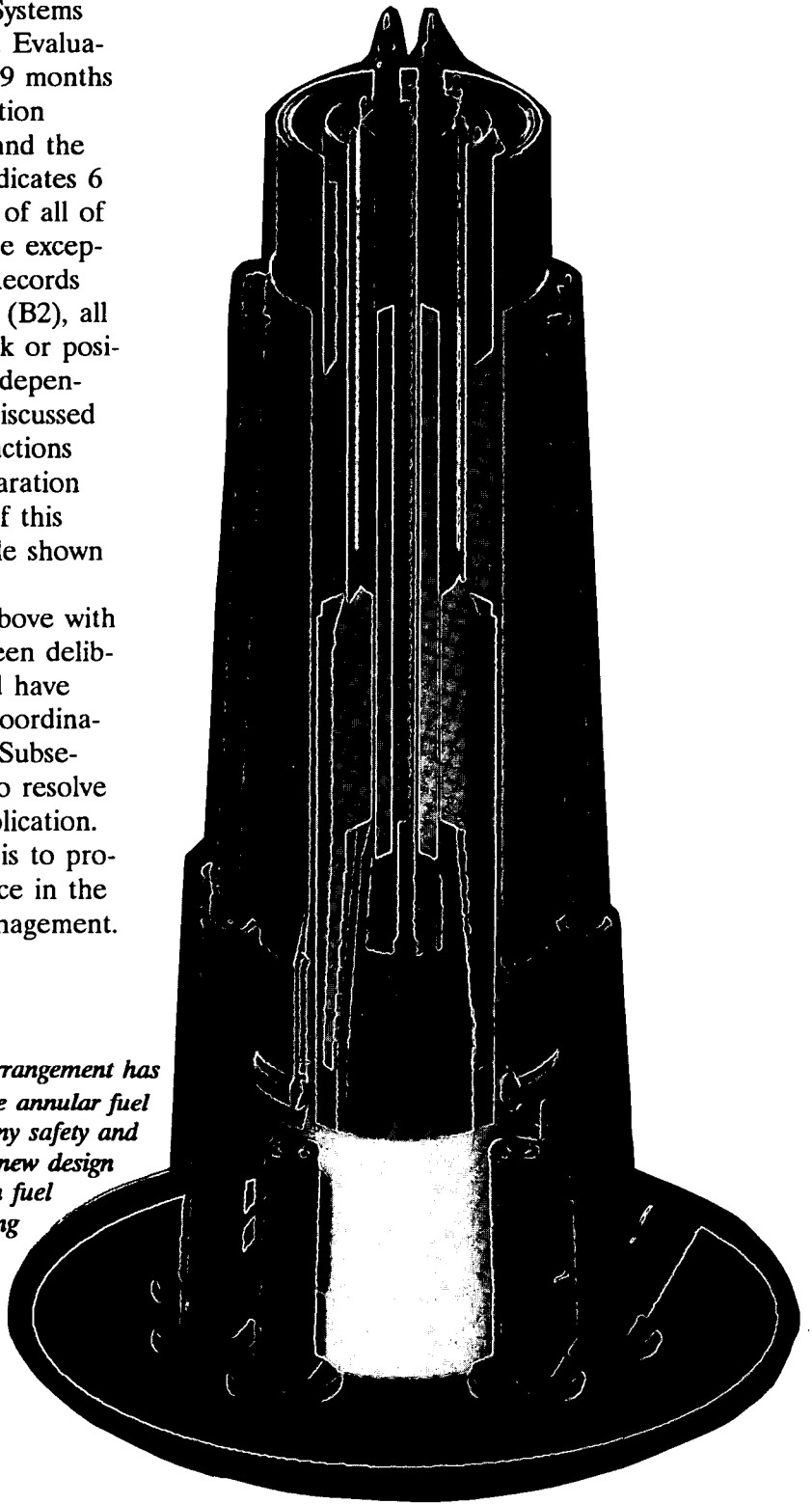
content of the drafts rather than waiting for a fully approved release.

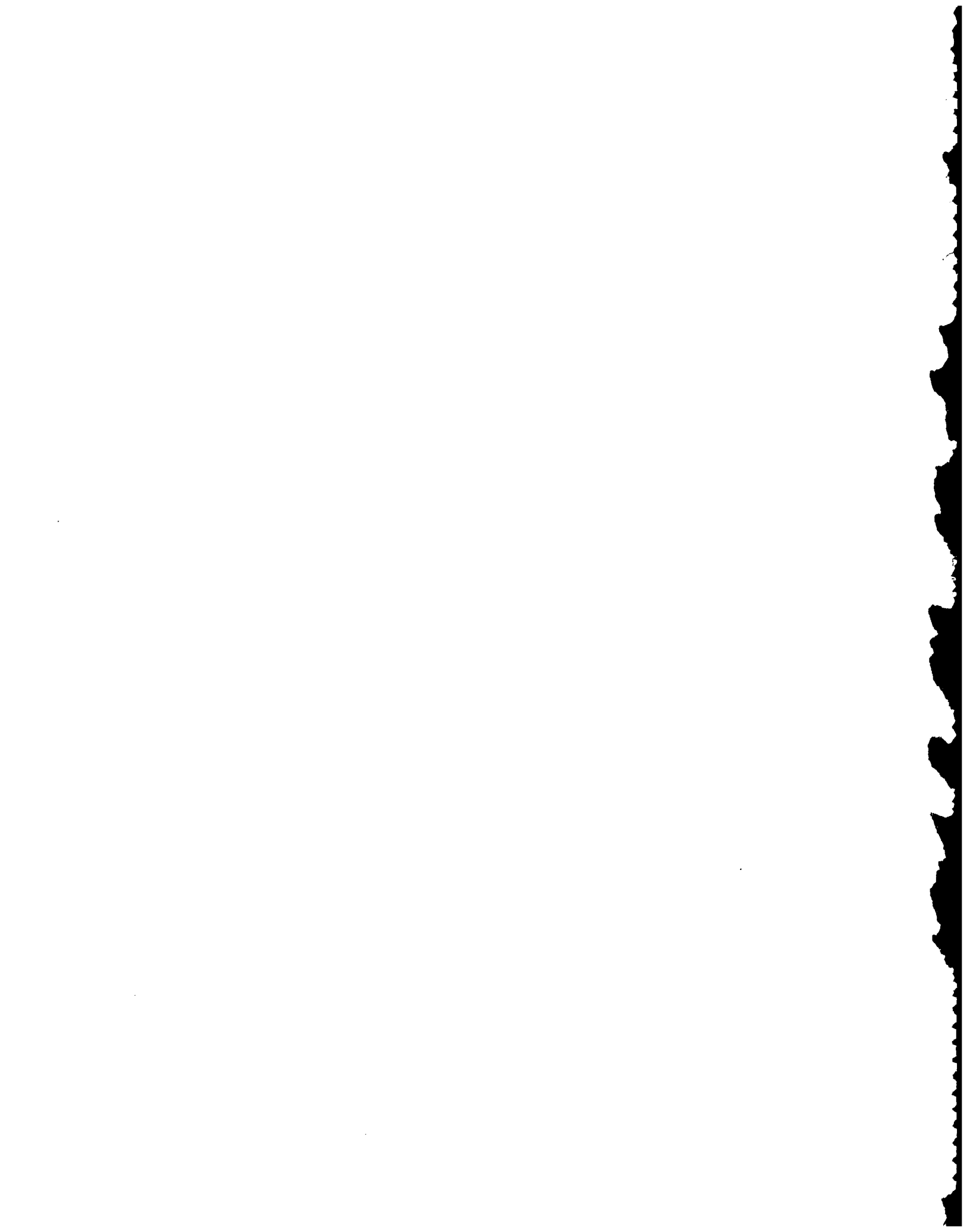
An evaluation of interdependencies was conducted for each and every document, and the results are indicated by identification of any positive (time is available) or negative (the item is late) slack. The legend used in Fig. 3.12 indicates the completion (or availability of information) point for appropriate documents as a capital letter. The time at which this information is needed by a dependent document is indicated by the corresponding lower-case letter. An example is the indication of the draft release of the Systems Engineering Plan at "C." This is the time when information is available to identify specific requirements for other documents. The documents dependent upon this information are identified by the letter "c" at the time related to that document's scheduled need for the input.

Following through with examples relative to the availability of data from the Systems Engineering Plan (B7), the Test and Evaluation Plan's (B9) scheduled start has 9 months of positive slack, while the Construction Management Plan (B10) has none, and the Records Management Plan (B18) indicates 6 months of negative slack. A review of all of the documents indicates that with the exceptions of the above-mentioned B18 Records Management Plan and the QA Plan (B2), all other documents have either no slack or positive slack relative to these schedule dependencies. The dependencies matrix discussed earlier as Table 3.1 deals with interactions between documents during the preparation phase, and the detailed scheduling of this aspect is not depicted in the schedule shown in Fig. 3.12.

The two documents identified above with negative slack (B2 and B18) have been deliberately planned for early release and have been or will be developed in close coordination with other related documents. Subsequent reviews and updates will act to resolve any remaining inconsistencies or duplication. The purpose of these early releases is to provide the project with specific guidance in the critical areas of QA and records management.

*A new research reactor core arrangement has been devised, using two separate annular fuel elements of different sizes, with many safety and performance advantages. The new design continues to use the well-proven fuel assembly technology from existing reactors, such as the HFIR at ORNL.*





## 4.1 SAFETY WORKSHOP

On October 25-26, 1988, about 60 people took part in an ANS Workshop, organized in cooperation with the ORO Office of DOE and held in Knoxville, Tennessee. Workshop participants were drawn from a diverse array of organizations, including DOE, NRC, the Tennessee Department of Health and the Environment, four national laboratories, four universities, three nuclear consulting concerns, and a public utility. Readers interested in a more detailed treatment than presented here are referred to the conference report issued by ORNL.<sup>24</sup>

After a plenary session at which ANS Project staff presented status reports on the ANS design, R&D, and safety analysis efforts, the workshop broke into three working groups, each covering a different topic: Environmental and Waste Management, Applicable Regulatory Safety Criteria and Goals, and Reactor Concepts. Each group was asked to review the Projects' approach to safety-related issues and to provide guidance on future reactor safety needs or directions for the Project.

Many constructive and positive comments and recommendations, to which the Project has been fully responsive, were made by the working groups. Selecting the most important or influential ones is difficult, but three broad findings (generalized from several more specific ones) follow:

1. The ANS Project is following, inter alia, DOE regulations for nuclear reactors; this is appropriate and also ensures compliance with applicable NRC regulations. The Project is working toward a Plant Design Requirements Document, which should include an identification of any NRC requirement that is not applicable to a research reactor of this type, together with the reasons that it is not applicable.
2. In the waste management area, the Project has taken a proactive stance toward environmental protection and safety. The effort to anticipate waste and effluent generation is important because many potential threats to the environment and to worker health and safety can be mitigated or virtually eliminated by appropriate facility design measures.
3. The recent effort by the Project to review passive safety enhancements, particularly of the basic cooling system design, is an important activity and should continue to receive attention.

During the 11 months following the workshop, the Project has taken the actions necessary to address these workshop findings. An ANS "Reference Documentation List" has been prepared and a draft issued; this document presents in an organized format the regulations, standards, and guides that are potentially applicable to the ANS, and lists

the NRC regulatory guides that are not applicable to the ANS design. In addition, an extensive study of primary coolant system design options began in June 1989 with the goal of incorporating the highest practicable level of inherently reliable features. This effort involves a multidisciplinary examination of various design options and will continue into 1990.

Subsections 4.1.1-4.1.3 briefly summarize the issues examined in the three working groups, their conclusions or recommendations, and actions taken in the intervening months since the workshop.

#### 4.1.1 Environmental and Waste Management Issues Session

This first session was chaired by T. H. Row, Director of the ORNL Environmental and Health Protection Division, and by reporter C. M. Kendrick of ORNL. Presentations were given in four areas to provide session participants with specific background information:

1. ANS Waste Generation and Handling—Fred J. Peretz, ORNL
2. Interface with ORNL Waste Management—Cindy M. Kendrick, ORNL
3. Environmental Impact Assessment for ANS—Johnnie B. Cannon, ORNL
4. ANS Site Evaluation Study—Brent Sigmon, SAIC

After extensive discussion of these topics, the consensus was that environmental and waste management issues will require continuing attention by the ANS Project team throughout the project cycle. Many potential threats to the environment and worker health and safety can be mitigated or virtually eliminated by incorporation of preventative measures into the facility design. Other concerns will be addressed through regular information transfer and interface with ORNL

support resources, such as Health Physics, Industrial Hygiene, Waste Management, and Environmental Monitoring and Compliance. New instrumentation, procedures, training program elements, and other elements will need to be incorporated by ORNL to accommodate specific aspects of the new facility (e.g., the use of tritium and heavy water) that are not currently being addressed. Four conclusions and recommendations merit specific emphasis. Following each recommendation is an indication of the action that the project has taken or plans to take:

1. *Recommendation:* Heavy water and tritium are not currently encountered in many operations at ORNL. Adjustment of worker training, radiation protection, environmental monitoring, and waste management programs will be required. Early interface with each of the affected organizations is under way and is further encouraged.  
*Action:* Continuing Project policy is to maximize interface with the ORNL support groups that will have to implement the needed safeguards. Long-term project plans call for extensive worker training and retraining.
2. *Recommendation:* Process monitoring (e.g., cooling loops, pool water, stack, ambient air, process waste, solid waste, etc.) would help give early indications of problems and was recommended for inclusion in the design, if not already included.  
*Action:* A significant I&C development effort is included in the project R&D plans. One major goal of this activity will be to determine the optimum level of process instrumentation and automation.
3. *Recommendation:* Public awareness should be managed by a planned campaign. Early involvement of regulators helps anticipate and avoid problems before they can cause project delays. A reading room in the Oak Ridge Public Library, a portable ANS display for technical meetings across the

country, and expanded use of the planned newsletter were suggested.

*Action:* This long-range recommendation will be pursued on a timely basis in coordination with the Environmental Impact Assessment schedule.

4. *Recommendation:* Information exchange with other sites was recommended. Regular visits to Canada, Los Alamos National Laboratory (LANL), BNL, Savannah River Plant, and ILL (Grenoble, France) were suggested, as well as interaction with the fusion community.  
*Action:* Project personnel have traveled widely during FY 1989, to BNL, National Institute of Standards and Technology (NIST), and to meetings of the newly formed Aluminum-Fueled Reactors Users Group, which provides a forum for representatives of the DOE reactors at BNL, INEL, and Savannah River Laboratory (SRL) to share safety-related reactor experience. Tours of the heavy-water handling facilities in Canada and at the highly successful ILL reactor in Grenoble, France, are scheduled for FY 1990. Contact with outside groups has made valuable experience available to the Project and will do so to an even greater degree in the future.

#### 4.1.2 Applicable Regulatory Safety Criteria and Goals Session

This second session was chaired by J. R. Buchanan, Director of the Nuclear Operations Analysis Center at ORNL, and reported by Michael D. Muhlheim, JBF Associates, Inc. This workshop session was structured to present the ANS Project approach and to elicit opinions and discussions from workshop participants as to the correctness and completeness of the ANS approach to defining safety goals and criteria. To stimulate discussion and provide participants with background information, presentations were given in four areas:

1. Identification of Regulations, Guides, and Standards Applicable to the ANS Design—J. R. Buchanan, ORNL
2. Permitting Process for ANS Regulatory Review—David Gruber, Impell
3. LANL DOE/Energy Research Safety Role—J. E. Hyder, LANL
4. Licensing Perspective for NRC Research Reactors—Ted Michaels, NRC

The overall conclusion of this working group discussion is that the safety criteria and goals applicable to the ANS must be identified before the completion of the conceptual design stage. An obvious and basic tenet of the ANS project approach is that DOE regulations for nuclear reactors apply to the ANS project. Especially significant is DOE 5480.6, which is intended to ensure the "Reactors are sited, designed, constructed, modified, operated, maintained, and decommissioned in a manner that gives adequate protection for health and safety and will be in accordance with uniform standards, guides, and codes which are consistent with those applied to comparable licensed reactors." This regulation also requires that the General Design criteria specified in the *U.S. Code of Federal Regulations*, "Title 10, Part 50, Appendix A," shall be applied to all new DOE reactors. Therefore, both DOE and much of the NRC regulations and standards are applicable to the ANS.

To develop a list of NRC regulations applicable to the ANS, the project has initiated a comprehensive review of the NRC research and power reactor regulations. Because many of the NRC regulations are prescriptive to specific reactor types, it will be necessary for the review to consider the intent behind each regulation and to determine if an intent could reasonably be applied to some aspect of the ANS design.

The following specific recommendations and conclusions were reached:

1. *Conclusion:* In the current climate of DOE's rapid organization and philosophical change, it is essential that the ANS

Project continue the established policy of seeking guidance from the NRC regulations.

*Action:* This is a basic tenet of the ANS Project Policy and will continue to be so for the foreseeable future.

2. *Recommendation:* The ANS Project needs to document its position on NRC regulations. The Plant Design Description (PDD) document should specify criteria and regulations that the ANS facility design will follow, and the lower level System Design Descriptions (SDDs) should detail implementation of the regulatory criteria.

*Action:* An ANS PDD is being developed that will specify regulations, standards, and goals for the facility. The systems level documents, the SDDs, are to be developed later in the conceptual or detailed design phases of the project. The SDDs will specify how the applicable standards are to be implemented and will identify what, if any, parts of the potentially applicable regulations are inappropriate for application to the ANS.

### 4.1.3 Reactor Concepts Session

This session was chaired by John F. Marchaterre, Director of the Reactor Analysis and Safety Division at ANL and reported by Phillip B. Thompson, Martin-Marietta Energy Systems Engineering. The objectives were to review the approach being taken by the ANS project team, define any safety issues, and identify design variations or considerations for the project team to include in their planning base for future work. Mike Harrington (ORNL) presented a brief review of salient ANS safety issues, and introduced talks to which the workshop participants were encouraged to respond in an interactive manner:

1. Transient Protection—L. C. Oakes, ORNL
2. Coolant Systems—F. J. Peretz, ORNL

3. Inherent Safety Considerations—B. S. Maxon, ORNL
4. Severe Accident Analysis—S. R. Greene, ORNL

Since the design at the time of the workshop was in the preconceptual stage, the working group discussions provided a valuable forum for the participants to discuss different options and choices for the reactor design. The following specific comments, conclusions, and recommendations reached in the workshop:

1. *Recommendation:* The design of the fuel plates is a welded-structure concept. The axial thermal growth should also be considered in this design to ensure that the plates will not fail (buckle) when exposed to the limiting maximum temperature differential conditions. It is understood that a finite-element model analysis is planned and the welded ends are needed to match critical velocity requirements.  
*Action:* Extensive laboratory testing and computer calculations are included in the R&D plan to evaluate the structural behavior of the fuel and core. One goal of this task is to define an acceptable design envelope for use in accident analyses.
2. *Recommendation:* Calculations supporting reactivity coefficients will require continued refinement to gain confidence in these calculations as input to the design of the control systems.  
*Action:* Planned ANS R&D will provide an orderly progression of interim to final calculations, and then measurement (in a critical facility) of the reactivity coefficients used in the accident analysis of the reactor.
3. *Recommendation:* The reference design concept of control rod scram systems as spring-driven and gravity-assisted is considered to be an appropriate choice.

*Action:* The Project has continued the development of suitable spring-driven, gravity-assisted control rod designs for the shim-safety rods.

4. *Recommendation:* Verification of the codes used to calculate these control systems' characteristics is essential. Careful validation is necessary to ensure that results match ANS requirements and conditions.

*Action:* The transient response code utilized by the I&C Division to perform analyses of the reactor response to transient upsets has been successfully benchmarked against the SPERT-II reactivity insertion data.<sup>25</sup>

5. *Recommendation:* Probabilistic risk assessment (PRA) input should be used as guidance for actual events to be considered in the failure modes and effects studies. It is understood that the present accident analysis effort is used as a screening tool; however, this must be followed by more definitive assessments derived from the PRA activity.

*Action:* Project safety analysis plans provide resources for increasingly detailed PRA studies in the coming years.

6. *Recommendation:* The addition of loss-of-heat-sink accident to the list of events being evaluated should be considered for possible core damage parameters.

*Action:* The loss-of-heat-sink accident is included in the list of design basis events currently under development for the ANS PDD.

7. *Recommendation:* A loss-of-flow accident would favor using an upflow design and should receive considerable attention in any final assessment of flow direction options.

*Action:* The adoption of upflow for core cooling, under tentative consideration at the time of the workshop, is the current reference design for the ANS.

8. *Recommendation:* Consideration should be given to variations in the placement of

the main heat exchangers, which include increasing the elevation above the core to enhance natural circulation, the elimination of any long horizontal piping runs to enhance stability, and possible inversion of the U-tubes within the heat exchangers. In any event, all nonessential loop seals, which may act as liquid traps during a thermosyphon process from the core, should be eliminated.

*Action:* The current ANS reference design has eliminated liquid traps by horizontal placement of the main heat exchangers. The ongoing cooling system design options studies are considering various alternative cooling system designs using, among others, the criterion that nonessential loop seals be avoided.

9. *Recommendation:* Passive vs active systems are preferred but must be evaluated with respect to a high-power density core design.

*Action:* The ongoing cooling system design studies have as a basic ground rule that the maximum practicable degree of passive cooling is to be built into the cooling system.

10. *Recommendation:* An overall strategy for loss-of-coolant accidents (LOCAs) must be defined (size of breaks specified) for design analyses to be conducted effectively and design choices to be made and defended.

*Action:* The overall strategy for pipe break events has been selected and will depend heavily on the leak-before-break approach to show that double-ended breaks in large piping are not credible. The specification of design basis breaks is currently under development, and the tentative decision is to specify that the design basis pipe break be a sudden opening in the primary coolant pressure boundary of flow area equal to or greater than the area of the largest pipe connecting the major (152-mm diameter, or greater) primary coolant piping.

Piping diameters <152 mm will be considered breakable because the conservatism of the leak-before-break approach becomes diminished as the diameter of the pipe decreases. The reactor protection and cooling systems must function to prevent significant fuel damage in the design basis pipe-break event. The incredible event of rapidly occurring double-ended break in major ( $\geq 152$  mm) piping will be analyzed as part of the ANS severe accident analyses for the Level II PRA; fuel damage is a distinct possibility for such worst-case evaluations.

11. *Recommendation:* Depressurization accidents are not fully dependent on large pipe breaks and will require separate evaluation and assessment.

*Action:* The list of design basis accidents being developed for the ANS PDD includes anticipated depressurization events independent of pipe break, such as the stuck-open letdown valve with coincident loss of the makeup pumps event or a stuck-open safety valve event.

12. *Recommendation:* Double-ended pipe-break accidents are not considered to be likely (or probable) for the ANS systems design but will still require appropriate review and evaluation. The use of a probabilistic approach, which will also require appropriate peer reviews and validation is being considered.

*Action:* Work performed for the Project at BNL has scoped out a probabilistic fracture mechanics leak-before-break approach that subsequently has been reviewed by ORNL. The ANS leak-before-break design and safety analyses will receive appropriate review in the coming years.

13. *Recommendation:* Consideration should be given to reducing the system operating pressure with respect to actual margins needed and the advantages to be gained with respect to accident response characteristics.

*Action:* For the 67.4-L final pre-conceptual core design selected in January 1989, a lower operating pressure has been specified: 3.7 MPa at the core inlet.

14. *Recommendation:* Because the design is at an early stage, now is the time for simplification and attention to providing as much passive safety as possible in the design.

*Action:* The ongoing cooling system design studies have as a basic ground rule that the maximum practicable degree of passive cooling is to be built into the cooling system.

15. *Recommendation:* The Project should ensure early interaction between the design team and the severe accident analysis effort.

*Action:* Since the workshop, several severe accident studies have been completed; these studies, and most severe accident studies, have implications mainly for containment design. The principal investigator for ANS severe accident analysis is a charter member of the recently formed containment design options study team.

16. *Recommendation:* Continued focus on key issues is perceived to be the appropriate direction in which to concentrate limited resources. Detailed severe accident evaluations should be resisted until the design has evolved sufficiently to support increased activity.

*Action:* Broad, conservative scoping evaluations are being conducted instead. Detailed severe accident evaluations will be initiated  $\sim 2$  years from now for the Level II PRA.

17. *Recommendation:* The use of university programs in which student assignments might be available should be considered to support development of the truly significant issues to the next level of understanding. This approach would offer a means to proceed on crucial topics without major increase in funding requirements.

*Action:* Talks have been held and discussions are on-going with representatives of Rensselaer Polytechnic Institute about possible severe accident topics appropriate for university research.

18. *Recommendation:* A careful evaluation of the applicability of the "commercial reactor" approach to the ANS analyses should be made. The specific concern here is directed to the issue of hydrogen detonation—cold sources in proximity to the core. While the specific concern was hydrogen detonation, the general concern was that care must be used in applying LWR codes to ANS. Appropriate tools must be developed for use in analysis of a new research reactor, including the correct application of existing codes.
- Action:* The severe accident studies conducted since the workshop have demonstrated the difficulty of direct implementation of some of the codes developed for severe accident analysis of light-water power reactors, especially where specific geometries, masses, materials, or phenomenological models have been built into the code. Significant resources are designated in the safety plan for the adaptation and improvement of severe accident analysis codes.

## 4.2 REGULATORY SAFETY CRITERIA

To identify regulations, standards, and guides that must or should be followed, the ANS project enlisted the help of the ORNL Engineering Technology Division's Nuclear Operations Analysis Center. This group has provided technical assistance regarding regulatory-related issues to the NRC for over a decade and has recognized expertise to make judgments in this area. NRC, as well as DOE, regulations were screened for applicability to the ANS reactor project. Their efforts culminated in a compilation of all the

regulations, guides, and standards potentially applicable to the ANS reactor. This compilation, entitled "Reference Documentation List for the ANS," was issued in draft form in April 1989 and includes not only the DOE and NRC but other primary federal agencies and a myriad of organizations issuing industrial and institutional standards and guides. The Reference Documentation List (RDL) for the ANS is intended to be utilized as a resource book for the preparation of the ANS PDD and for the lower-level SDDs. In any case, the authors have been careful to indicate regulations, standards, and guides that are considered mandatory and directly applicable to the ANS and that are cited in DOE or NRC regulations as examples of good practice and not mandatory. In either case, the ANS PDD and SDDs will specify in detail how the regulations, standards, and guides are to be applied to the design. A significant resource used in the preparation of the ANS RDL was a similar document compiled for the ATR; the Project is indebted to D. W. Croucher (INEL) for providing this assistance. The following paragraphs briefly summarize the contents of the ANS RDL.

Reference documents are listed in the ANS RDL in two different ways: by issuing organization and by plant system. Appendix A of the ANS RDL lists the reference documents by issuing organization in alphabetical order, from "A" (Air Conditioning and Refrigeration Institute) almost to "Z" (Water Resources Council). In Appendix D of the RDL, the same reference documents are organized by functional category: (1) General, (2) Site Characteristics, (3) Principal Design Criteria, (4) Safety Class System Design, (5) Non-safety Class System Design, (6) Radioactive Waste Management, (7) Radiation Protection, (8) Accident Analysis, (9) Conduct of Operations, (10) Operating Controls and Limits, (11) Quality Assurance, (12) Human Factors Engineering and Human Reliability, and (13) Miscellaneous. The net result is a comprehensive, usable listing of potentially applicable regulations, standards, and guides.

### 4.3 TRANSIENT THERMAL-HYDRAULIC ANALYSIS

The basic objective of this activity for FY 1989 was to have an accepted computer code for transient thermal-hydraulic accident analysis in place at ORNL, with the necessary accompanying input data for the ANS conditions. For reasons enumerated later, the computer code RELAP5<sup>26</sup> was selected for ANS accident analysis. It was decided that optimum progress could be made by a cooperative effort between ORNL, the lead laboratory for the ANS project, and INEL, the laboratory that developed the RELAP5 code and continues to maintain and improve the code. Early planning discussions revealed that some of the basic thermal-hydraulic correlations in RELAP5 might not be directly applicable to the geometry and fluid conditions of the ANS. This year's activity therefore included a code improvement effort, as described in Sect. 4.3.1. A. E. Ruggles of ORNL identified the needed modifications, and code development personnel at INEL implemented the recommended changes to RELAP5.

The process of calculating the input parameters necessary to describe the geometry, fluid and thermal characteristics of a particular reactor is known as "modeling" and is a difficult process that requires experience with the mathematical attributes and capabilities of the code. As discussed in Sect. 4.3.2, model development for a RELAP5 model of the ANS reactor and primary coolant system was successfully completed and test cases were run for a variety of pipe-break accidents. The model development was performed at INEL by C. D. Fletcher, and the QA function of review and checking was performed by N. C. J. Chen of ORNL. In coming years, necessary modifications to the RELAP5 programming will continue to be performed at INEL and analysis done at ORNL or at INEL, depending on the scheduled analyses and availability of personnel.

Section 4.3.3 describes the results of an investigation by N. C. Chen of the thermal-hydraulic limits for low-flow and natural-circulation cooling of the ANS fuel. This effort, of no direct relation to the RELAP5 code improvement and modeling efforts, was undertaken to provide guidance to the ongoing coolant system design options study.

The transient thermal-hydraulic code RELAP5 has been chosen as the preferred code to do LOCA and two-phase, natural-circulation analysis for ANS safety assessment. It is a one-dimensional, nonequilibrium system code developed by INEL through NRC programs. RELAP has been used over the past 15 to 20 years by both regulators and industry to assess the performance of LWRs under various postulated accident conditions. Code improvements are still supported by NRC funding; the Code is recognized throughout the industry as a primary thermal-hydraulic accident analysis code. RELAP5 was chosen for the following reasons:

1. RELAP5 versions already contain some of the modifications necessary for ANS analysis (e.g., D<sub>2</sub>O properties, low-pressure modifications, etc.), and the code has already been used for analysis of ATR postulated accidents.
2. Multidimensional effects, for which RELAP does not account, are expected to play a minor roll in dictating overall system behavior because of ANS system design features such as its highly subcooled D<sub>2</sub>O in upflow. However, if RELAP5 analysis indicates that two-phase multidimensional effects are important for certain system designs or certain transients, this decision will have to be reevaluated for those particular conditions.
3. ORNL personnel have used various RELAP versions on many projects over the past several years and are very familiar with the operation of this code.
4. RELAP5 has also been chosen to do the HFIR LOCA analysis, and similarity between HFIR and ANS cores lead to

synergism in the code development process.

5. RELAP5 can be executed in combination with the modular SCDAP code in order to analyze certain scenarios involving fuel damage. This capability may prove useful for ANS severe accident analysis.

Various transients are to be studied both for design input and safety analysis. The major transients of interest fall into three broad categories: (1) loss-of-pressure transients, (2) increasing power transients, and (3) low coolant flow transients. Loss-of-pressure transients occur in highly subcooled systems when there is a primary system leak. The most severe location for a leak or pipe break is on the pump exit side of the primary loop. This allows pressures at the core inlet to reach 1 atm, and core exit pressures to become subatmospheric. In turn, these exit pressures may be below the local saturation pressure, causing vapor voiding or choked-flow conditions at the core exit. The consequences of this event depend on the time required for the coolant to reach saturation conditions.

Increasing power transients would be initiated by a reactivity disturbance, such as a spurious withdrawal of control rods. Coolant pressure and flow remain at or close to initial values, but reactor power would increase until arrested by inherent negative reactivity feedback or by insertion of the control rods. As power increases, the coolant temperature at the core outlet increases, and hot channel or hot-spot boiling is a possibility. The consequences of an increasing power transient depend on the magnitude and speed of the reactivity disturbance.

Low coolant flow transients result from a mechanical or electrical failure in one or more of the coolant pumps. The result is a decrease of coolant flow to the reactor core and an increase in the coolant temperatures. The consequences of these transients depend on the character of the coolant flow reduction

and its accompanying simultaneous loss or degradation of primary coolant pressure.

### 4.3.1 RELAP5 Code Improvement

Following selection of the code, a task was undertaken to examine RELAP5 and to determine if the models and correlations used in the code were appropriate for investigating ANS geometry and fluid conditions. A. E. Ruggles distributed two memoranda that describe his review of the RELAP5 hydraulic and thermal models and assessment of their applicability in the narrow rectangular flow channels used to cool the fuel element of the ANS reactor. Several RELAP5/MOD3 models were identified that are not appropriate for use in narrow rectangular channels or in high mass flux (i.e.,  $G > 10,000 \text{ kg/m}^2\text{s}$ ) subcooled flows. These models influence subcooled void generation, subcooled boiling pressure drop, boiling natural circulation, and positive-quality critical heat flux. Presently, three specific modifications to the RELAP5/MOD3 code have resulted from the review. The code with these modifications is only applied within the fuel element region of the reactor model.

The first modification replaces the original Dittus-Boelter single-phase, forced-convection heat-transfer coefficient with the Petukhov correlation that has been selected for ANS design work. The 1930 Dittus-Boelter model does not explicitly include the effect of thermophysical property variations. The ANS reactor operates at high heat flux levels and with substantial subcooling. Thus the heat transfer coefficient will increase significantly because of the lower viscosity near the heated wall. The Petukhov correlation<sup>27</sup> has replaced Dittus-Boelter because it more appropriately models property variations, and because it compares more favorably with experimental data in the velocity and property range of interest. Although it gives only a 2% increase in the heat transfer coefficient at full-power operation, the increase in the

calculated heat transfer coefficient becomes more significant as the power level is increased toward the critical heat flux value. The single-phase, forced-convection, heat-transfer coefficient is important to oxide growth calculations and influences the critical heat flux and incipience of boiling predictors.

The second modification extends the critical heat flux correlation developed by Groeneveld.<sup>28</sup> The Groeneveld correlation is based on tabulated values extending to a mass flux of 750 kg/m<sup>2</sup>s. The Gambill-Weatherhead correlation is used when mass flux values exceed 10,000 kg/m<sup>2</sup>s and is well-validated by subcooled critical heat flux data taken in high mass flux situations. This extension of the Groeneveld model is necessary because the ANS fuel element nominal coolant mass flux is ~27,000 kg/m<sup>2</sup>s.

The third code modification alters the interfacial drag terms in the slug flow regime to reflect the drift flux behavior in narrow channels first reported by Griffith.<sup>29</sup> Used by Mishima, et al.,<sup>30</sup> the Griffith model has successfully predicted measured flow behavior in narrow channels. This change essentially lowers the interfacial drag and results in a lower void fraction for a given flow quality. The existing bubbly-to-slug and slug-to-annular flow regime transition criteria were retained. The implementation of this model is important to accurate prediction of boiling natural circulation and positive-quality critical heat flux during low mass flux situations.

Several areas of concern were not addressed directly by the code modifications. The models for subcooled void generation and subcooled boiling pressure drop in RELAP5/MOD3 are not validated for ANS flow conditions and still require attention. The positive-quality critical heat flux model is also not validated for the narrow channel geometry. Experimental efforts planned for 1991 and beyond will improve our understanding in these areas.

### 4.3.2 Development of a RELAP5 Model of the ANS

A careful and orderly process was followed for the development of the ANS RELAP5 model. After initial investigation and planning, a meeting was held at INEL to review the proposed modeling approach and to elicit comments and recommendations from a peer group of expert developers and analysts. Subsequently, the detailed work of developing code input for the ANS model proceeded in a step-by-step fashion: each major segment of the code was developed, copies of the resulting model development notebook were sent to ORNL for detailed review, and the segment was tested for proper execution on the computer. There are five major model segments: (1) core and CPBT/reflector tank, (2) main loop piping and components, (3) emergency loop piping and components, (4) the makeup/letdown equipment, and (5) core neutronics. The specific design parameters utilized for the input parameters are those specified in the March 1989 draft of ORNL/ANS/INT-1, *Preliminary Description of the Advanced Neutron Source*.

After all five segments were completed, they were combined into one RELAP5 input file that describes the ANS reactor. Test cases, including small (51-mm diam), medium (152-mm diam), and large (325-mm diam) pipe-break accidents were calculated. As discussed in Sect. 4.1.3 (Item 10) of this report, the 152- and 325-mm breaks are not in the ANS design basis (leak-before-break approach used instead); however, the system response to these accidents determines the margins to fuel damage for beyond-design-basis analysis of severe accidents. The 51-mm break is within the ANS design basis, and RELAP5 analyses are necessary to demonstrate the efficacy of cooling-system mitigative features in preventing fuel damage in the event of such an accident. Each of the pipe breaks for the test cases is located between

the primary coolant pump discharge and the core inlet because this location results in the greatest depressurization and, hence, a challenge to adequate fuel cooling.

The 325-mm pipe break begins with a rapid subcooled depressurization of the primary coolant system. The pressure condition needed to initiate the reactor scram is calculated to occur at 0.02 s, and scram rod insertion begins after detection and unlatching, at about 0.02 s. Before insertion of scram rod reactivity, core coolant voiding produces only a modest reduction in core power, and a hot channel fuel plate temperature excursion begins at 0.044 s, when the local heat flux at the top of the lower fuel

element hot channel exceeds the critical heat flux (CHF). Figure 4.1 illustrates the coolant system pressure responses and the fuel plate centerline temperatures. As discussed at the end of this section, these results should be considered as very preliminary until additional code performance checking, planned for FY 1990 is completed. The results for the medium break (not shown) are qualitatively similar, but major events take slightly longer to unfold because of the smaller break size.

In the 51-mm pipe break, the depressurization is slower and the scram reactivity insertion prompt enough to prevent fuel plate heatup. As shown on Fig. 4.2, the reactor pressure decreases rapidly, recovers partially

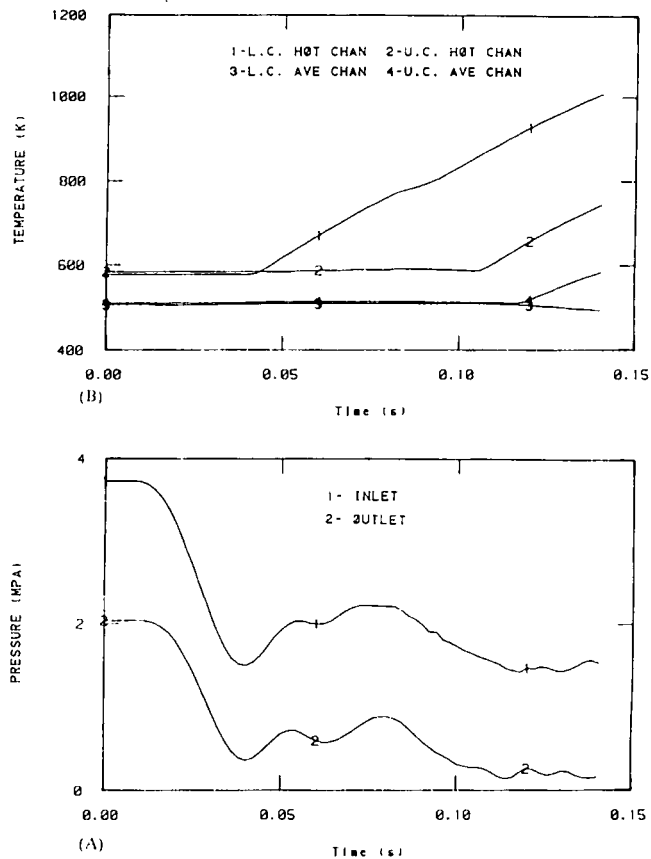


Fig. 4.1. RELAP5 preliminary calculations of (A) primary coolant core inlet and outlet pressures and (B) hot spot fuel plate centerline temperatures after large pipe break (325 diam) from full power.

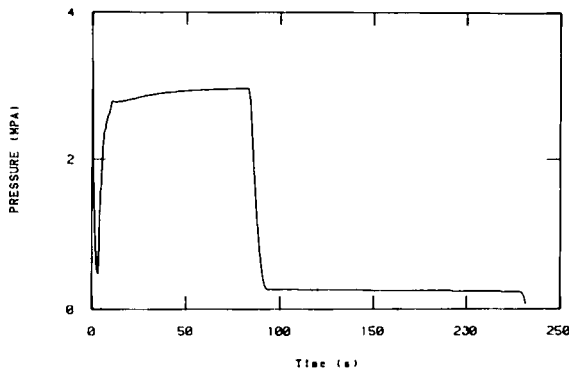


Fig. 4.2. RELAP5 preliminary calculations of primary coolant core inlet pressure after small pipe break (51-mm diam) from full power.

after the standby injection pump starts, and then falls to a low level after the injection tank is pumped dry. The fuel plate temperatures remain low throughout the calculation period; however, calculation time became unacceptably long after cavitation of the emergency pumps began, and the computation was stopped after about 230 s of reactor time.

After RELAP5 code execution was obtained for each of the pipe-break test cases, a peer review group convened on Sept. 12, 1989, at INEL. The reviewers concluded that the test case results appear to be reasonable with the following exceptions and qualifications:

1. The calculated behavior in the uppermost core cells following dryout and heatup in the medium- and large-break LOCA calculations appears to be faulty. Following fuel plate dryout, about half of the fuel plate heat flux is directed to the liquid phase; a much smaller fraction would seem reasonable to represent film-boiling heat transfer. The liquid heat addition leads to continued vapor generation, pressurization of the upper core cell, and flow stagnation in the affected core channel. Thus the behavior following dryout, but not the occurrence of the dryout itself, appears questionable.

2. The numerical difficulties preventing completion of the small-break calculations appear to be caused by the large variations in fluid properties (mainly the vapor density, saturation temperature, and sound speed) as functions of pressure at sub-atmospheric pressures. A stable solution may require much smaller time-steps than may be economically feasible. A potential remedy may be to tighten the criteria for time-step control based on changes in pressure and void. Existing criteria are based on success with problems near atmospheric pressure, not at vacuum conditions.
3. The INEL reviewers concur with those from ORNL that the calculated behavior of the main coolant pumps in the presence of void at the pump inlets appears suspect. Specifically, the pump inlet region experiences significant flashing and voiding that should result in significant pump performance degradation. In the model, degradation is based on pump center, rather than inlet, voiding. Because these are high head pumps the calculated pump center void is much lower than the pump inlet void. As a result, the pump inlet condition is highly voided and horizontally stratified at vacuum conditions, but the calculated pump performance is only slightly degraded.

These uncertainties are to be addressed during the early part of FY 1990.

Test case results lead to several tentative conclusions of importance to the ongoing coolant system design effort: (1) automatic main coolant pump motor trip upon low pressure is required to avoid pump inlet voiding and possible flow interruption; and (2) even with main pump motor trip (the pony motors continue running), subatmospheric pressure may be encountered, and careful analysis of the extent of voiding and its effect on coolant circulation is required.

### 4.3.3 Decay Heat Removal Calculations

In addition to the RELAP5 work, calculations were made by N. C. Chen to examine the behavior during low-flow transients by assuming that the system operated under quasi-steady-state conditions. The onset of net vapor generation (ONVG) criterion by Saha-Zuber<sup>31</sup> has been used to predict allowable ANS core power under both normal and emergency conditions. This analysis focused on decay heat removal by natural circulation; therefore, only that part of the Saha-Zuber correlation for ONVG at low pressure and low flow was studied. Also, a saturated exit limit was included as a reference.

In subcooled boiling, the Saha-Zuber low-pressure-flow correlation predicts that the Nusselt number remains constant if the Peclet number is  $<70,000$ . For the ANS configuration, this would require core velocities to be  $<4$  m/s. Consequently, the allowable core power depends on the core mass flux and the degree of subcooling if core inlet conditions are specified.

The Saha-Zuber correlation was implemented, and calculations of allowable heat flux for decay heat removal by natural circulation were made. Upward flow of  $D_2O$  coolant in the core and core dimensions as specified in Ref. 42, were assumed. A uniform power density profile in the hot channel was assumed to be 1.3 times that of the average channel with an exit peaking factor of 1.7.

Results of the allowable heat flux and exit coolant temperature for a core exit pressure at 0.2 MPa (29 psia) are presented in Fig. 4.3 and Table 4.1, respectively. The exit pressure is the sum of the atmospheric pressure and a 10-m water head. Some findings are that (1) a saturated exit limit predicts a higher allowable heat flux than that of Saha-Zuber low mass flux correlation at all velocities (between 0 and 4 m/s), (2) allowable heat flux

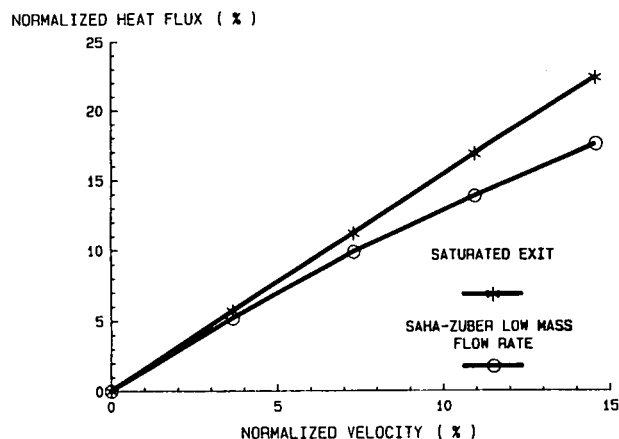


Fig. 4.3. Comparison of normalized heat flux vs flow predicted by onset of net vapor generation criteria and saturated exit limit (nominal heat flux =  $6$  MW/m<sup>2</sup>, nominal velocity =  $27.4$  m/s, T-core inlet =  $49^{\circ}\text{C}$ , and P-core exit =  $0.2$  MPa).

increases with both coolant velocity and the degree of subcooling, and (3) the coolant bulk temperature at the ONVG limit tends to decrease with both coolant velocity and inlet subcooling.

## 4.4 SEVERE ACCIDENT ANALYSIS

The onset of a severe accident begins when the reactor fuel is exposed to conditions beyond its design basis. For reactors with metallic fuel or clad, the degree of severity is proportional to the fraction of the core that undergoes melting. Therefore, the ANS would experience a severe accident if a large fraction of the reactor fuel were to exceed the melting point of aluminum, the core's major structural material. The ANS fuel plates are manufactured by sandwiching the "meat" ( $U_3Si_2$  particles dispersed in 1100 Aluminum powder) between 6061 aluminum-clad plates. The melting point of aluminum is well below the  $1665^{\circ}\text{C}$  melting point of the ceramic-like  $U_3Si_2$  fissile material. Even

Table 4.1. Coolant bulk temperature at core exit predicted by onset of net vapor generation (ONVG) using Saha-Zuber low mass flow rate correlation ( $P_{\text{exit}} = 0.2 \text{ MPa}$ ,  $T_{\text{sat}} = 121^\circ\text{C}$ )

Velocity (m/s)	ONVG (Saha-Zuber) $T_{\text{inlet}}$ ( $^\circ\text{C}$ )		
	49	73	97
1	101	108	114
2	98	106	113
3	95	104	113
4	93	103	112

though the  $\text{U}_3\text{Si}_2$  would be far from its melting point, experiments on cermet fuels have shown that the release of large fractions of the very volatile noble-gas fission products begins with melting of the aluminum clad/matrix material, and the other important but less volatile fission products begin to be released at temperatures only moderately above the melting point of aluminum ( $649^\circ\text{C}$  for 6061 Aluminum and  $660^\circ\text{C}$  for 1100 Aluminum). The object of severe accident analysis is to gain an understanding of core melt progression and the release, transport, and containment of fission products.

A severe accident would be an extremely hypothetical event for the ANS: the reactor cooling and protective systems are being designed to achieve a severe core damage risk goal of 1/100,000 core damage events per year. Nevertheless, severe accident studies are needed to (1) determine if containment is sufficiently robust to contain radioactivity released in the event of fuel damage, (2) provide input for the probabilistic risk analyses that will be conducted for the ANS, (3) verify that the site suitability source-term accident analyzed per 10 CFR 100 is sufficiently conservative, and (4) to develop knowledge of severe accident progression for emergency

preparedness procedures and guidelines. Severe accident evaluation has been initiated for the ANS at a relatively early stage of the project design cycle to provide the information that will allow designers to optimize the severe accident resistance of the reactor.

The pace of severe accident analysis accelerated during the current reporting period. Scoping studies on hydrogen explosion, steam explosion, and core debris recriticality were completed, and studies on core melt progression and fission product release were initiated. In the most recent annual report, the results of calculations of the severe accident containment pressurization caused by generalized fission product heat dissipation and hydrogen deflagration are reported. The studies summarized below relate to specific phenomena that might have some effect on containment performance during severe accidents.

#### 4.4.1 Severe Accident Debris Recriticality

The ANS core comprises two semiconcentric, multiplate fuel elements in an annular configuration with control rods in the central

nonfuel region and control rods on the outside. In the event of severe overheating, the highly enriched  $U_3Si_2/Al$  fuel would melt and be transported away from the annular region poisoned by control rods; that is, a severe accident would separate the highly enriched uranium from the control poison. This section summarizes the results of a study undertaken by D. L. Moses and C. O. Slater (ORNL Engineering Physics and Mathematics Division) to determine if the debris would be subcritical after a severe accident. The problem is approached in a parametric fashion because no mechanistic predictions are currently available that would predict the nature of the debris resulting from a severe core damage accident or precisely where and in what geometry the debris would accumulate.

To ensure the accuracy of the hypothetical debris multiplication ratio calculations, the performance of the KENO<sup>32</sup> and DORT<sup>33</sup> computer codes were benchmarked against configurations known to be exactly critical by actual experiment (experimentally determined multiplication ratio, or k-effective, equal to 1.0). This involved a variety of experiments that utilized highly enriched uranium: (1) uranium metal spheres reflected by light and heavy water and (2) uranium solution spheres and cylinders moderated by light and heavy water. Both light- and heavy-water moderated and reflected experimental configurations were sought because a likely resting place for debris would be at the bottom of a primary coolant pipe with heavy water inside the pipe and light water outside the pipe. The comparisons between critical experiment and calculation are very favorable. For the lumped critical configurations, the average of nine values is 1.0039 with a standard deviation of 0.0027; for the solution criticals, the average of 19 values is 1.0045, with a standard deviation of 0.0046. To achieve 99% confidence in subcriticality, the predicted k-effective would have to be  $<1.0$  by at least 3 standard deviations; that is,  $\sim <0.985$ . The benchmarking for this task was extremely

thorough and has established a solid foundation for future similar analyses.

K-effective calculations were performed for five hypothetical postaccident debris configurations: three cases with the fuel debris lumped at the bottom of a 488-mm inside diam coolant pipe, and two cases with the fuel debris dispersed in a low concentration within 1-m and 2.1-m sections of the 488-mm-diam pipe. The pipe material in all cases was taken to be 304 stainless steel. Conservatism adopted for these cases include: (1) the debris was assumed to be at ambient temperature (293 K); (2) the complete beginning-of-life fuel inventory was estimated at the beginning of the study to be  $\sim 25$  kg of  $^{235}U$  (the most recent preconceptual inventory is only 18 kg); (3) the debris was assumed to have no fission product poisoning; (4) for the lumped cases the fuel material was assumed to be at its maximum theoretical density; and (5) the coolant pipe was assumed to be optimally reflected by light water, but the neutron moderation inside the pipe was taken to be heavy water without significant light-water contamination to provide competing neutron parasitic capture.

The results of the five hypothetical cases are summarized in Table 4.2. The key result that emerges from these preliminary calculations is that lumped configurations have little potential for exceeding criticality. This is a very positive result for ANS severe accident analysis because the stable configuration for severe accident debris would be in some sort of a lump or layer at the bottom of one of the coolant pipes. On the other hand, case (4) shows potential for debris to become critical if a majority of the core's fissile inventory became suspended in a submerged coolant pipe, away from the reactivity control elements, at a concentration of  $\sim 0.1$  kg  $^{235}U/L$ . Two variants of case (4), one with an air-reflected coolant pipe and the other with a boronated steel pipe wall, show that such a critical configuration could be made subcritical by reducing neutron reflection. The potential

Table 4.2. Criticality of hypothetical core debris configurations

Case	Mass of $^{235}\text{U}$ (kg)	Configuration	K-effective	
			KENO	DORT (or TORT)
1	26.4	Lumped: 175-mm-diam sphere of $\text{U}_3\text{Si}_2$ at bottom of $\text{D}_2\text{O}$ -filled 304 stainless steel, $\text{H}_2\text{O}$ -submerged pipe (488-mm ID)	0.9674+-0.0025	0.9638
2	26.4	Lumped: 220-mm-diam sphere of $\text{U}_3\text{Si}_2/\text{Al}$ at bottom of $\text{D}_2\text{O}$ -filled 304 stainless steel, $\text{H}_2\text{O}$ -submerged pipe (488-mm ID)	0.8728+-0.0023	0.8663
3	22.5	Lumped: hemicylinder (175 × 175 × 42 mm depth) of $\text{U}_3\text{Si}_2$ at bottom of $\text{D}_2\text{O}$ -filled 304 stainless steel, $\text{H}_2\text{O}$ submerged pipe (488-mm ID)	0.8192+-0.0032	
4	26.4	Dispersed: $\text{U}_3\text{Si}_2$ uniformly suspended in a 1-m-long section of $\text{D}_2\text{O}$ -filled 304 stainless steel, $\text{H}_2\text{O}$ submerged pipe (488-mm ID)	1.0911+-0.0037	1.084
5	4.5	Dispersed: $\text{U}_3\text{Si}_2$ uniformly suspended in a 2.1-m-long section of $\text{D}_2\text{O}$ -filled 304 stainless steel, $\text{H}_2\text{O}$ submerged pipe (488-mm ID)	0.844+-0.0036	

for re-criticality will be examined in greater detail when more detailed, mechanistic severe accident analyses are available. For the present, it is sufficient to note that the agglomerated debris configurations are clearly sub-critical and that engineered fixes will be available if credible dispersed configurations would exceed criticality.

#### 4.4.2 Severe Accident Initiated Steam Explosion

Steam explosion is a phenomenon in which a portion of the thermal energy of molten material in contact with water is converted into mechanical energy by the

extremely rapid generation of steam. Steam explosions have been observed in conjunction with molten materials in the metal refining<sup>34</sup> and iron working industries. Steam explosion can be triggered by a disturbance or movement that causes vapor film collapse: the resultant extremely rapid generation of steam is feasible because the initiation of the explosion involves the propagation of an interaction wave that fragments the coherent melt into many small particles having a very large aggregate heat transfer area. In the event of a severe accident of the ANS, some molten material would come into contact with water, and it is therefore necessary to gain an appreciation of the likelihood of steam explosion under ANS severe accident conditions and its potential effect on containment integrity. The paragraphs below briefly summarize the results of a study by R. P. Taleyarkhan (ORNL) documented in detail in ORNL/TM-11324, *Steam-Explosion Safety Considerations for the Advanced Neutron Source Reactor at the Oak Ridge National Laboratory*.

The ANS scoping study of steam explosion included a literature survey. It was found that steam explosion events have occurred at reactors having plate-type aluminum fuel: the BORAX test reactor, the SPERT-I test reactor,<sup>35</sup> and the SL-I prototype reactor (all at the National Reactor Test Station in Idaho). In each case the steam explosion followed an intentional prompt critical reactivity excursion initiated by rapid control rod withdrawal without reactor scram. The SPERT-I and BORAX power excursions were initiated to study the effects of hypothetical reactor accidents; the SL-I accident<sup>36</sup> occurred during the refueling of a military prototype pressurized-water reactor and is thought to have been the direct result of a suicidal act of sabotage. Such an accident would not occur at the ANS for many reasons; one of these is inherent in the nature of a heavy-water-moderated and -cooled reactor, that is, the long neutron lifetime of the ANS

(about ten times longer than that of the light-water-moderated SPERT-I and SL-I reactors) means that the reactor power would increase more slowly for a given reactivity disturbance. However, given the occurrence of a sufficiently energetic melt, the possibility of a steam explosion cannot be discounted and must therefore be studied. In the steam explosion scoping study Taleyarkhan recommends that small-scale laboratory experiments should be conducted to assess the relative propensity of molten ANS fuel mixtures to undergo steam explosion.

The destructive potential of a steam explosion is related to the total thermal energy of the molten material before the explosion and the fraction of the thermal energy that can be converted to mechanical energy. The thermal energy of the melt is determined by the rate at which the material is being heated and limited by natural forces that tend to disassemble the molten mass. For a core melted by decay heat, the force of gravity would tend to disrupt the core before the melt reached a temperature much above the melting point. A core melt with the reactor at power (such as one that could follow a loss-of-coolant flow with coincident failure to scram) would reach higher temperatures before being disrupted by either gravity or hydraulic forces. The destructive potential of a steam explosion is determined by how efficiently the thermal energy of the melt is turned into mechanical energy. Theoretical thermodynamic estimates of conversion efficiency range up to ~32%; more practical estimates based on scale experiments range closer to 10%.

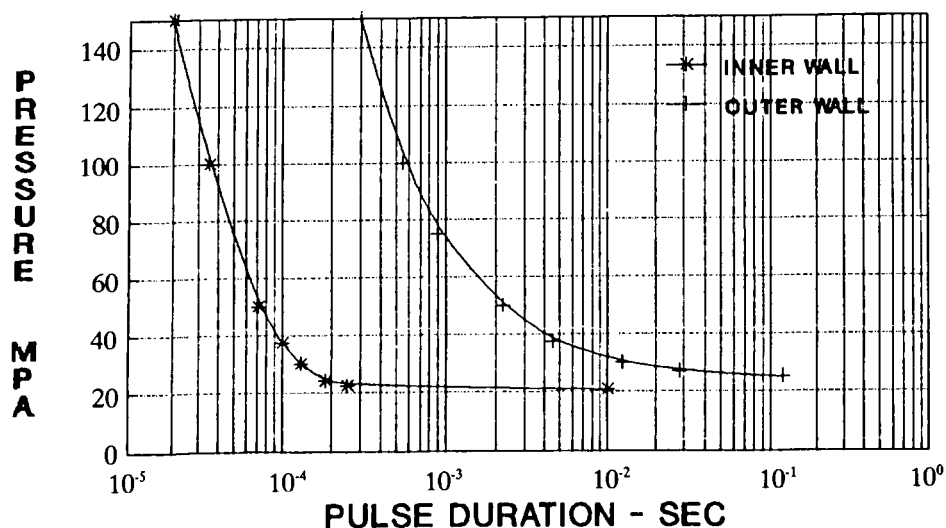
During a steam explosion, an initial pressure pulse occurs in the immediate vicinity of the explosion site during the first several milliseconds of the explosion. After the initial pressure peak, the pressure quickly decays as the steam bubble expands and steam is condensed. In the course of his literature survey, Taleyarkhan found a concise

expression for estimating the initial pressure pulse associated with a steam explosion initiated from molten material of a given temperature. The expression is an equation of state that requires information available only in a parametric sense; however, with reasonable input parameters, it compares well with the range of peak pressures seen in experimental steam explosion data for molten aluminum and tin,<sup>37</sup> as well as against pressure pulses observed in the SPERT-I test and the SL-1 destructive incident. For hypothetical ANS severe accidents, this expression was used to predict the possible ranges of peak pressure associated with the initial pressure pulse assuming the inception of steam explosion for each of three severe accident scenarios considered.

To assess the possible effect of the pressure pulses upon relevant structural components, R. C. Gwaltney and C. R. Luttrell (ORNL ETD) used the general-purpose finite-element code ADINA<sup>38</sup> to perform a dynamic structural evaluation to estimate the potential effect of rapid pressure pulses of

various magnitudes and durations on a 20-mm-thick, 242-mm midradius CPBT and a 12.7-mm-thick, 1756 midradius reflector tank. The results are depicted on Fig. 4.4. The predicted failure pressure of the CPBT is very close to its estimated 20-MPa static failure pressure for all pressure loadings lasting longer than  $\sim 0.3$  ms, a much shorter period than even the initial pressure pulse phase of a steam explosion. The reflector tank, however, could withstand much higher pressures for transient pressure loadings in the millisecond range. The estimates of the pressure pulses for ANS conditions and the ADINA results are listed on Table 4.3. The results of these scoping calculations show that a steam explosion involving a large fraction of the core would very likely rupture the CPBT but that a melt at power would be required to rupture the reflector tank.

Additional work beyond the already-completed scoping study will be required to characterize steam explosions fully and the implications for containment design. Results from work in other areas, such as the PRA,



Note: Tube Midradius = 242 mm  
Wall Thickness = 20 mm

Fig. 4.4. Failure envelopes for CPBT (inner wall) and reflector tank (outer wall) loaded by triangular pressure pulse.

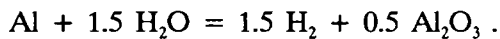
Table 4.3. ANS steam explosion pressure pulse estimates and effect on CPBT and reflector tank

<u>Accident</u>	<u>Debris temperature reached (°C)</u>	<u>Probable range, pressure pulse peak (MPa)</u>	<u>Effect on CPBT</u>	<u>Effect on reflector tank</u>
Insufficient cooling on decay heat	873	25-80	Probably ruptured	Intact
Insufficient cooling at power (i.e., without scram)	1684	100-150	Ruptured	Probably ruptured
Reactivity excursion without scram	1327	60-100	Ruptured	Possibly intact

will influence the conclusions. It is not now clear whether additional design features will be necessary to protect the containment from steam explosions. If the steam explosion does not cause rupture of the reflector tank, it is very unlikely that there would be any effect on the containment dome. But, even if a steam explosion were retained inside the reflector tank, there could be damage to the neutron beam tubes (thin aluminum tubes that direct slow neutrons from the reflector tank, through the pool wall and into the beam room), and a careful analysis will be required to determine the subsequent leakage, if any, from the reflector tank into the beam room. If the reflector tank is ruptured, the possibility of missiles or water plume that might damage containment must be examined and design provisions provided if the PRA shows the probability of a large release in excess of one in a million per year (per recent draft of DOE safety policy).

#### 4.4.3 Hydrogen Explosion

This section explains the results of a scoping study of potential hydrogen detonation loads upon containment. Estimates of the containment loads associated with hydrogen burning, a much slower process, are given in the most recent ANS Project annual report.<sup>39</sup> The two ways in which hydrogen or deuterium gas could be produced under accident conditions are considered: (1) escape of deuterium from one or both of the cold sources or (2) fuel melting with hydrogen production by aluminum water reaction. According to a recent estimate, each cold source contains  $< \sim 8$  kg of deuterium, equivalent to 4 kg of hydrogen gas. The ANS preconceptual core design has an active fuel volume of 67.4 L and would therefore yield  $\sim 10$  kg of hydrogen gas if all the aluminum in the fuel plates were to react completely with water via the reaction:



There are at least two ways to estimate the peak pressure of a hydrogen-oxygen explosion. The first is to convert the amount of hydrogen into an equivalent amount of standard TNT explosive and then utilize the widely available tabulations of overpressure vs explosive charge and distance. The other way is to use published hydrogen explosion data. Both methods were utilized for this study, but the explosion parameter estimates reported below are based on data published<sup>40</sup> for actual hydrogen explosions: overpressure as a function of the distance from the center of experimentally detonated 0.8- and 0.455-m radius balloons filled with a stoichiometric mixture of hydrogen and oxygen. The estimates of ANS hydrogen explosion parameters were straightforward because the data correlate well with the distance from the center of the explosion divided by the radius of the pocket of gas (conservatively assumed to be spherical). An explosion would have to involve isolated pockets of gas because the amount of hydrogen is not enough to raise the very voluminous ANS containment above the lower flammability limit (4 v/o), much less the lower detonation limit (~14 v/o).<sup>41</sup>

Figure 4.5 presents the peak overpressure that would impact a structure 5, 10, and 15 m from the center of the explosion of 4, 10, and 18 kg of hydrogen (or twice the masses of deuterium). A factor of 2 was used to convert the "side-on" pressure data to the "reflected" pressure that is more appropriate to the loading that a structure in the path of the detonation shock would experience. The pulse durations (between 5 and 14 ms) were inferred from the corresponding impulse results of Ref. 40 by assuming that the pressure pulse has a triangular shape. The results have been presented here in a parametric fashion because design data are not available to allow the analyst to postulate the most likely site for an explosion and to identify the nearby structures. If some catastrophe were

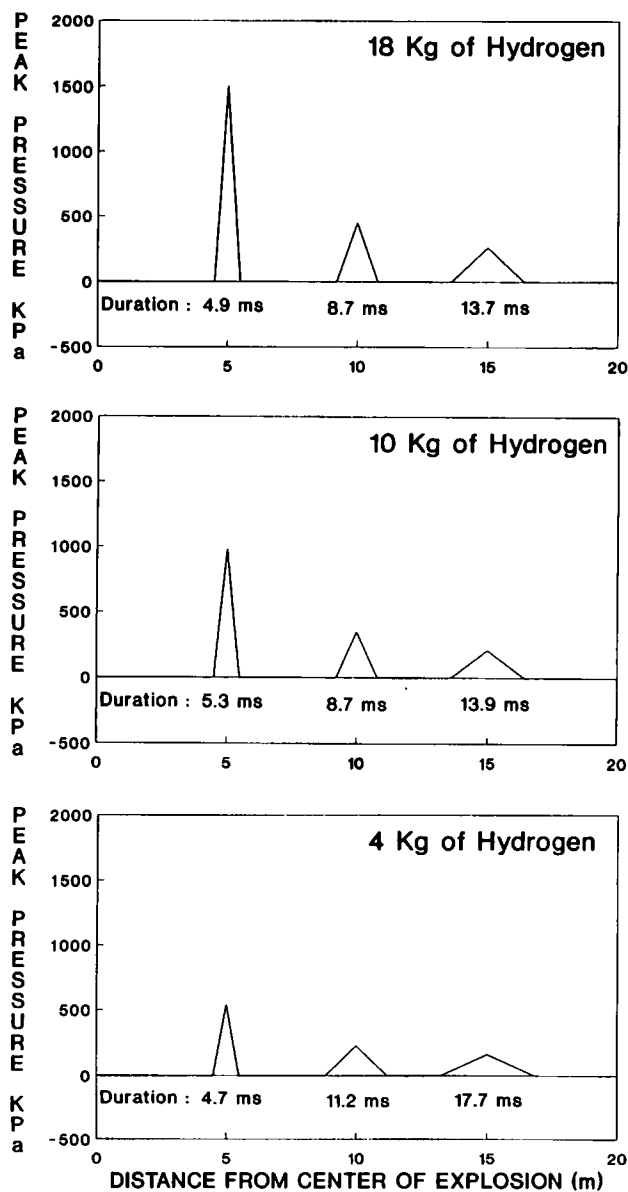


Fig. 4.5. Pressure pulse vs distance for atmospheric pressure detonation of 4, 10, and 18 kg hydrogen (total pressure given).

to result in the explosion of 18 kg of hydrogen (36 kg deuterium) directly above the reactor pool, the peak reflected pressure differential at the ceiling of the containment would be ~164 kPa—well in excess of the design pressure differential of the containment inner shell (which will be in the neighborhood of 33 kPa)—but this loading would

last for only ~14 ms. The structural response of the inner shell cannot be determined without dynamic analysis, but it is possible that a dynamic analysis would show that the shell would not be damaged by such a load.

The information presented in this subsection is expected to be useful at some point in the containment design process. Hydrogen design criteria need to be adopted early in the containment design and appropriate structural evaluations performed. A reasonable criterion would be that containment must be able to withstand, without loss of integrity or function, the detonation of the entire cold source inventory plus the hydrogen equivalent that would result from the complete oxidation of the aluminum in the fuel plates. In this subsection, this amount is estimated at 18 kg of hydrogen (or equivalent deuterium) but could change as the conceptual design of cold sources and core evolves.

#### 4.4.4 Other Ongoing Studies

Two other studies are in midcourse at the end of the current reporting period. The first is a scoping study to characterize severe accident core melt progression and fission product release issues, and the other is a scoping study to characterize the potential for postsevere accident core debris to escape from the primary coolant system and cause degradation of the concrete floors of the subpile room or the reactor pool. The results of these studies will be documented during the next reporting period.

### 4.5 PROBABILISTIC RISK ASSESSMENT

Early in FY 1987, the decision was made to initiate a PRA of the evolving design of the ANS facility. BNL has been used as a subcontractor for ANS risk analyses performed to date; under the guidance of the

task leader, R. R. Fullwood, significant progress was made, as described below for the current reporting period and as previously described in past annual reports.

Two advantages of doing PRA during the design process are to (1) help minimize the possibility of expensive backfits and (2) enable the project to demonstrate compliance with DOE and NRC safety goals for nuclear reactors. This risk assessment task includes the process of describing the failure rates of components and systems and the dependencies between systems and subsystems and determining and enumerating accident initiators that could lead to core damage. Methods for calculating probabilities of unacceptable consequences are selected and results expressed in such a way that the dominant accident sequences are apparent. The results must be communicated to project designers who can effect design changes if necessary to meet the safety goals.

Recent DOE policy developments in nuclear safety philosophy have stressed safety awareness and accountability, defense-in-depth, and PRA. The most recent draft of the DOE nuclear safety policy statement provides qualitative safety goals for individual and societal radiological risks that are very similar to those prescribed by the familiar NRC reactor safety goals policy and states two very stringent quantitative guidelines for the risk associated with new DOE production reactors: (1) the probability of severe core damage or meltdown at individual new DOE reactors should normally be less than one per hundred thousand reactor-years, and (2) the frequency of accidents accompanied by severe releases of radioactivity should normally be less than one in a million reactor-years. Even though the last two goals are applicable only to the new defense production reactors currently under study by DOE, they have been adopted by ANS project management as goals because the ANS is also a major new facility.

The following three major PRA activities were completed during the reporting period:

(1) investigation of large pipe-break probability, (2) evaluation of hydrogen safety risks, and (3) determination of dominant severe core damage initiators. Large break is a potential sticky wicket for a high-power-density research reactor because of thermal-hydraulic uncertainties surrounding fuel cooling during the extremely rapid depressurization that would follow an instantaneous large pipe break. The ANS large-pipe-break study, summarized below, concludes that the probability of large break can be made sufficiently low by application of the leak-before-break approach. Although it consumed only a small proportion of the total resources expended during the reporting period, the hydrogen safety risks study prompted the development and articulation of a cold-source hydrogen safety philosophy. The effort to develop a list of initiating events and accompanying severe core damage event trees resulted in initial bottom-line estimates of core damage probabilities that indicate that the  $10^{-5}$ /year core damage goal is achievable.

#### 4.5.1 Large Pipe Break Core Damage Risk Study

This section summarizes the results, conclusions, and recommendations of R. R. Fullwood's (BNL) study of the core damage risk posed by breakage of large pipes in the ANS primary coolant system. Piping in the "large" category includes any piping of nominal diameter  $\geq 152$  mm (6 in.); the ANS preconceptual primary coolant arrangement includes both 356- and 610-mm (6-, 14-, and 24-in.) pipes.

Probabilistic fracture mechanics methods were applied to the preconceptual ANS primary coolant system piping layout to estimate the pipe-break frequency, and then large break event trees were drawn and corresponding fuel damage probabilities estimated. The event trees include a "leak detected" event that averts fuel damage because the reactor is

shut down before the break occurs and not restarted until the crack that caused the leak is repaired. This is the heart of the leak-before-break approach recently approved by the NRC<sup>42</sup> for the elimination of certain pipe-break-related loads from the design basis of commercial nuclear power plants.

**Estimation of Pipe-Break Probabilities.** A PC code, named PRAISDPD (PRAISE Discrete Probability Distributions) by Fullwood because it utilizes the probabilistic fracture mechanics approach of the more sophisticated PRAISE-B computer code, but employs a simplified, faster method of calculating the effect of the multiple input data distributions. The new computer code was written to avoid the anticipated inconvenience and expense of using a large code for a parametric study and because PRAISE-B output did not include the individual probabilities needed for this study.

The most basic assumption of the present study is that the reason for pipe breaks would be the existence of flaws in the installed piping, and the most likely place for these flaws would be in the weld zones. [An extrapolation for the leak/break probability in the base metal was scaled, using the model of Thomas (see "Pipe and Vessel Failure Probability," *Reliability Eng.*, 1981, Vol 2, pp. 83-124).] If a flaw exists, stress cycles cause the flaw to grow, both in depth and length. When the flaw (crack) depth exceeds the piping wall thickness, leakage begins; when the crack length reaches some appreciable fraction of the piping circumference (exceeds the "critical" length), the crack becomes unstable and the pipe ruptures.

Input parameters required by the PRAISDPD code include the pipe diameter, wall thickness, and stress intensity. Basic properties of the piping material are taken from a study by Harris<sup>43</sup> of PWR plants having 304-L stainless steel piping. For example, these data show the occurrence of flaws to follow a Poisson distribution with a mean value of  $6.1 \times 10^{-6}$  flaws per cubic centimeter

of weld material. The initial flaw depth probability is exponentially distributed with a mean depth of 6.2 mm. The nondestructive testing probability of crack detection is taken to be a log-normal distribution with a 99% chance of nondetection for a 5-mm-deep crack (aspect ratio  $\sim 1.2$ ). Other important input and hard-wired data for the PRAISDPD calculations include: the occurrence of 22 stress cycles per year (consistent with the ANS 2-week fuel cycle); for all but one calculation discussed below, an assumed stress intensity factor ten times greater than the minimum required to initiate fatigue crack growth; and critical crack length of two-thirds of the pipe circumference. It was necessary to assume a stress intensity factor because piping stress analysis has not yet been performed.

The results of PRAISDPD calculations are presented in Table 4.4 in terms of the yearly probability of failure for one weld in piping of different diameters, thicknesses (i.e., Schedule 40 and Schedule 80), stress intensities, and number of years since nondestructive examination. It should be emphasized that these calculations are not leak-before-break; for example, a weld that fails catastrophically after 32 years may have been leaking for 16 years. The fuel damage risk calculations *did* consider leak detection, as discussed below. Parameters that significantly affect the leak and break probabilities include "age" since nondestructive examination, wall thickness, pipe diameter, and stress intensity. Perhaps the most interesting parameter is the stress intensity. A halving of the stress intensity reduced the risk of failure by  $\sim 4$  orders of magnitude. This is why it is essential for piping designers to work hand-in-hand with the fracture mechanics analysts for plants that exclude large pipe breaks from their list of design basis accidents.

**Risk of Large-Pipe-Break Initiated Core Damage.** An event tree was drawn (Fig. 4.6) to aid in the calculation of fuel damage risk. Nine events were included: (1) leak, (2) leak detected and repaired, (3) no break, (4)

scram, (5) no cooling channel blockage upon depressurization, (6) break under pool water, (7) main cooling flow continues, (8) isolate reactor, and (9) shutdown cooling. The outcome of each branch of the tree is either no fuel damage (NFD) or fuel damage (FD). Most of the FD branches are of insignificant probability because, in addition to the break, an equipment failure would be required for fuel damage. Branch FD3 is dominant by at least an order or magnitude, because of the assumed 50% probability for Event 5; that is, that fuel damage occurs during the depressurization immediately following the break, regardless of any automatic mitigative actions by the installed cooling and protective systems. This high probability was assessed because preliminary ANS RELAP5 calculations (see Sect. 4.3.2) predict fuel damage following large-pipe breaks; other research reactors of similarly high-power density, such as the ATR and the HFIR have recognized in their PRAs the likelihood of severe fuel damage in the extremely unlikely event of large pipe break. Other event probabilities contributing to the FD3 severe core damage probability for Schedule 40 pipe include leak probability of  $7.2 \times 10^{-4}$ /year (Event 1), leak non-detection probability of  $2.2 \times 10^{-2}$  (Event 2), conditional pipe break probability of  $4.7 \times 10^{-2}$  given the occurrence of the leak (Event 3), and reactor scram probability of  $\sim 1$  (Event 4).

Figure 4.7 presents the fuel damage risk estimates (major core damage events per year) as a function of "age," the elapsed time since the initial nondestructive examination of the installed pipe welds, for four different piping alternatives. The probability of pipe-break-initiated core damage is seen to increase dramatically over the first  $\sim 5$  years, and more slowly thereafter. The base case, and highest, risk profile is the "Reference Sch. 40" curve on Fig. 4.7; that is, the baseline preconceptual primary coolant piping layout<sup>44</sup> implemented in Schedule 40 piping, which is of adequate thickness for the  $\sim 4.8$ -MPa (697-psi) ANS primary coolant system

Table 4.4. Aging probability of failure per weld-year  
calculated with PRAISDPD

Pipe OD (mm)	Wall thickness (mm)	Stress intensity (MPa · m <sup>1/2</sup> )	Age (years)	Leak probability (per year)	Break probability <sup>a</sup> (per year)
610	31	50.55	1	$1.87 \cdot 10^{-12}$	$1.65 \cdot 10^{-16}$
			4	$8.12 \cdot 10^{-11}$	$4.00 \cdot 10^{-12}$
			16	$7.56 \cdot 10^{-10}$	$3.72 \cdot 10^{-11}$
			32	$1.39 \cdot 10^{-9}$	$6.85 \cdot 10^{-11}$
610	17.5	50.55	1	$1.18 \cdot 10^{-9}$	$3.08 \cdot 10^{-15}$
			4	$2.66 \cdot 10^{-8}$	$1.31 \cdot 10^{-9}$
			16	$1.40 \cdot 10^{-7}$	$6.88 \cdot 10^{-9}$
			32	$2.07 \cdot 10^{-7}$	$1.02 \cdot 10^{-8}$
610	31	25.28	1	$6.67 \cdot 10^{-18}$	$5.91 \cdot 10^{-22}$
			4	$8.29 \cdot 10^{-15}$	$4.08 \cdot 10^{-16}$
			16	$1.87 \cdot 10^{-12}$	$9.21 \cdot 10^{-14}$
			32	$1.51 \cdot 10^{-11}$	$7.42 \cdot 10^{-13}$
356	19.1	50.55	1	$3.21 \cdot 10^{-10}$	$3.82 \cdot 10^{-14}$
			4	$7.98 \cdot 10^{-9}$	$3.93 \cdot 10^{-10}$
			16	$4.55 \cdot 10^{-8}$	$2.24 \cdot 10^{-9}$
			32	$6.92 \cdot 10^{-8}$	$3.41 \cdot 10^{-9}$
356	11.2	50.55	1	$1.71 \cdot 10^{-8}$	$8.06 \cdot 10^{-14}$
			4	$2.35 \cdot 10^{-7}$	$1.16 \cdot 10^{-8}$
			16	$8.23 \cdot 10^{-7}$	$4.05 \cdot 10^{-8}$
			32	$1.08 \cdot 10^{-6}$	$5.32 \cdot 10^{-8}$
168	10.9	50.55	1	$8.32 \cdot 10^{-9}$	$4.69 \cdot 10^{-12}$
			4	$1.12 \cdot 10^{-7}$	$5.49 \cdot 10^{-9}$
			16	$3.83 \cdot 10^{-7}$	$1.89 \cdot 10^{-8}$
			32	$5.01 \cdot 10^{-7}$	$2.47 \cdot 10^{-8}$
168	7.1	50.55	1	$4.93 \cdot 10^{-8}$	$2.67 \cdot 10^{-12}$
			4	$4.20 \cdot 10^{-7}$	$2.06 \cdot 10^{-8}$
			16	$1.04 \cdot 10^{-6}$	$5.10 \cdot 10^{-8}$
			32	$1.31 \cdot 10^{-6}$	$6.44 \cdot 10^{-8}$

<sup>a</sup>Assuming no interaction between leak and break.

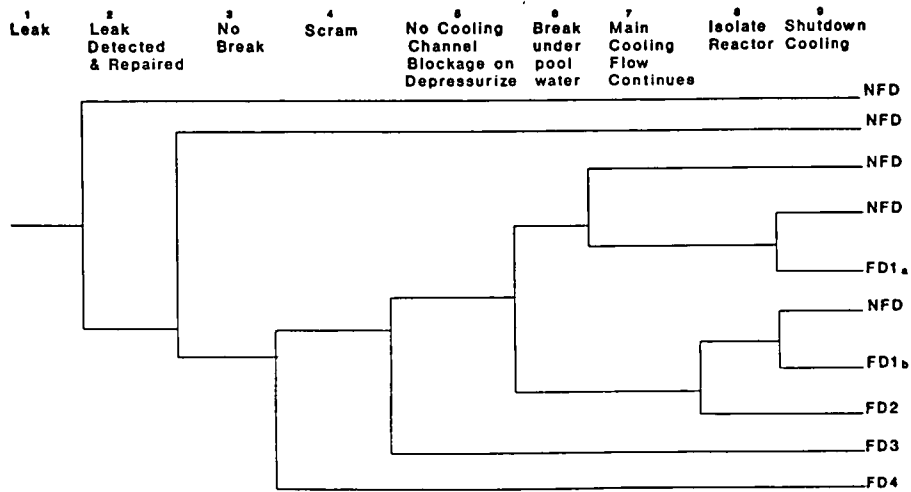


Fig. 4.6. Large-pipe-break event tree (FD = fuel damage and NFD = no fuel damage).

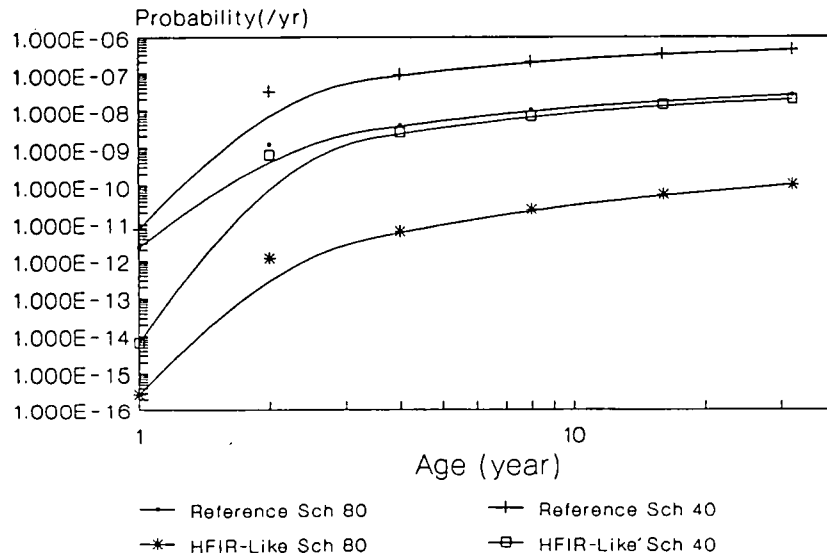


Fig. 4.7. Large-pipe-break fuel damage risk.

design pressure. This presents a total core damage risk of less than one in a million per year and is therefore compatible with the ANS overall core damage goal of one in one hundred thousand per year.

If the reference layout were implemented in Schedule 80 piping (approximately twice the wall thickness of Sch. 40 pipe), the core damage risk would be reduced by  $\sim 1$  order of magnitude. Further risk reductions could

be achieved with the "HFIR-like" piping layout: a piping arrangement in which larger piping is used to the maximum extent possible by using large ( $\sim 500$ - to  $\sim 600$ -mm-diam) headers to route the primary coolant from the reactor to the heat exchanger cells. The risk can be reduced with larger piping because: (1) cracks have further to go to penetrate the wall; (2) cracks must be longer for unstable tearing to begin; and (3) the total amount of pipe and, hence, the number of initial flaws is reduced. The primary coolant piping system is currently being redesigned and is expected to fall somewhere between the "Reference" and "HFIR-like" assumptions used in Fig. 4.7.

*Recommendations.* Based on his work as summarized above, R. R. Fullwood made the following recommendations for consideration by the ANS project design team:

1. On a priority basis, determine if the rapid depressurization that accompanies a large pipe break will damage the fuel to the extent that cooling channels are blocked. Also determine whether the damage, if it occurs, will propagate to otherwise undamaged fuel (see Sect 4.3.2 for a partial answer to this recommendation).
2. Investigate the appropriateness of including a vacuum breaker valve as indicated to avoid the need for fast isolation of the reactor from the main cooling loop [the details of this question are discussed in Fullwood's report on this work (February 1989 draft)].
3. If rapid reactor isolation is retained in the design, analyze its accident potential as soon as feasible to determine the risk.
4. Re-examine the piping design to determine the advantages that accrue in the reference design to outweigh the obvious advantages of the HFIR-like option (i.e., by consolidating smaller loop piping into larger headers wherever possible).
5. Investigate relocating the pumps and heat exchangers so that natural circulation can be provided without the shutdown cooling

system, thereby allowing the elimination of that system.

6. Perform calculations to determine the correct stress intensity factors for the ANS piping design.
7. Specify pipe that is thicker than necessary from pressure considerations to reduce the pipe-break probability.
8. Note that a break in the CPBT would overpressure the reflector tank. Such an event should be investigated for accident potential and mitigated by a pressure relief valve if necessary.

#### 4.5.2 Determination of Dominant Accident Sequences

This task was undertaken by R. Fullwood and W. Shier of BNL to determine which of the many potential accident sequences dominate the risk of severe fuel damage for the ANS. Identification of the dominant accidents is required to allow the determination of where improvements in safety or cooling systems should be sought to yield the greatest improvement in safety. A by-product of this task was a very preliminary indication of the total severe core damage risk.

Accidents were grouped in nine categories by initiating event: (1) pressurizer pump events, (2) reactor scram scenarios, (3) instrument air failures, (4) flow blockage, (5) reactivity excursion transients, (6) degraded primary flow, (7) degraded secondary cooling, (8) loss of preferred ac power, and (9) large-pipe-break scenarios. This list is compatible with available operating data and represents a broad spectrum of events that could possibly lead to fuel damage. The probabilistic analysis of small-pipe-break events was not finished in time to be included in this progress report.

The process of determining dominant accidents requires the estimation of core damage risk for each type of accident scenario. An event tree was constructed for

each accident sequence to express in an orderly manner the combinations of various system failures necessary to cause fuel damage if the initiating event has occurred. A per-year frequency was assigned to each initiating event, and conditional probabilities were assigned to the subsequent failures that comprise each branch of the event tree. A PC-based event tree code, BETA (Brookhaven Event Tree Analyzer), written by R. Fullwood under ANS funding, was used to calculate the core damage probabilities for each event tree.

Because detailed design information does not yet exist for the ANS, improvisation was necessary to select relevant input data for initiating event frequency and for equipment failure probabilities required for the event tree calculations. Fortunately, a PRA has been completed on the HFIR reactor, which is the progenitor of many of the ANS design concepts. Failure probabilities for components were developed for the HFIR PRA by detailed study and tabulation of the 17-year operating history of the HFIR, and these were used for the present ANS study. The HFIR data were not always *directly* applicable to ANS systems, but fault trees were used as necessary to combine the available component data to calculate system failure probabilities.

The following event tree calculations results reveal that the fuel damage risk of the ANS would be dominated by the core flow blockage:

<u>Accident initiator</u>	<u>Percent of total risk</u>	<u>Percent of total risk without flow blockage</u>
Flow blockage	84.4	0 (N/A)
Reactivity transients	7.7	49
Large pipe breaks	4.7	30
Pressurizer pump failure	2.6	17
Degraded secondary cooling	0.25	1.6
Degraded primary flow	0.22	1.4
Loss of preferred ac power	0.07	0.45
Instrument air failure	0.05	0.32
Reactor scram	0.03	0.2

Therefore, the most cost-effective place to concentrate risk reduction resources would be in ways to further reduce the risk of core flow blockage. In fact, some authorities in

PRA circles feel that an unbalanced risk profile is inherently bad, no matter how low the total risk. Therefore, the ANS Project should actively pursue ways to reduce the risk of core flow blockage either in core design, refueling techniques and designs, or coolant system design.

The total core damage risk caused by the nine accident initiators listed above is less than the ANS goal of one severe core damage event per hundred thousand years. This is a positive result for the ANS project, but it must be realized that these results are highly preliminary because of the very rapidly changing nature of the ANS design. This task is to be revisited in FY 1990 when the results of the currently on-going design options studies are available and more conceptual design decisions have been made. The rest of this section elaborates on the top five accident sequences resulting from the BNL event tree studies.

#### 4.5.2.1 Core Flow Blockage (85% of Total Core Damage Risk)

Flow blockage usually does not show up in reactor PRAs as a dominant accident for extensive core damage risk. The reason it does figure prominently in the HFIR and ANS PRAs is the assumption of fuel damage propagation. For the HFIR PRA, and for the preliminary ANS PRA work described here, a very basic conservative assumption was made that essentially any blockage lodged at the core inlet would cause local fuel damage that would propagate and involve the whole fuel element—about half of the two-element core. This assumption seemed necessary because the ANS core has very thin, closely-spaced fuel plates (1.27-mm-thick fuel plates are separated by only 1.27 mm) and because of the high power density of the ANS core at full power. Fuel damage propagation is possible because debris from a single molten fuel plate could lodge in the two adjacent fuel channels, causing overheating of the two adjacent fuel plates, which, in turn, could melt

and spew debris into two more coolant channels, etc. Propagation over any appreciable fraction of the core is typically not a problem with other reactors because of nonfuel barriers within the core and because extra time for detection and shutdown is afforded by the slower adiabatic heat-up rates that obtain with low-power density. Thermal-hydraulic work is planned for FY 1990 to quantify the amount of core inlet blockage that the ANS core can accommodate without fuel damage.

For the present calculations, three fine-mesh flow screens were assumed: one in the main cold-leg pipe, one near the core inlet, and one near the core outlet. The BNL analysis examined the chance that core flow blockage could occur because of internally and externally generated debris. An intermediate conclusion of the investigation was that there would be negligible risk of introducing external debris during refueling because of the use of a refueling machine that could be very carefully charged at a location remote from the reactor, obviating the need for the reactor access hatch to remain open in the pool during refueling. About 70% of the flow blockage risk was determined to come from the risk of failure of the lower (core inlet) strainer itself and the other 30% found to come from external debris inadvertently introduced during main (cold leg) strainer or shutdown cooling loop inspection and maintenance. As a result of their study, the BNL PRA analysts made the following recommendations:

1. The ANS should have a HFIR-like main screen with mesh smaller than the reactor core coolant channel width (i.e., <1.27 mm).
2. The lower and upper strainers appear to be susceptible to failure because of the probable large flow forces and vibrations, and the high radiation levels close to the core.
3. The lower screen is valuable, but not practical as a fine mesh. The upper screen is

of little use because the ANS has decided to use upflow core cooling.

4. Monitoring of the main strainer pressure drop is advantageous to warn of incipient failure or clogging.
5. A strainer with mesh smaller than the core coolant channel width should be provided for the pressurizer pump outlet.
6. For in-service cleaning of the main strainer, vacuum cleaning is recommended to avoid having to remove the main strainer. Any removal of the main strainer introduces the risk that debris could be dropped into the primary coolant piping.

#### 4.5.2.2 Reactivity Addition Initiated Transients (8% of Total Risk)

The ANS is provided with very rapidly-acting safety instrumentation and fast-scramming control rods to accommodate even severe reactivity disturbances. As a practical matter, it is not known how a severe reactivity disturbance could occur. The BNL risk evaluation takes into account the mild reactivity addition that could occur as a result of the precipitous starting of an idle main heat exchanger/pump combination. Any decrease in core moderator temperature results in positive reactivity (via the desirable negative reactivity coefficient) that would initiate an increase in power level. If the reactor power increases sufficiently and is not interrupted by the reactor protection system, fuel damage results.

The present calculations reflect the risk of a mild reactivity insertion exacerbated by total failure of the reactor scram system (the insertion of even one control rod would prevent fuel damage in this case). The  $5.2 \times 10^{-5}$  per demand failure probability of the ANS shim-safety rods was based on the extensive operating experience with the HFIR shim-safety control elements upon which the ANS design concept is based. This analysis took no credit for the outer safety rods located in the RT.

The following observations for possible design improvement were made by the BNL analysts:

1. The coolant may be premixed by either a bypass valve around the main pump check valve, permitting flow on demand, or by a small bleed line around the check valve so that a small flow in the idle loop is continuous. Of these two suggestions, the latter seems preferable because the continuous low mixing keeps the idle loop at the same temperature as the operating loops and prevents colder water injection from an unplanned startup.
2. If needed, additional mixing could be achieved by a rotation of the coolant in the headers, either as a result of the pump action or by short vanes in the pipe.
3. The high core outlet temperature trip is considered a backup to the high power-to-flow ratio trip in this scenario and does not significantly reduce the fuel damage probability.

#### **4.5.2.3 Large Pipe Breaks (4.7% of Risk)**

(See Sect. 4.5.1)

#### **4.5.2.4 Pressurizer Pump Failures (3% of Risk)**

For this analysis it was assumed that the ANS primary coolant pressurizer pumps (i.e., makeup pumps) utilize the same type of speed-reduction coupling between pump motor and pump as the HFIR pressurizer pumps. This coupling fails to reduce the speed when its cooling fails, a failure that has been observed at the HFIR. The scenario that results in most of the risk from this type of event involves overspeed of the operating pressurizer pump, successful trip of the pump followed by failure of the standby pump, subsequent depressurization of the primary coolant system, and failure of the reactor

scram function and inadequate core cooling and thus widespread fuel damage is possible.

The other type pressurizer pump event, simple trip or failure of the operating pump, was not dominant in this event category because of the letdown valves and letdown isolation valves that were assumed to be capable of closing rapidly enough after the pump failure to halt the loss of primary coolant pressure.

The BNL PRA team noted the following considerations for safety enhancement:

1. The pressure relief valve(s) should be designed to prevent overpressurization from a single pressurizer overspeed event with no letdown flow.
2. The design of the scram system should allow for the independence of the inner control plate and outer shutdown systems. If this independence is established, considerable reduction in the fuel damage probabilities will be realized.
3. It is recommended that more advanced speed control systems be investigated for the pressurizer pumps; for example, a synchro-converter. Such a device would eliminate the eddy current drive heating problem that is a potential source of the pump overspeed and would reduce common mode coupling failures between pumps.

#### **4.5.2.5 Loss of Secondary Coolant Heat Removal (0.25% of Total Risk).**

If a major malfunction with the secondary coolant system were to occur, other heat sinks for decay heat would be available, for example, the reactor pool or, in the preconceptual ANS design, the separate secondary coolant system of the shutdown heat removal system. The fuel damage risk of this category expresses the probability that a failure in the backup systems could result in inadequate cooling of the fuel.

### 4.5.3 Hydrogen-Oxygen Safety Risks

One of the essential ANS research capabilities will be the beams of extremely slow ("cold") neutrons created by collecting neutrons that have passed through the liquid deuterium in the two cold sources. The deuterium in the double-walled cold sources is maintained in a liquid state at about 20 K by cryogenic cooling systems. The cold sources are located outside the CPBT in the reflector tank at about the midheight of the core. As discussed in Sect. 4.4.3, each cold source contains  $\sim 8$  kg of deuterium, equivalent to  $\sim 4$  kg of hydrogen. Because deuterium is expected to have characteristics very similar to hydrogen, a primary safety goal of the ANS is the prevention of deflagration or detonation of the cold source deuterium.

In January 1989, R. R. Fullwood (BNL) completed a study entitled "Survey of Energetic Hydrogen-Oxygen Reactions of Possible Relevance to the ANS." The objective of this report was to study the record of accidents involving detonation or deflagration of hydrogen to determine if conclusions valid to the ANS could be drawn. The emphasis of the study was on an event that occurred in 1983 at the High Flux Beam Reactor (HFBR, located at BNL) in which the moderator chamber of the HFBR cold neutron facility was destroyed by an energetic hydrogen-oxygen reaction.

As a result of his study, Fullwood concluded that the ANS design is different from the HFBR cold source design but made several observations relevant to the safety of the ANS design:

1. The elimination of residual oxygen gas either by purging or evacuation is essential.
2. If purging is used, the composition of the purge gas should be analyzed to assure air removal.
3. Cold surfaces can result in cryogenic

pumping of air that can only be prevented by leak-proof boundaries and valves.

4. Ignition of combustible hydrogen-air mixtures in enclosures is nearly guaranteed. It may be initiated by minor disturbances such as the movement of crystals of frozen air.
5. Cryogenic trapping of the deuterium supply may lead to problems rather than solving them because of the cryopumping of the traps. It may be better to independently assure that the deuterium supply is negligibly low in oxygen content resulting in a flammable mixture than to depend on cryotrapping of the deuterium.

After the initial draft of Fullwood's study was published, T. L. Ryan, ANS project cryogenic and cold source designer, articulated a five-point safety philosophy for ANS cold source design—the major elements of which are reported below.

**Minimize the Chances for Leaks.** One of the main design goals with deuterium systems, cryogenic or not, is the prevention of leaks. Therefore, the ANS cold source will be an all-welded assembly to eliminate mechanical joints. This will require the cutting and rewelding of lines for replacement of components, but because this will not occur often, it will not impose any significant operational constraint on the ANS. In addition, a double containment with a vacuum annulus that is monitored 100% of the time will be provided. The vacuum containment will also provide a secondary pressure boundary for containment of the deuterium and will provide an extremely high sensitivity leak-detection capability.

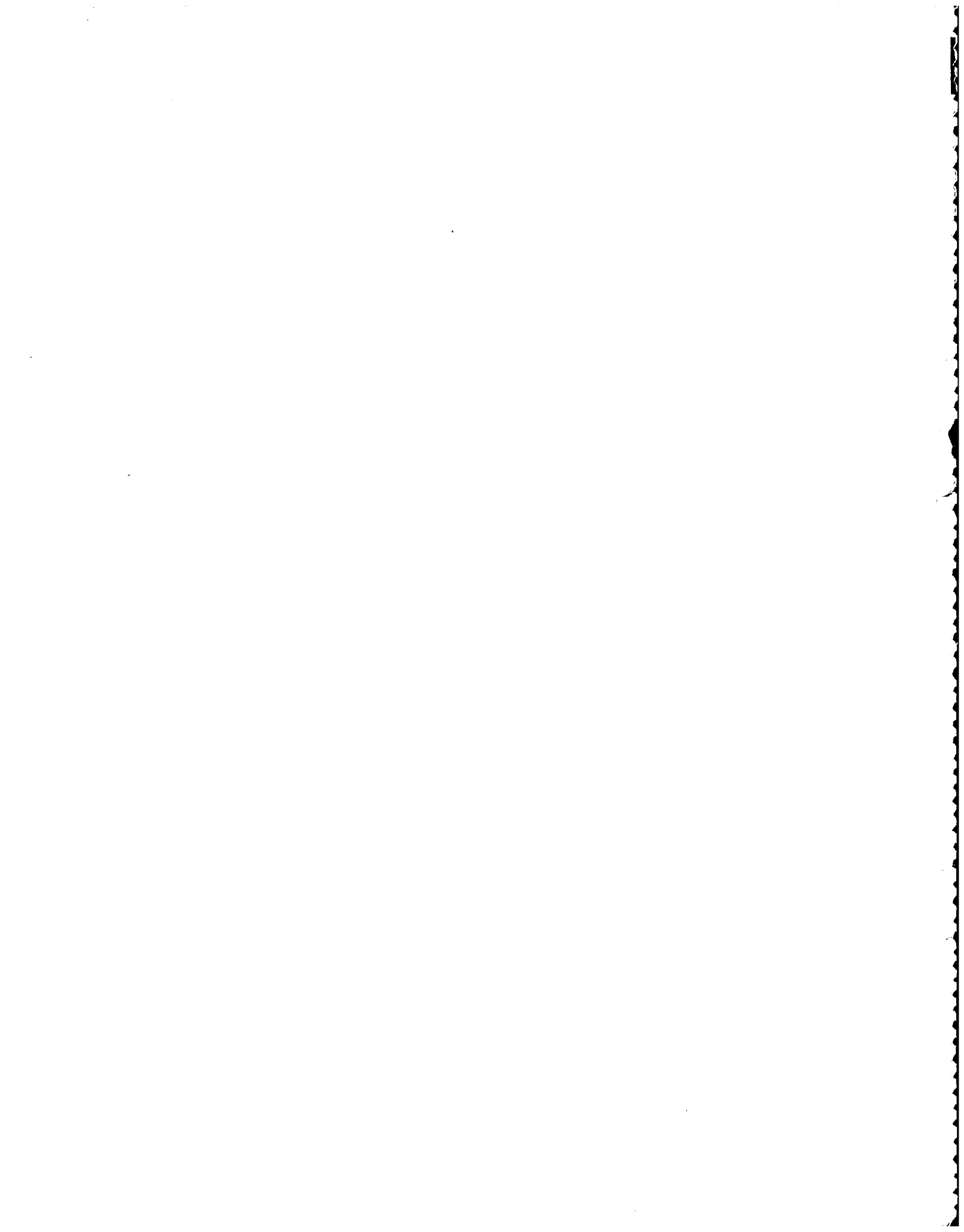
**Minimize the Probability for Failure.** The system will be designed without valves within the cryostat. The elimination of cryogenic valves greatly enhances the reliability of the system. The combination of a system with no valves, or other moving parts, in a completely welded double enclosure provides a system with an extremely small chance for failure.

**Minimize the Chance for Operational Error.** In the description of the failure that occurred in the BNL HFBR cold source, note a very complicated procedure was performed to charge the cold source. The ANS procedure will be much simpler. The plan is to completely vacuum purge the system for initial charging. Once the system has been pumped down to a low vacuum level, the system will be helium leak checked. Both the primary and secondary systems will be checked. After passing this leak check, the system will be charged to 6 atms with warm deuterium gas, and the system will be locked up at  $\sim 0.6$  MPa of pressure and the charging station checked for leaks. If no deuterium or air is detected in the vacuum annulus, cool-down of the cold source can then be initiated. As the cold source is cooled, the deuterium gas in the cold source will be cooled eventually to the point where the liquid deuterium will begin to condense. The volume of the primary containment is sized such that the 0.6 MPa will provide a full charge in the cold source cryostat when the pressure within the primary containment reaches 0.1 MPa. When 0.1 MPa is reached, the cooling will be adjusted to the cold source to maintain that pressure and thereby maintain the correct quantity of liquid in the cryostat for cold source operation. When it is required to warm the cold source, helium cooling will be stopped, and the cold source liquid deuterium will be allowed to boil off and the system rise back to 0.6 MPa when the entire cold source is at ambient temperature. This operational philosophy does not require the removal, purge, or refilling of deuterium within the cryostat unless some failure occurs and the deuterium becomes contaminated or until the tritium level within the deuterium reaches set limits and the entire inventory of deuterium must be removed.

**Provide adequate monitoring and control.** The vacuum annulus will be monitored for leaks, and the deuterium will be monitored for contamination during all phases of opera-

tion. These monitoring functions will provide early warning of any incipient failure of the primary or secondary pressure boundaries.

**Provide a fail-safe design.** This can be accomplished by the extremely simple system that can be allowed to safely rise to ambient temperature even if all cooling and power is lost to the cold source. In addition, proper venting and relief features will be built into the system if some overpressure does occur and venting will be either carried to a burn facility or to a storage facility or the deuterium cannot be burned and vented to the atmosphere. The main point is that no operator action will be required to safely shut down the cold source in case of a malfunction or loss of reactor or cold source control systems.



## References

1. G. L. Copeland, et al., *Advanced Neutron Source Final Preconceptual Reference Core Design*, ORNL/TM-11234, Martin Marietta Energy Systems, Inc., Oak Ridge Natnl. Lab., August 1989.
2. W. R. Gambill and T. Mochizuki, "Advanced Neutron Source Design: Burnout Heat Flux Correlation Development", 1988 International Conference on Nuclear Fission: Fifty Years of Progress in Energy Security, *Trans. Amn. Nuc. Soc.*, Vol. 57, pp. 298-99, November 1988.
3. G. L. Copeland, et al., *Advanced Neutron Source Final Preconceptual Reference Core Design*, ORNL/TM-11234, Martin Marietta Energy Systems, Inc., Oak Ridge Natnl. Lab., August 1989.
4. J. C. Griess, et al., *Effect of Heat Flux on the Corrosion of Aluminum by Water. Part III Final Report on Tests Relative to the High-Flux Isotope Reactor*, ORNL-3230, Martin Marietta Energy Systems, Inc., Oak Ridge Natnl. Lab., December 1961.
5. J. C. Griess, H. C. Savage, and J. L. English, *Effect of Heat Flux on the Corrosion of Aluminum by Water. Part IV Tests Relative to the Advanced Test Reactor and Correlation with Previous Results*, ORNL-3541, Martin Marietta Energy Systems, Inc., Oak Ridge Natnl. Lab., February 1964.
6. D. L. Selby, R. M. Harrington, and F. J. Peretz, *Advanced Neutron Source (ANS) Project Annual Report, April 1987-March 1988*, ORNL/TM-10860, Martin Marietta Energy Systems, Inc., Oak Ridge Natnl. Lab., February 1989.
7. B. H. Montgomery, R. E. Pawel, and G. L. Yoder, "The Advanced Neutron Source Test Loop Facility", *Trans. Am. Nuc. Soc.* 57, 1988.
8. R. E. Pawel, *On the Kinetics of the Aluminum-Water Reaction During Exposure in High-Heat Flux Test Loops. I. A Computer Program for Oxidation Calculations*, ORNL/TM-10602, Martin Marietta Energy Systems, Inc., Oak Ridge Natnl. Lab., January 1988.
9. R. E. Pawel and D. W. Yarbrough, *Modeling Heat Generation and Flow in the Advanced Neutron Source Test Loop Specimen*, ORNL/TM-10603, Martin Marietta Energy Systems, Inc., Oak Ridge Natnl. Lab., January 1988.
10. G. H. Hanson, G. W. Gibson, J. C. Griess, R. E. Pawel, N. E. Pace, and J. M. Ryskamp, *Report of the Advanced Neutron Source (ANS) Aluminum Cladding Corrosion Workshop; November 16-17, 1988; Idaho Falls, Idaho*, ORNL/CONF-8811203, Martin Marietta Energy Systems, Inc., Oak Ridge Natnl. Lab., February 1989.
11. D. R. Miller, "Critical Flow Velocities for Collapse of Reactor Parallel-Plate Fuel Assemblies," *J. Eng. Power, Trans. ASME*, pp. 83-95 (April 1960).

12. G. S. Rosenberg and C. K. Youngdahl, "A Simplified Dynamic Model for the Vibration Frequencies and Critical Coolant Flow Velocities for Reactor Parallel Plate Fuel Assemblies," *Nuc. Sci. Eng.*, 13(2): 91-102 (June 1962).
13. G. E. Smissaert, "Static and Dynamic Hydroelastic Instabilities in MTR-Type Fuel Elements, Part II. Theoretical Investigation and Discussion," *Nuc. Eng. Des.*, 9: 105-22 (1969).
14. G. E. Smissaert, "Static and Dynamic Hydroelastic Instabilities in MTR-Type Fuel Elements, Part I. Introduction and Experimental Investigation," *Eng. Des.*, 7: 535-46 (1968).
15. R. D. Groninger and J. J. Kane, "Flow Induced Deflections of Parallel Flat Plates," *Nuc. Sci. Eng.*, 16: 218-26 (1963).
16. W. L. Zabriskie, *An Experimental Evaluation of the Critical Flow Velocity Formulas for Parallel Plate Assemblies*, AECU-3936, General Engineering Laboratory, General Electric, October 1958.
17. R. J. Scavuzzo, *An Experimental Study of Hydraulically Induced Motion in Flat Plate Assemblies*, Bettis Technical Review, WAPD-BT-25 (May 1962).
18. PATRAN Plus graphical pre- and postprocessor for FEA, version 2.3, developed by PDA Engineering, Costa Mesa, CA, 1988.
19. FIDAP CFD software version 4.15, developed by Fluid Dynamics International, Inc., Evanston, IL, 1988.
20. H. Hoffman, *Thermodynamic and Fluid Dynamic Experiments for the Horizontal Cold Source of the Grenoble High Flux Reactor*, ILL report Re 972 N(p) 008, October 1983 (in French).
21. J. B. Hayter, *Proceedings of the Oak Ridge National Laboratory/Brookhaven National Laboratory Workshop on Neutron Scattering Instrumentation at High-Flux Reactors—June 5-7, 1989*, CONF-8906311, Martin Marietta Energy Systems, Inc., Oak Ridge Natnl. Lab., in progress.
22. C. Michelson (to E. P. Epler), *Design and Experimental Evaluation of Electromagnets in Research Reactors*, ORNL 57-9-48, Martin Marietta Energy Systems, Inc., Oak Ridge Natnl. Lab., September 6, 1957.
23. B. Sigmon, A. C. Heitzman, Jr., and J. Morrissey, *Oak Ridge Reservation Site-Evaluation Report for the Advanced Neutron Source*, ORNL/TM-11419, Martin Marietta Energy Systems, Inc., Oak Ridge Natnl. Lab., in progress.
24. J. R. Buchanan et al., *Report of the Advanced Neutron Source (ANS) Safety Workshop*, ORNL Conference Report, CONF-8810193, Martin Marietta Energy Systems, Inc., Oak Ridge Natnl. Lab., December 1988.

25. J. A. March-Leuba, *Advanced Neutron Source Reactor Dynamics Calculations: Comparison with SPERT-II Experimental Results*, TANSO 60 1-792(1989), pp. 435-36.
26. V. H. Ransom, *RELAP5/MODf2 Code Manual, Vol. 1: Code Structure, Systems Models, and Solution Methods; Vol. 2: Users Guide and Input Requirements*, NUREG/CR-4312, U.S. Nuclear Regulatory Commission, 1985.
27. S. B. Petukhov, *Advances in Heat Transfer*, Academic Press, New York, 6,503 (1970).
28. D. C. Groeneveld et al., *1986 TECL-UO Critical Heat Flux Lookup Table*, *Heat Transfer Engineering*, Vol. 7, No. 1-2, pp. 46-62.
29. P. Griffith, "The Prediction of Low Quality Boiling Voids," *ASME J. of Heat Trans.*, August 1964, pp. 327-33.
30. K. Mishima, et al., "A Study of Air-Water Flow in a Narrow Rectangular Duct Using Image Processing Technique," U.S./Japan Seminar on Two-Phase Flow Dynamics, Ohtsu, Japan, July 1988.
31. P. Saha and N. Zuber, "Point of Net Vapor Generation and Vapor Void Fraction in Subcooled Boiling," Fifth International Heat Transfer Conference, Tokyo, Japan, September 3-7, 1974.
32. C. V. Parks, ed., *SCALE: A Modular Code System for Performing Standardized Computer Analyses for Licensing Evaluation*, NUREG/CR-0200 (also ORNL/NUREG/CSD-2/V1 to V3/R3), 1984.
33. W. A. Rhoades and R. L. Childs, *An Updated Version of the DOT 4 One- and Two-Dimensional Neutron/Photon Transport Code*, ORNL-5851, Martin Marietta Energy Systems, Inc., Oak Ridge Natnl. Lab., July 1982.
34. P. D. Hess and K. J. Brondyke, "Causes of Molten Aluminum-Water Explosions and Their Prevention," *Metals Progress* 45 (April 1969).
35. R. W. Millet, et al., *Report of SPERT-I Destructive Test Program on Aluminum, Plate-Type, Water-Moderated Reactor*, IDO-16883, Phillips Petroleum Co., Atomic Energy Div., Idaho Falls, Idaho, June 1964.
36. Idaho Test Station, *Final Report of SL-1 Excursion*, IDO-19313, The General Electric Co., Idaho Falls, Idaho, July 1962.
37. C. J. Fry, et al., *CSNI Joint Interpretation Exercise on Fuel-Coolant Interactions. Results from Selected Experiments Performed in the Thermir Facility at AEE Winfrith*, AEEW-M-1778, AKAEA Atomic Energy Establishment, Winfrith, United Kingdom, May 1980.
38. Adina Research & Development Co., Inc., *ADINA (Automatic Dynamic Incremental Non-linear Analysis) Users Manual*, Report No. ARD-87-1, December 1987.

39. D. L. Selby, et al., *Advanced Neutron Source (ANS) Project Annual Report, April 1987-March 1988*, ORNL/TM-10860, Martin Marietta Energy Systems, Inc., Oak Ridge Natnl. Lab., February 1989.
40. B. D. Fishburn, "Some Aspects of Blast from Fuel-Air Explosives," *Acta Astronautica* 3, 1049-65 (April 1976).
41. M. P. Sherman, "Hydrogen Combustion in Nuclear Plant Accidents and Associated Containment Loads," *Nuc. Eng. and Design* 82, 13-24 (1984).
42. U.S. Nuclear Regulatory Commission, *U.S. Code of Federal Regulations*, 52 FR 41288 (published 8/21/87, effective 11/27/87).
43. D. O. Harris, et al., *Probability of Pipe Fracture in the Primary Coolant Loop of a PWR Plant, Volume 5: Probabilistic Fracture Mechanics Analysis Load Combination Program Project I Final Report*, NUREG/CR-2189, U.S. Nuclear Regulatory Commission, August 1981.
44. F. J. Peretz, *Preliminary Description fo the Advanced Neutron Source, March 1989 Draft*, ORNL/INT-1, Martin Marietta Energy Systems, Inc., Oak Ridge Natnl. Lab., March 1989.

## Internal Distribution

- |                          |  |
|--------------------------|--|
| 1. C. W. Alexander       | 53-54. M. R. McBee                     |
| 2. R. G. Alsmiller       | 55. M. T. McFee                        |
| 3. J. L. Anderson        | 56. T. J. McManamy                     |
| 4. B. R. Appleton        | 57. G. S. McNeilly                     |
| 5. Y. Y. Azmy            | 58. G. R. McNutt                       |
| 6. V. B. Baylor          | 59. P. E. Melroy                       |
| 7. R. A. Brown           | 60-61. B. H. Montgomery                |
| 8. J. R. Buchanan        | 62. R. M. Moon                         |
| 9. R. M. Canon           | 63. J. A. Murray                       |
| 10. N. C. J. Chen        | 64. R. K. Nanstad                      |
| 11. R. D. Cheverton      | 65. F. S. Patton                       |
| 12. G. L. Copeland       | 66. R. E. Pawel                        |
| 13. B. L. Corbett        | 67. F. J. Peretz                       |
| 14. W. G. Craddick       | 68. R. T. Primm, III                   |
| 15. F. C. Difilippo      | 69. C. C. Queen                        |
| 16. J. R. Dixon          | 70. S. Raman                           |
| 17. H. L. Dodds          | 71. J. S. Rayside                      |
| 18. F. F. Dyer           | 72. A. E. Ruggles                      |
| 19. C. C. Eberle         | 73. T. L. Ryan                         |
| 20. S. R. Ervin          | 74. W. K. Sartory                      |
| 21. D. K. Feld           | 75-76. D. L. Selby                     |
| 22. R. E. Fenstermaker   | 77. T. E. Shannon                      |
| 23. G. F. Flanagan       | 78-79. H. B. Shapira                   |
| 24. C. P. Frew           | 80. W. D. Shults                       |
| 25. W. R. Gambill        | 81. J. O. Stiegler                     |
| 26. R. K. Genung         | 82. W. F. Swinson                      |
| 27-28. M. L. Gildner     | 83. R. P. Taleyarkhan                  |
| 29. R. W. Glass          | 84-85. P. B. Thompson                  |
| 30. H. A. Glover         | 86. K. R. Thoms                        |
| 31-32. R. M. Harrington  | 87. A. W. Trivelpiece                  |
| 33-34. J. B. Hayter      | 88. D. B. Trauger                      |
| 35-36. D. R. Hicks       | 89-90. C. D. West                      |
| 37. R. W. Hobbs          | 91. J. Westbrook                       |
| 38. D. T. Ingersoll      | 92. M. K. Wilkinson                    |
| 39-40. J. A. Johnson     | 93. B. A. Worley                       |
| 41. R. L. Johnson        | 94. G. T. Yahr                         |
| 42. J. E. Jones, Jr      | 95. G. L. Yoder                        |
| 43-44. L. M. Jordan      | 96. A. Zucker                          |
| 45. H. T. Kerr           | 97. ORNL Patent Office                 |
| 46. M. W. Kohring        | 98. Central Research Library           |
| 47. R. A. Lillie         | 99. Document Reference Section         |
| 48. M. F. Marchbanks     | 100-101. Laboratory Records Department |
| 49-50. J. A. March-Leuba | 102. Laboratory Records (RC)           |
| 51-52. B. S. Maxon       |  |

## External Distribution

103. Alexander Adams, U.S. Nuclear Regulatory Commission, MS-10-0-21, Washington, DC 20555
104. P. Ageron, Institut Laue Langevin, 156X 38042, Grenoble Cedex, France
105. Jurgen Ahlf, Joint Research Center, Institute for Advanced Materials, 1755 ZG Petten, P. O. Box 2, The Netherlands
106. William Anderson, Babcock & Wilcox, Mt. Athens Road, P. O. Box 785, Lynchburg, VA 24505
107. Peter Armbruster, Institut Laue-Langevin, 156X, 38042 Grenoble Cedex, France
108. Takumi Asaoka, Deputy Director General, Tokai Research Establishment, Japan Atomic Energy Research Institute, Tokai-mura, Naka-gun, Ibaraki-ken, Tokyo 319-11, Japan
109. John Axe, Brookhaven National Laboratory, Building 510A, Upton, NY 19973
110. Anton Axmann, Hahn-Meitner Institute Berlin, N3, Glienicke Str. 100, D-1000 Berlin 39, Federal Republic of Germany
111. Lewis J. Baker, Materials Physics & Metallurgy Division, Building 521.11, Harwell Laboratory, Oxfordshire OX11 0RA, United Kingdom
112. Frank Bates, Department of Chemical Engineering and Material Science, University of Minnesota, 151 Amundson Hall, 421 Washington Avenue, SE, Minneapolis, MN 55455
113. Gunter S. Bauer, Paul Scherrer Institute, CH-5234 Villigen, Switzerland
114. J. M. Baugnet, Nuclear Services Program, S.C.K./C.E.N., Boeretang 200, B2400 Mol, Belgium
115. Dr. Klaus Böning, Fakultät für Physik E21, Technische Universität München, D-8046 Garching, Federal Republic of Germany
116. Paul Breant, CEN Saclay, SPS ORPHEE, 91191 Gif-sur-Yvette Cedex, France
117. H. A. Capote, Burns & Roe, 800 Kinderkamack Road, Oradell, NJ 07649
118. Kurt N. Clausen, RISO National Laboratory, Physics Department Postbox 49, DK-4000 Roskilde, Denmark
119. M. F. Collins, Nuclear Reactor, McMaster University, Hamilton, Ontario, L8S, 4K1, Canada
120. C. Desandre, Technicatome, Centre d'Etudes Nucleaires de Saclay, BP17, 92291 Gif/Yvette Cedex, France
121. A. F. DiMeglio, Rhode Island Atomic Energy Commission, Rhode Island Nuclear Science Center, South Ferry Road, Narragansett, RI 02882
122. B. Farnoux, CEN Saclay, Laboratoire Leon Brillouin, 91191 Gif/Yvette Cedex, France
123. C. D. Fletcher, Idaho National Engineering Laboratory, P. O. Box 1625, Idaho Falls, ID 83415
124. Dr. B. Chalmers Frazer, Materials Science Division, Office of Basic Energy Sciences, Office of Energy Research, U.S. Department of Energy, Germantown, ER-132, Washington, DC 20545
125. R. R. Fullwood, Building 130, Brookhaven National Laboratory, Upton, NY 11973
126. W. Glaser, Fakultät für Physik, Technische Universität München, D-8046 Garching, West Germany
127. Otto K. Harling, Massachusetts Institute of Technology, 77 Massachusetts Avenue, Cambridge, MA 02139

128. Masatoshi Hayashi, Research Reactor Institute, Kyoto University, Kumatori-cho, Sennan-gun, Osaka 590-04, Japan
129. Dr. L. C. Ianniello, Deputy Associate Director, Office of Basic Energy Sciences, Office of Energy Research, U.S. Department of Energy, Germantown ER-11, Washington, DC 20545
130. Masashi Iizumi, Japan Atomic Energy Research Institute, 222, Uchisaiwai-cho, Chiyoda-ku, Tokyo, Japan
131. Professor K. Kanda, Research Reactor Institute, Kyoto University, Kumatori, Osaka 590-04, Japan
132. Nobuhiki Kunitomi, Osaka University, 1-1 Yamadaoka, Suita-Shi, Osaka 565 Japan
133. Wilfried Krull, GKSS, Postfach 1160, D-2054 Geesthacht, Federal Republic of Germany
134. J. A. Lake, Manager, Nuclear Engineering and Reactor Design, Idaho National Engineering Laboratory, P. O. Box 1625, Idaho Falls, ID 83415
135. Dale Lancaster, Georgia Institute of Technology, Atlanta, GA 30332
136. Albert G. Lee, Atomic Energy of Canada, Ltd., Whiteshell Nuclear Research Establishment, Pinawa, Manitoba, R0E 1L0, Canada
137. L. LeSage, Argonne National Laboratory, 9700 South Cass Avenue, Argonne, IL 60439
138. Charles Lewis, Babcock & Wilcox, P. O. Box 785, Lynchburg, VA 24505-0785
139. Mr. Robert F. Lidstone, Atomic Energy of Canada, Ltd., Whiteshell Nuclear Research Establishment, Pinawa, Manitoba, R0E 1L0, Canada
140. John Marks, Research and Test Reactor Fuel Elements, Babcock and Wilcox Co., P. O. Box 785, Lynchburg, VA 24505
141. Shajiro Matsuura, Japan Atomic Energy Research Institute, Tokai Research Establishment, Tokai-mura, Naka-gun, Ibaraki-ken, Japan
142. M. H. McBride, Oak Ridge Operations, U.S. Department of Energy, Building 7900, MS-6387, P. O. Box 2008, Oak Ridge, TN 37831-6387
143. J. Charles McKibben, Research Reactor Facility, University of Missouri-Columbia, Research Park, Columbia, MO 65211
144. Ross Miller, Atomic Energy of Canada, Ltd., Research Company, Chalk River Nuclear Laboratories, Chalk River, Ontario, K0J 1J0, Canada
145. Hirokatsu Nakata, Project Engineering Division, Department of JMTR Project, Japan Atomic Energy Research Institute, Oarai Ibaraki-ken, Japan
146. Robert J. Neuhold, U.S. Department of Energy, Germantown, NE-472, Washington, DC 20545
147. Les C. Oakes, Electric Power Research Institute (EPRI), Building 2, Room 252, P. O. Box 10412, Palo Alto, CA 94303
148. Stephen L. Ostrow, Ebasco Services, Inc., 2 World Trade Center, 89th Floor, New York, NY 10048
149. Yuri V. Petrov, Leningrad Nuclear Physics Institute, Academy of Science of USSR, 188350 Gatchina, Leningrad District, USSR
150. Henry J. Prask, National Institute for Standards & Technology, A-106 Reactor, Gaithersburg, MD 20899
151. Harry E. Preble, Babcock & Wilcox, P. O. Box 785, Lynchburg, VA 24505-0785
152. Thomas J. Raney, Ebasco Services, Inc., 2 World Trade Center, 89th Floor, New York, NY 10048

153. Hans-Joachim Roegler, Interatom GmbH, Friedrich-Ebert-Strasse, D-5060 Bergisch-Gladbach 1, Federal Republic of Germany
154. Mike Rowe, National Institute of Standards and Technology, Washington, DC 20234
155. John J. Rush, National Bureau of Standards, Washington, DC 20234
156. John M. Ryskamp, Idaho National Engineering Laboratory, P. O. Box 1625, Idaho Falls, ID 83415
157. Professor Toshikazu Shibata, Atomic Energy Research Institute, Kinki University, Kowakae, Higashi-Osaka, Osaka 577, Japan
158. Eiji Shirai, Department of Research Reactor Operation, Japan Atomic Energy Research Institute, Tokai-mura, Naka-gun, Ibaraki-ken 319-11, Japan
159. J. B. Slater, Atomic Energy of Canada, Ltd., Research Company, Chalk River Nuclear Laboratories, Chalk River, Ontario, K0J 1J0, Canada
160. Roland Smith, Argonne National Laboratory, P. O. Box 2528, Idaho Falls, ID 83403
161. J. L. Snelgrove, Coordinator, Engineering Applications, RERTR Program, Argonne National Laboratory, 9700 South Cass Avenue, Argonne, IL 60439
162. Dr. D. K. Stevens, Associate Director, Office of Basic Energy Sciences, Office of Energy Research, U.S. Department of Energy, Germantown ER-10, Washington, DC 20545
163. T. G. Theofanous, Theofanous & Company, Inc., 857 Sea Ranch Drive, Santa Barbara, CA 93109
164. Dr. Iran L. Thomas, Director, Materials Science Division, Office of Energy Research, U.S. Department of Energy, Germantown ER-13, Washington, DC 20545
165. Masahiko Utsuro, Research Reactor Institute, Kyoto University, Kumatori-cho, Sennan-gun, Osaka, Japan
166. Jacques Verdier, Centre d'Etudes Nucleaires, SBT, 85X, 38041 Grenoble Cedex, France
167. R. P. Wadkins, Idaho National Engineering Laboratory, P. O. Box 1625, Idaho Falls, ID 84515
168. James M. Warren, Gilbert Commonwealth, 320 Cedar Bluff Road, Suite 300, Knoxville, TN 37923
169. R. F. Wichman, Atomic Energy of Canada Ltd., Research Company, Chalk River Nuclear Laboratories, Chalk River, Ontario, K0J 1J0, Canada
170. D. K. Wilfert, Energy Programs, U.S. Department of Energy, Oak Ridge Operations, Building 7900, MS-6387, P. O. Box 2008, Oak Ridge, TN 37831-6387
171. R. J. Willard, U.S. Department of Energy, Oak Ridge Operations, P. O. Box 2001, Oak Ridge, TN 37831-2001
172. Houston G. Wood, III, Associate Professor, Department of Mechanical and Aerospace Engineering, Thornton Hall, University of Virginia, Charlottesville, VA 22901
173. Office of Assistant Manager for Energy Research and Development, U.S. Department of Energy, Oak Ridge Operations, P. O. Box 2001, Oak Ridge, TN 37831-2001
- 174-175. Office of Scientific and Technical Information, P. O. Box 62, Oak Ridge, TN 37831